UNIVERSITY OF GENOA

POLYTECHNIC SCHOOL

Department of Civil, Chemical and Environmental Engineering

MASTER DEGREE

IN

CHEMICAL AND PROCESS ENGINEERING

Numerical investigation of conjugate heat transfer within the vascular system in the presence of a bioprosthesis

Supervisors

Prof. Jan Oscar Pralits

Prof. Pier Francesco Ferrari

Candidate

Viola Prando

Academic year 2023-2024

A me.

Abstract

Vascular bioprostheses offer promising solutions for replacing small-caliber vessels. However, their clinical feasibility demands comprehensive evaluation beyond mechanical and biological compatibility. This research focuses on investigating thermal effects associated with the implantation of polymer-based (PCL:PGS) vascular prostheses, as even minor temperature variations might significantly affect clinical outcomes. The analysis employs numerical simulations based on Computational Fluid Dynamics (CFD) to explore conjugate heat transfer phenomena within vascular systems incorporating bioprostheses. Multiple geometries—linear, curved, and bifurcated vessels—were modeled using OpenFOAM, varying velocity and diameters to assess thermal behavior under realistic physiological conditions. Results demonstrate minimal temperature variations (less than 0.1 K) introduced by the prosthesis, irrespective of geometry complexity. Although slight temperature increases occurred locally near the scaffold, these were deemed negligible, confirming the prosthesis's thermal safety and suitability for clinical implantation. This study validates the thermal compatibility of PCL:PGS vascular prostheses, significantly supporting their clinical implementation. Additionally, the established CFD modeling framework provides an adaptable platform for future investigations under diverse physiological conditions, potentially facilitating targeted patient-specific assessments and extended clinical applicability.

Contents

Introduction

This thesis falls within the field of chemical bioengineering and fluid dynamics applied to vascular bioprostheses. The primary objective of this research is to analyze the thermal and fluid dynamic behavior of a synthetic vessel fabricated through electrospinning, using a polymer blend of polycaprolactone (PCL) and polyglycerol sebacate (PGS). Numerical simulations are performed using OpenFOAM to study the temperature profile and fluid behavior under realistic operating conditions. The interest in vascular bioprostheses arises from the need to develop more effective alternatives to traditional synthetic grafts. Cardiovascular diseases represent one of the leading causes of mortality worldwide, with conditions such as atherosclerosis, aneurysms, and arterial stenosis often requiring surgical intervention through vascular replacement or bypass procedures. In this context, innovative bioprostheses offer solutions that are more compatible with physiological processes, reducing postoperative complications and improving patients' quality of life. Bioprostheses made from bioresorbable materials provide the advantage of promoting tissue regeneration, avoiding long-term complications associated with permanent implants. The selection of the PCL-PGS blend comes from its mechanical and elastic properties, as well as its ability to gradually degrade, allowing for the formation of new biological tissue. The research is structured into multiple phases. Initially, a detailed analysis of the circulatory system's anatomy is provided, with particular focus on the characteristics of blood vessels and the biomechanical requirements that vascular prostheses should fulfill. Subsequently, bioprostheses are discussed in general, with an in-depth examination of polymeric materials used in biomedical applications, particularly the properties of PCL and PGS. Electrospinning, the fabrication technique adopted for the preparation of experimental samples, is analyzed in detail to highlight the role of process parameters in defining the structural characteristics of the bioprosthesis. A fundamental aspect of this study involves the fluid dynamic modeling within

the synthetic vessel. The flow is considered laminar, and blood is modeled as an incompressible fluid. The Navier-Stokes equations serve as the mathematical reference for fluid behavior analysis, while for the thermal aspect, an equivalent condition is adopted to simplify the problem without neglecting the influence of the material's thermal conductivity. This condition is based on the assumption that when the vessel diameter is significantly larger than the wall thickness, the latter can be considered negligible in conduction calculations. However, a corrective equation is introduced to account for the thermal conductivity of blood and the polymer blend used, ensuring a more realistic model. Finally, the numerical simulation phase is conducted using OpenFOAM, an open-source software widely employed for fluid dynamic and thermal analysis. The vascular geometries are modeled using Onshape, enabling the creation of precise and customized three-dimensional structures. The simulation process involves the implementation of the Navier-Stokes equations within the computational domain, with appropriate boundary conditions to represent blood flow under physiological conditions. Numerical discretization techniques based on the finite volume method are applied, ensuring high accuracy in solving the governing equations. Post-processing is performed in ParaView, where the obtained data are analyzed to visualize velocity, pressure, and temperature profiles along the synthetic vessel. This phase allows the identification of critical regions of flow instability or thermal accumulation, which are essential for model validation and bioprosthesis design improvements. The results will help assess the effectiveness of the bioprosthesis from a thermal and fluid dynamic perspective, providing useful insights for future material and production process optimizations. This thesis, therefore, aims to combine an engineering approach to bioprosthesis design with advanced numerical simulation tools, contributing to the understanding of vascular bioprosthesis behavior and the definition of design criteria based on scientific evidence. The integration of computational modeling and experimental analysis is a crucial aspect in advancing next-generation bioprostheses, offering a solid foundation for optimizing materials and fabrication processes. Furthermore, the findings of this research could serve as a reference for future studies aimed at refining simulation methodologies and evaluating additional material combinations for biomedical applications. The approach adopted not only provides a rigorous method for bioprosthesis analysis but also opens new perspectives for the customization of implantable devices, with the ultimate goal of enhancing clinical efficacy and improving patients' quality of life.

Chapter 1

Anatomy of the circulatory system

1.1 The human circulatory system and blood

The human circulatory system is a complex apparatus that ensures the continuous transport of oxygen, nutrients, hormones, and metabolic waste products throughout the body. Its primary function is to maintain homeostasis by supplying tissues with an adequate amount of oxygen while facilitating the removal of carbon dioxide and other waste substances. This system is composed of an interconnected network of blood vessels that enable blood circulation, driven by the propulsive action of the heart. The heart is the central organ of the circulatory system, a hollow muscular structure divided into four chambers (two atria and two ventricles), responsible for propelling blood through the vessels. The circulatory system is divided into two main circuits[1]:

- *Systemic circulation*

  Transports oxygenated blood from the left ventricle of the heart to the entire body via the aorta and major arteries. After delivering oxygen to the tissues and collecting carbon dioxide and metabolic waste products, the deoxygenated blood returns to the right atrium through the venae cavae.

- *Pulmonary circulation*

  Carries oxygen-poor blood from the right ventricle to the lungs through the pulmonary artery. In the lungs, the blood becomes enriched with oxygen and releases carbon dioxide before returning to the heart via the pulmonary veins.

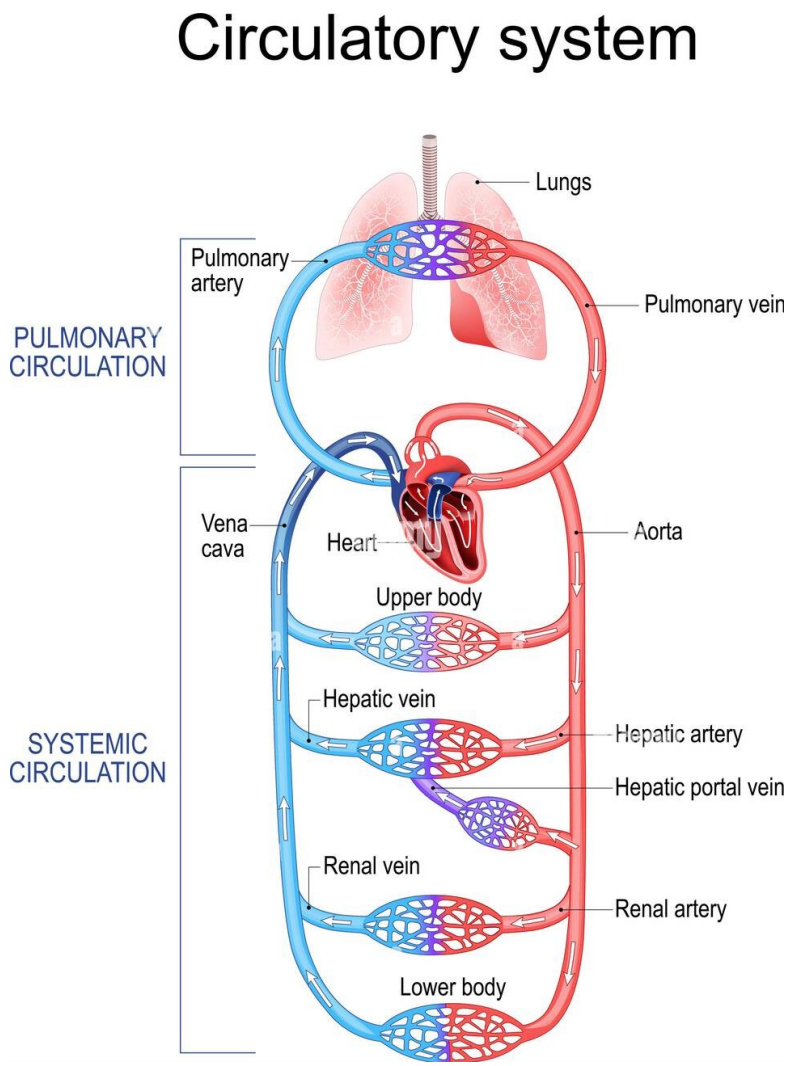

Figure 1.1: *Systemic and pulmonary circulation in human body.*

Blood is the fluid that circulates within the circulatory system and performs multiple vital functions. It is composed of 55% plasma and 45% formed elements. Plasma is a yellowish liquid containing plasma proteins (albumin, globulins, fibrinogen), electrolytes (sodium, potassium, calcium), glucose, lipids, vitamins, and dissolved gases. The formed elements of blood play essential roles in maintaining physiological functions and are categorized into three main types of cells[1][2]. Erythrocytes, commonly known as red blood cells, are responsible for oxygen transport due to the presence of hemoglobin. Their characteristic biconcave shape optimizes the surface area available for gas exchange, facilitating

the release of oxygen to tissues and the uptake of carbon dioxide for elimination through the lungs. Leukocytes, or white blood cells, serve as the body's primary defense system against infections and pathogens. These immune system cells can be further classified into different subtypes. Granulocytes are involved in inflammatory responses and bacterial infections, lymphocytes play a crucial role in specific immunity, and monocytes have the ability to differentiate into macrophages, assisting in the destruction of microorganisms and the removal of cellular debris. Lastly, platelets are small cell fragments that play a crucial role in blood coagulation. In the event of vascular injury, these structures rapidly aggregate at the site of damage, forming a hemostatic plug that prevents excessive blood loss and facilitates the repair process of the injured vessel[3][2]. The circulatory system also plays a fundamental role in regulating body temperature and distributing hormones. Any alteration in its functionality can lead to various pathologies, including hypertension, atherosclerosis, and thrombosis, ultimately impairing the proper delivery of blood to tissues[4].

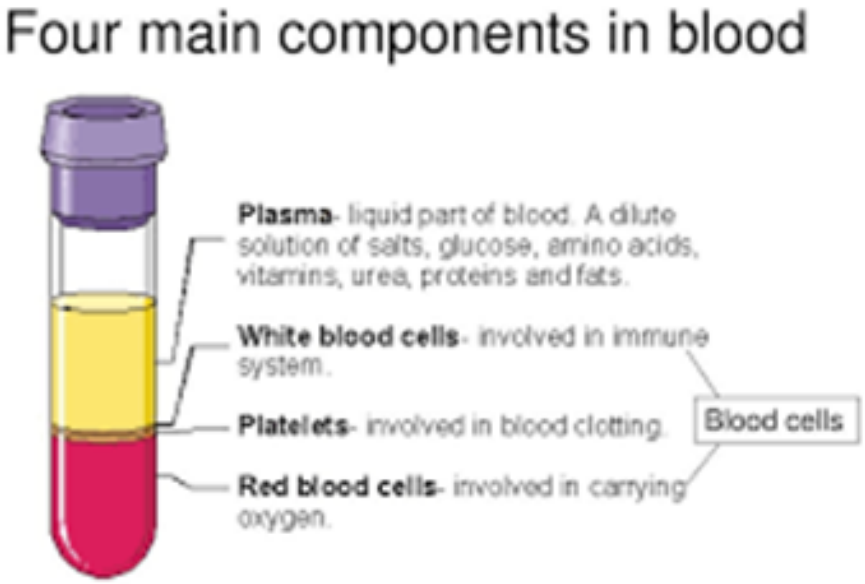

Figure 1.2: *The diagram illustrates the primary components of blood separated by centrifugation: plasma, white blood (leukocytes), platelets, red blood cells (erythrocytes).*

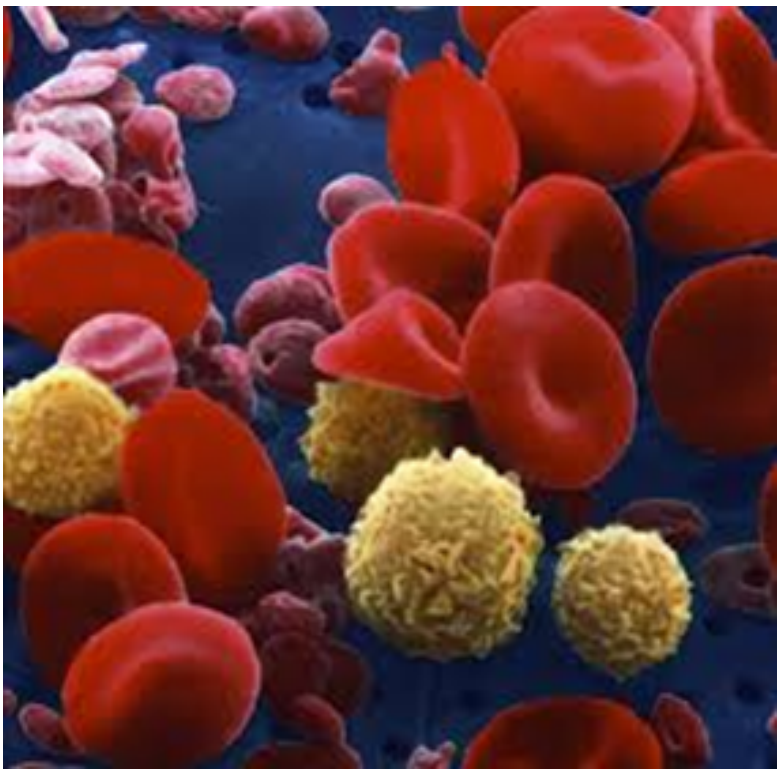

Figure 1.3: *The image presents a high-magnification view of blood cells, highlighting their structural differences. The red blood cells (erythrocytes) appear as biconcave discs. The white blood cells (leukocytes), visible in yellow. The platelets, seen as small irregularly shaped fragments, are involved in the blood clotting process.*

1.2 Blood vessels

1.2.1 Introduction

Blood vessels form the transport network for blood within the body and play a crucial role in maintaining homeostasis. They facilitate the distribution of oxygen and nutrients to tissues, the removal of metabolic waste products, and the transport of regulatory molecules such as hormones and growth factors[2]. Their structure and function vary depending on their type and anatomical location, yet they all share a general organization composed of specialized layers that ensure strength, elasticity, and the regulation of blood flow. Blood vessels can be classified into three main categories based on their function and the direction of blood

flow[1]:

- *Arteries*

  Transport oxygenated blood from the heart to the tissues.

- *Veins*

  Return deoxygenated blood from the tissues to the heart.

- *Capillaries*

  Facilitate the exchange of gases, nutrients, and metabolic waste between the blood and tissues.

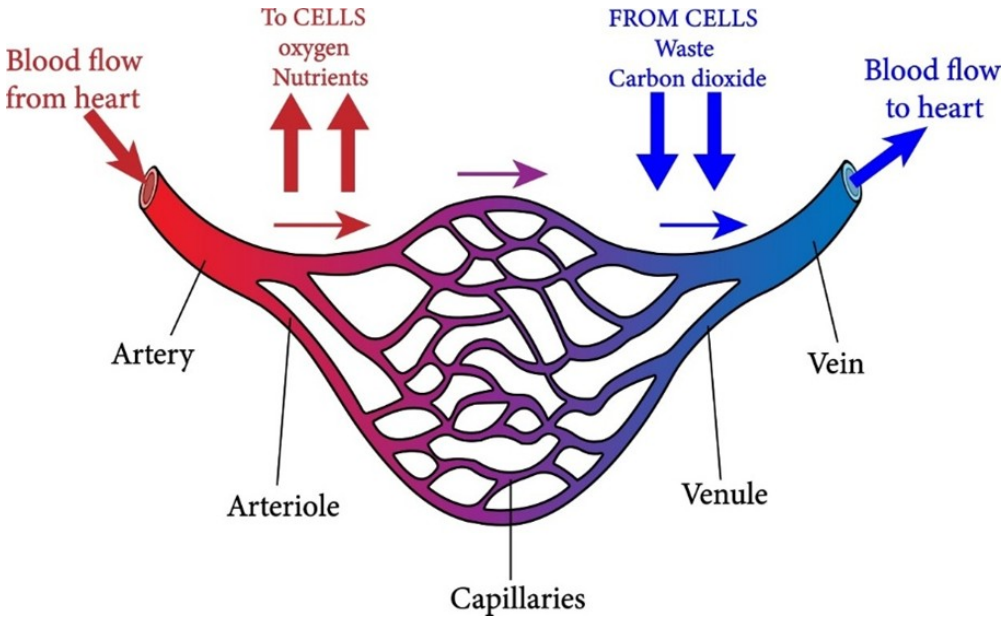

Figure 1.4: *The diagram illustrates the transition of blood flow through the vascular system. Arteries carry oxygen-rich blood from the heart, which then moves through arterioles into the capillary network. At the capillary level, oxygen and nutrients diffuse into the surrounding cells, while carbon dioxide and waste products are collected. The deoxygenated blood then flows into the venules and subsequently into the veins, which return it to the heart for reoxygenation. This process ensures efficient nutrient exchange and waste removal, maintaining homeostasis in tissues.*

In addition to these primary categories, there are also arterioles and venules, which serve as transitional vessels between arteries and capillaries and between

capillaries and veins, respectively. Arterioles play a fundamental role in regulating blood pressure and distributing blood flow across different areas of the body. Arteries can be further classified into elastic arteries and muscular arteries. Elastic arteries, such as the aorta and pulmonary arteries, contain a large amount of elastic fibers in their walls, allowing them to expand and contract with each heartbeat. This elasticity helps maintain continuous blood flow even when the heart is in its relaxation phase. In contrast, muscular arteries have a higher proportion of smooth muscle tissue, which regulates the vessel diameter and, consequently, the blood flow to different tissues[1]. Unlike arteries, veins have thinner walls and are less elastic. However, they are equipped with one-way valves that prevent blood from flowing backward, facilitating venous return to the heart, particularly in the lower limbs, where gravity opposes the upward movement of blood. Capillaries are the smallest blood vessels in the body and play a crucial role in the exchange of gases, nutrients, and metabolic waste between the blood and surrounding tissues. Despite their small size, capillaries exhibit structural variations that influence their function and distribution across different organs. Continuous capillaries are the most common type and are characterized by tightly connected endothelial cells. This structure limits the passage of large molecules, ensuring a selective exchange between the blood and tissues. These capillaries are primarily found in muscles and the central nervous system, where an effective protective barrier is required to regulate substance flow[5]. Fenestrated capillaries, on the other hand, have small openings, or fenestrations, in their endothelial cells, allowing for an increased exchange of substances between the blood and surrounding tissues. This structural adaptation is particularly beneficial in organs involved in filtration and secretion. In the kidneys, fenestrated capillaries facilitate plasma filtration, playing a crucial role in the formation of urine. Similarly, in the endocrine glands, they enable the rapid transfer of hormones into the bloodstream, ensuring efficient hormonal signaling throughout the body[2]. Lastly, sinusoidal capillaries possess large openings between endothelial cells, making their walls highly permeable. Due to this feature, they allow the passage of not only large molecules but also entire cells, facilitating the transfer of substances and cellular components between the blood and organs. This type of capillary is typically found in the liver and spleen, where extensive macromolecule exchange and blood cell turnover are essential for maintaining physiological balance [5][6].

1.2.2 Structure of blood vessel walls

With the exception of capillaries, blood vessels have a layered structure composed of three concentric layers, each with a specific function. The tunica intima, also known as the inner layer, is the innermost layer and is in direct contact with the blood. It consists of a single layer of endothelial cells that regulate vascular permeability, prevent coagulation, and modulate vascular tone by releasing vasoactive substances such as nitric oxide and endothelin. These factors play a crucial role in maintaining proper blood flow and preventing abnormal clot formation. The tunica media is the middle layer, primarily composed of smooth muscle cells and elastic fibers. Its thickness varies depending on the type of vessel: in arteries, it is well-developed to withstand high pressures, while in veins, it is thinner and less rigid. This muscular layer allows blood vessels to contract and relax, actively regulating blood flow and pressure distribution across the circulatory system. The tunica adventitia, or outer layer, is mainly composed of connective tissue rich in collagen fibers, providing structural support and anchoring the vessel to surrounding tissues. Within this layer, small blood vessels known as vasa vasorum are present, supplying oxygen and nutrients to the walls of larger blood vessels, ensuring their proper function and structural integrity[1][2].

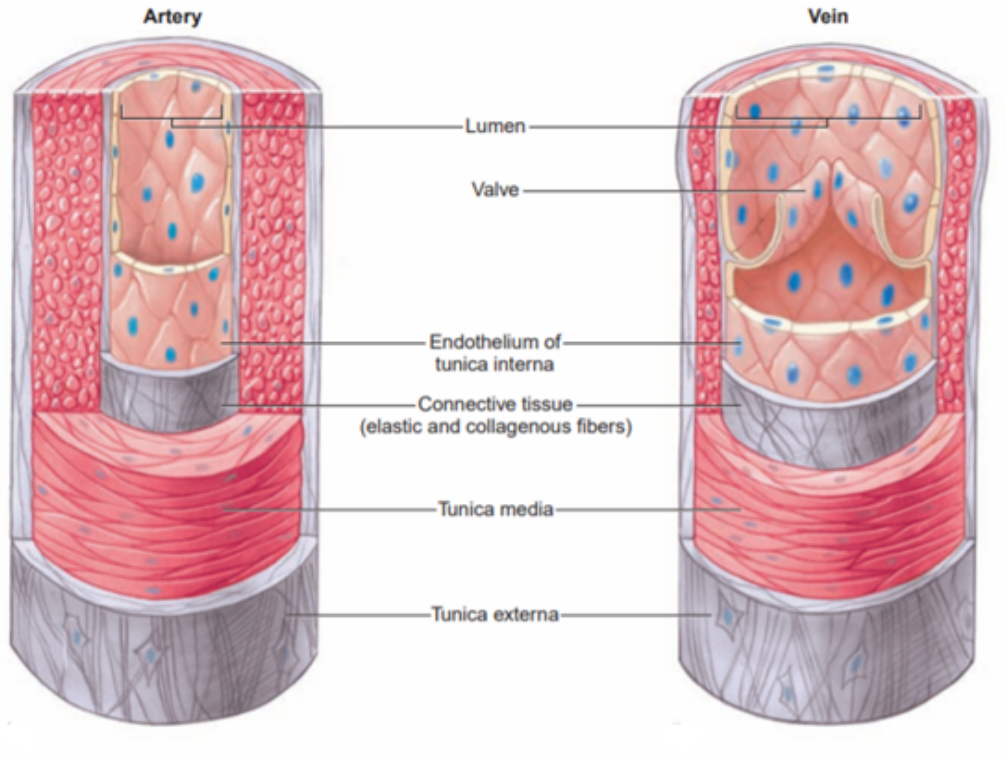

Figure 1.5: *The image highlights the differences between arteries and veins. Arteries have thicker walls with a well-developed tunica media, while veins have thinner walls and contain valves to prevent blood backflow.*

1.2.3 Vascular tissues

The walls of blood vessels are composed of various types of tissues, each playing a specific role in regulating blood flow and ensuring the mechanical resistance of the vessel. These tissues work together to maintain the functionality of the circulatory system, adapting to the body's physiological needs. The endothelial tissue forms the inner lining of blood vessels and is essential for regulating blood flow, inflammatory responses, and coagulation mechanisms. The endothelium is in constant interaction with the bloodstream and responds to mechanical and chemical stimuli by releasing vasoactive substances such as nitric oxide, which modulate vasodilation and vasoconstriction. Additionally, it regulates vascular permeability and prevents the adhesion of platelets and inflammatory cells to the

vessel wall, thereby reducing the risk of thrombus formation. The smooth muscle tissue, located in the tunica media, is responsible for the contraction and relaxation of blood vessel walls. This function is essential for regulating vessel diameter and, consequently, controlling blood pressure and the distribution of blood flow to various organs. Depending on the body's needs, the vascular muscle tone can be adjusted to either increase or decrease blood supply to tissues, ensuring an optimal balance between oxygen and nutrient demand and supply. The connective tissue, primarily found in the tunica adventitia, plays a crucial role in providing mechanical strength and elasticity to blood vessels. Its structure is rich in collagen and elastic fibers, which enable vessels to withstand pressure variations while maintaining their structural integrity. Additionally, this tissue offers support by anchoring blood vessels to surrounding tissues and shielding them from external mechanical stress[1]. The interplay between these tissues allows blood vessels to continuously adapt to hemodynamic variations, ensuring efficient and stable circulation throughout the body. Blood vessels are fundamental components of the circulatory system, facilitating blood distribution and the exchange of substances between tissues. Their complex structure, composed of multiple specialized layers and tissues, enables them to meet the body's physiological demands. A comprehensive understanding of their types, structure, and function is essential for advancing the study of vascular diseases and developing effective therapeutic solutions[2].

1.3 Circulatory system diseases

The circulatory system plays a fundamental role in maintaining the body's homeostasis by ensuring the transport of oxygen, nutrients, and metabolites across different tissues[7]. However, it is susceptible to numerous diseases that can compromise vascular function, leading to serious health consequences. Among these, diseases affecting small blood vessels, particularly arteriosclerosis, hold significant importance due to their impact on microcirculation and the functionality of vital organs. Vascular diseases can be classified based on the nature of the damage and the type of vessel involved[8]. The main categories include:

- *Atherosclerosis and arteriosclerosis*

  Characterized by the thickening and hardening of arterial walls.

- *Thrombosis and embolism*

  Conditions that involve the formation of blood clots, which can obstruct blood flow.

- *Vasculitis*

  Inflammation of blood vessels, often of autoimmune or infectious origin.

- *Aneurysms*

  Abnormal dilations of arteries that may lead to vascular rupture.

Among these conditions, arteriosclerosis of small vessels is particularly critical as it can lead to chronic ischemia and organ dysfunction, significantly affecting the microvascular network responsible for essential metabolic exchanges.

1.3.1 Arteriosclerosis in small blood vessels

Arteriosclerosis is a degenerative disease characterized by the loss of elasticity in the arteries, leading to thickening and increased rigidity of their walls. Its most common form is atherosclerosis, which involves the formation of lipid plaques on the inner walls of arteries, progressively narrowing the vessel lumen and restricting blood flow[9]. The World Health Organization (WHO) classifies the progression of atherosclerotic plaques into three stages. In the initial phase, known as the fatty streak, lipids begin to accumulate within the arterial wall, although this does not yet cause a significant narrowing of the vessel. As the disease progresses, the fibrous plaque develops, characterized by the proliferation of connective tissue covering the lipid deposits, making the arterial wall stiffer and less elastic. In the advanced stages, the plaque may ulcerate, leading to the formation of thrombi that can completely obstruct the vessel and severely restrict blood flow[7]. Atherosclerotic lesions tend to develop in areas exposed to high hemodynamic stress, such as arterial bifurcations. In small blood vessels, the progressive narrowing can result in chronic ischemia, causing irreversible tissue damage. The organs most affected by this condition include the heart, brain, kidneys, and lower limbs. A reduction in blood flow within coronary arterioles can lead to myocardial infarction, while blockages in small cerebral vessels may result in strokes or transient ischemic attacks (TIAs). When arteriosclerosis affects renal arterioles, it can contribute to hypertensive nephropathy, whereas in the peripheral arteries of the lower limbs, it may cause claudication intermittens and, in severe cases, gangrene[10].

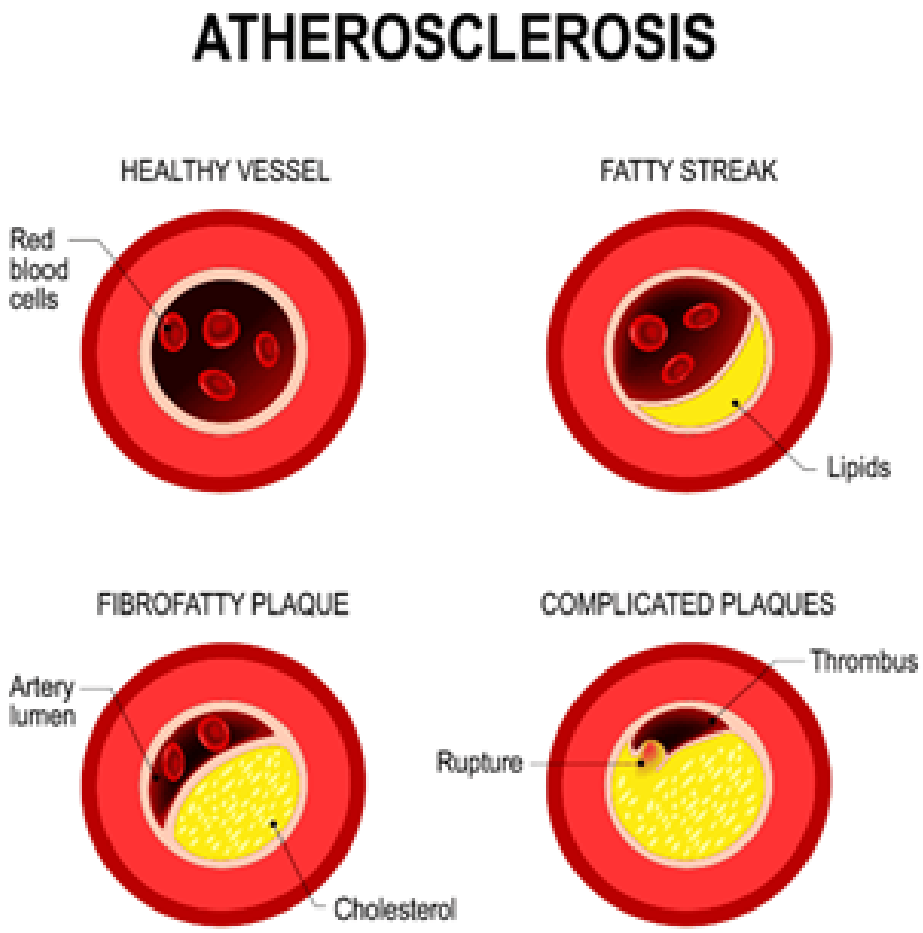

Figure 1.6: *Stage of arteriosclerosis in human vessel.*

1.3.2 Causes and risk factors

Atherosclerosis is a multifactorial disease influenced by several risk factors, which can be categorized as modifiable or non-modifiable. Non-modifiable factors include advanced age, male sex, and genetic predisposition. These elements contribute to an individual's susceptibility to the disease, making early monitoring crucial for high-risk populations[8]. Modifiable risk factors, on the other hand, include smoking, hypercholesterolemia, hypertension, diabetes, obesity, physical inactivity, and a diet rich in saturated fats. These factors play a significant role in disease progression, as they contribute to endothelial dysfunction, lipid accu-

mulation, and increased vascular resistance. Managing these risk factors through lifestyle modifications and medical supervision is a key strategy for preventing and slowing the advancement of the disease[9].

1.4 Treatments for small blood vessel diseases

Diseases affecting small blood vessels pose a significant challenge in modern medicine[6]. The narrowing of vascular diameter, primarily caused by arteriosclerosis and atherosclerosis, can lead to chronic ischemia in tissues and impair the function of vital organs such as the heart, brain, and kidneys[11]. The treatment of these conditions relies on a combination of pharmacological therapies, minimally invasive endovascular techniques, and, in advanced cases, surgical solutions and innovative biotechnological approaches, such as bioengineered vascular prostheses[12].

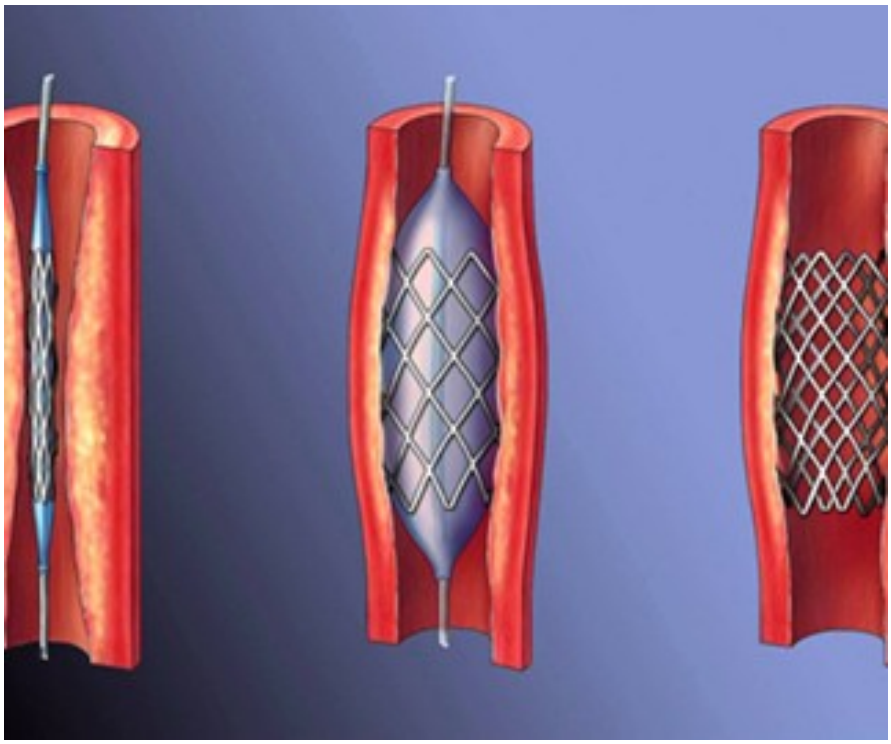

Figure 1.7: *The image illustrates the stages of angioplasty, where a balloon catheter expands a narrowed artery, followed by the deployment of a stent to keep the vessel open and restore blood flow.*

1.4.1 Pharmacological approaches

Pharmacological therapy represents the first-line intervention for the treatment of small blood vessel diseases. The primary goal is to slow disease progression, improve blood flow, and prevent thrombotic events. Several classes of drugs are commonly used to manage these conditions[13]. Statins are widely prescribed to lower LDL cholesterol levels, stabilize atherosclerotic plaques, and reduce the risk of ischemic events. By inhibiting cholesterol synthesis in the liver, statins help prevent further narrowing of the vessels and decrease inflammation within the arterial walls. Antiplatelet agents, such as aspirin and clopidogrel, play a crucial role in preventing the formation of blood clots within damaged vessels. These drugs work by inhibiting platelet aggregation, thereby reducing the risk of thrombosis, which can lead to heart attacks and strokes[8]. Antihypertensive medications, including ACE inhibitors and beta-blockers, are essential for lowering vascular resistance and reducing the pressure load on small blood vessels. By maintaining optimal blood pressure levels, these drugs help prevent excessive strain on the microcirculation, which is particularly important in conditions such as hypertensive nephropathy. Antidiabetic medications are critical for controlling blood glucose levels, as diabetes accelerates the progression of atherosclerosis in small vessels. Poor glycemic control leads to endothelial dysfunction and increased oxidative stress, both of which contribute to vascular damage. Despite the effectiveness of these pharmacological treatments in managing the disease, disease progression may still require more advanced interventional procedures to restore adequate blood flow in severely affected vessels[9].

1.4.2 Endovascular techniques

Minimally invasive endovascular procedures are commonly used to restore blood flow in small blood vessels without the need for open surgery. One of the most widely performed techniques is balloon angioplasty, which involves the insertion of a catheter equipped with a small balloon. Once inflated, the balloon widens the narrowed vessel, improving circulation and reducing the risk of ischemia. This procedure is often combined with the implantation of a stent, a small metallic structure that helps keep the vessel open and prevents restenosis—the re-narrowing of the artery due to plaque buildup or excessive tissue growth. Another innovative procedure is atherectomy, which mechanically removes atherosclerotic plaques

from the inner wall of the vessel, further enhancing perfusion[14]. These interventions are particularly effective in the early and intermediate stages of vascular disease. However, in cases of severe occlusions, they may not be sufficient, requiring more invasive surgical approaches[8].

1.4.3 Surgical treatments

When endovascular techniques fail to restore adequate blood flow, more complex surgical interventions become necessary. One of the most widely used approaches is vascular bypass surgery, which reroutes blood circulation around a blocked or severely narrowed vessel to ensure adequate tissue perfusion[15]. This technique involves the creation of an artificial conduit that allows blood to bypass the occluded segment, restoring normal circulation. The bypass can be performed using autologous grafts, meaning segments of the patient's own veins or arteries, such as the saphenous vein or the internal mammary artery. When autologous vessels are not available or suitable, synthetic grafts made from biocompatible materials, such as polytetrafluoroethylene (PTFE) or Dacron, can be used as an alternative. These synthetic materials provide durability and structural integrity, although their long-term success in small-caliber vessels may be limited due to a higher risk of thrombosis and graft failure[13].

1.4.4 Vascular prostheses and vascular tissue engineering

Vascular tissue engineering has led to the development of bioengineered vascular substitutes designed to enhance the biocompatibility and long-term functionality of prosthetic blood vessels[16]. Small-caliber vascular prostheses must meet specific requirements to minimize thrombotic complications and ensure effective integration with biological tissues[17]. Among the most innovative solutions are polymeric vascular prostheses, such as those made from poly(-ϵ-caprolactone) (PCL)[18]. This material provides an excellent balance between biocompatibility and mechanical resistance, making it a promising option for small-diameter grafts[19]. Another promising approach involves bioabsorbable prostheses, which gradually degrade over time while being replaced by regenerated vascular tissue. This technique reduces long-term complications associated with permanent synthetic materials and promotes natural tissue remodeling[20]. A particularly advanced solution in this field is the development of vascular tissues through

electrospinning[21]. This technique allows the creation of fibrous scaffolds that mimic the native extracellular matrix, thereby facilitating cell proliferation and improving endothelial integration. These properties make electrospun scaffolds a highly effective strategy for promoting functional vascular regeneration in small-diameter vessels[14][22].

Chapter 2

Artificial vascular prostheses

2.1 History and evolution of artificial vascular prostheses

The development of artificial vascular prostheses is the result of a long historical journey that has accompanied the evolution of medicine and surgery. Since ancient times, the cardiovascular system has been the subject of study and experimentation aimed at restoring blood flow in vessels compromised by disease or trauma[23]. While early solutions were rudimentary and often ineffective, scientific and technological progress has led to increasingly advanced techniques. The true revolution occurred in the twentieth century when advancements in knowledge of vascular biomechanics and material biocompatibility enabled the creation of the first synthetic prostheses[14]. Initially, natural tissues and autologous vessels were used, but research soon shifted toward synthetic materials capable of withstanding hemodynamic stresses while ensuring proper integration with the human body. Wars and the need for rapid intervention in patients with vascular injuries accelerated research, leading to the discovery of polymers with properties suitable for clinical use. Modern prostheses are the result of decades of research on materials, design, and strategies for biological integration[24].

Figure 2.1: *A depiction of a surgical operation in a text from the second half of the 16th century.*

2.2 State of the art of artificial vascular prostheses

Artificial vascular prostheses represent a crucial solution for treating vascular diseases that compromise the functionality of arteries and veins. The primary objective of these devices is to restore blood flow in areas where the natural vessel is damaged or obstructed. Depending on their application, vascular prostheses can be classified into large-diameter prostheses (such as those for the aorta) and small-diameter prostheses (such as peripheral artery grafts)[25]. Small-caliber prostheses, in particular, pose greater design challenges due to the higher risk of thrombosis and the need for improved hemodynamic performance[20]. Currently, vascular prostheses are manufactured using a variety of synthetic and biomimetic materials. Among the most commonly used polymers in clinical practice are[26]:

- *Polyethylene terephthalate (PET) – Dacron*

  Widely employed for large-caliber prostheses, this material is durable and biostable, available in different fabric configurations (woven or knitted) to enhance flexibility and tissue integration.

- *Expanded polytetrafluoroethylene (ePTFE, known as Gore-Tex)*

  Commonly used for medium- and small-caliber prostheses, ePTFE offers

good mechanical resistance and reduced thrombogenicity due to its microporous surface.

- *Polyurethanes and poly(-ϵ-caprolactone) (PCL)*

  these polymers are emerging as more flexible and biocompatible alternatives, with the potential to enhance tissue integration and reduce postoperative complications.

Beyond material selection, current research focuses on improving prosthesis functionality through innovative strategies. Some prostheses are treated with pharmacological agents to reduce thrombus formation, while others are designed with a multilayer structure to mimic the biomechanical properties of natural vessels. The use of bioactive materials represents another promising approach, aiming to promote integration with surrounding tissues and enhance graft endothelialization[17].

Figure 2.2: *Vascular prostheses with different surface characteristics and sizes*

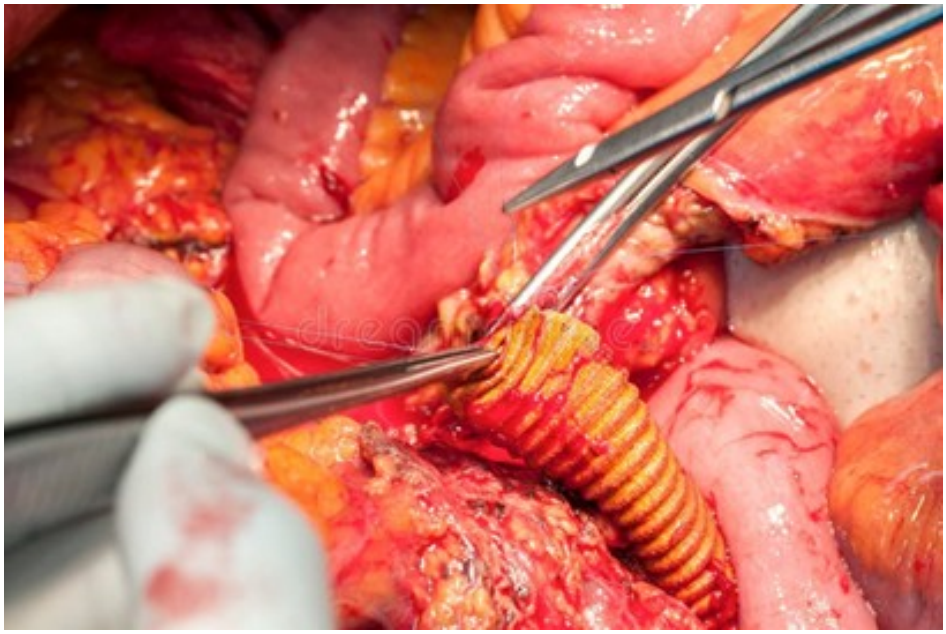

Figure 2.3: *Implantation of a vascular prosthesis in the abdominal region of an adult male.*

2.3 Small-caliber prostheses

Small-caliber vascular prostheses (<5 mm in diameter) represent one of the most complex challenges in biomedical engineering and vascular surgery. Unlike large-diameter prostheses, which achieve high long-term success rates, small-caliber prostheses are subject to a higher incidence of thrombosis and early occlusion, significantly limiting their clinical efficacy. The primary difficulties encountered with small-caliber prostheses arise from physiological phenomena related to the reduced lumen size. In these vessels, blood flow velocity is lower than in larger ones, increasing the contact time between blood and the prosthetic wall. This factor enhances platelet activation and thrombus formation, leading to rapid graft occlusion[6]. Another major issue is the lack of endothelialization on the prosthesis's internal surface. In natural vessels, the endothelium plays a crucial role in regulating platelet aggregation and vascular permeability. However, the synthetic surfaces of conventional prostheses, made of materials such as polyethylene terephthalate (Dacron) or expanded polytetrafluoroethylene (ePTFE), do not adequately support endothelial cell adhesion and proliferation, limiting their biological integration[27]. To overcome these limitations, research has focused on

several innovative strategies. One of the most promising approaches is endothelial cell coating, which involves seeding the prosthesis's internal surfaces with autologous endothelial cells or biomolecules that promote their proliferation. This technique aims to mimic the natural physiological environment and reduce the prosthesis's thrombogenicity[28]. Another solution is the development of more elastic and compliant materials, capable of better adapting to the biomechanics of the replaced vessel. Advanced polymers such as modified polyurethane and biodegradable copolymers offer greater hemodynamic compatibility than traditional materials, improving the transmission of pulsatile energy and reducing the risk of material degradation due to concentrated stress[29]. The introduction of microporous structures is another significant research area. Prostheses with calibrated micropores can facilitate the integration of surrounding tissues and promote cellular colonization, thereby enhancing biocompatibility and reducing occlusion risk. Finally, controlled drug release directly from the prosthesis surface is an innovative approach to improving graft patency. Coatings impregnated with anticoagulants such as heparin or growth factors that stimulate endothelialization have shown promising results in experimental models. Tissue engineering techniques are opening new possibilities in the development of fully biological prostheses. The idea is to use biodegradable scaffolds that serve as temporary frameworks for the growth of new vascular cells. These scaffolds can be colonized by endothelial cells and fibroblasts, ultimately leading to a structure that remodels over time into a fully functional vessel integrated within the patient's body[30]. One of the most advanced approaches in this field involves the use of dynamic bioreactors to culture cells under conditions that mimic physiological blood flow, enhancing tissue maturation before implantation. These technologies could lead to the creation of fully autologous vascular prostheses, minimizing the risk of rejection and thrombosis[21].

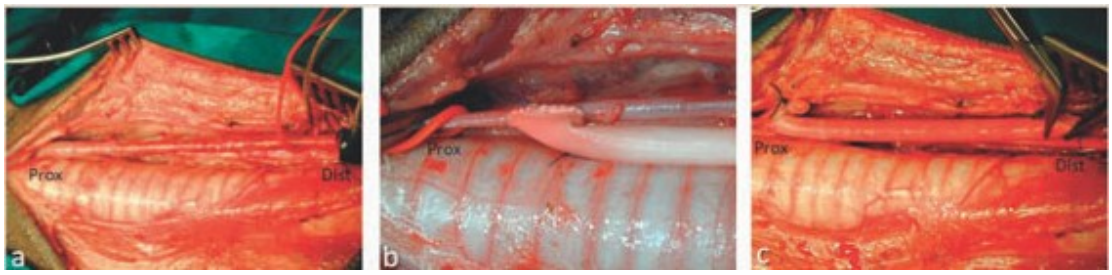

Figure 2.4: *Implantation of a small-caliber vascular prosthesis in the coronary artery..*

2.4 Use of prostheses in vascular surgery

Artificial vascular prostheses play a crucial role in modern vascular surgery, providing solutions for conditions where natural vessels are unsuitable or unavailable. These prosthetic grafts are employed in arterial bypass procedures, replacement of aneurysmal segments, and the creation of vascular access for hemodialysis. In bypass surgeries, they restore blood flow when native arteries cannot be used for revascularization. In aneurysm repair, they replace the dilated portion of an artery to prevent rupture. For patients with chronic renal failure, they ensure long-term vascular access for hemodialysis, facilitating life-sustaining treatments[19]. Despite their widespread use, artificial vascular prostheses face significant challenges that limit their long-term success. One of the most pressing issues is thrombogenicity, particularly in small-diameter grafts. The absence of a functional endothelial layer increases the risk of thrombus formation, leading to occlusion and graft failure. Ensuring that synthetic materials do not promote excessive clotting remains a major hurdle in vascular graft design. Various surface modifications, such as the incorporation of antithrombotic agents, are being explored to mitigate this risk and enhance blood compatibility. Another critical limitation is the mechanical mismatch between synthetic grafts and natural blood vessels. Many prostheses lack the elasticity and compliance of biological arteries, leading to abnormal blood flow patterns and mechanical stress at the graft-vessel junction. This mismatch can contribute to intimal hyperplasia, a pathological thickening of the vessel wall that can compromise long-term graft patency. Furthermore, while some prostheses are designed for permanent implantation, others are intended to degrade over time and be replaced by new tissue. However, controlling the degra-

dation rate is complex—too rapid a breakdown can result in vascular instability, while slow degradation may hinder proper tissue remodeling and integration[31]. Material degradation and chronic inflammatory responses also pose significant concerns. Synthetic prostheses must withstand prolonged exposure to physiological forces without structural failure. Over time, certain materials may degrade or lose mechanical integrity, leading to complications such as aneurysm formation or graft rupture. Additionally, some prosthetic materials may trigger chronic inflammatory reactions, further complicating long-term outcomes. The ultimate goal is to develop prostheses that integrate seamlessly with biological tissues, promoting healing while maintaining structural stability. To address these challenges, ongoing research is exploring innovative strategies to enhance vascular graft performance. Advances in 3D bioprinting allow for the fabrication of patient-specific grafts with tailored architecture and porosity, improving both mechanical properties and cellular integration. Smart biomaterials, capable of responding dynamically to physiological conditions, are being developed to improve graft adaptability and longevity. Additionally, hybrid prostheses combining synthetic polymers with biological components such as collagen, elastin, and chitosan are being investigated to enhance biocompatibility and encourage endothelialization[22]. As these technologies advance, the future of vascular prostheses is moving toward solutions that closely mimic the structural and functional characteristics of native blood vessels. The integration of bioactive materials and tissue engineering techniques holds the potential to create grafts that not only restore blood flow effectively but also support long-term vascular regeneration. These innovations will ultimately lead to safer and more durable prosthetic solutions, improving outcomes for patients with complex vascular conditions. By addressing the current limitations of artificial vascular prostheses, ongoing research is paving the way for next-generation grafts that combine durability, biocompatibility, and regenerative potential. The continuous refinement of materials and fabrication techniques promises to expand treatment options and enhance the success rates of vascular surgeries in the years to come[32].

2.5 Engineering and software in the study and development of vascular prostheses

The development of vascular prostheses has undergone significant evolution in recent decades due to biomedical engineering and the integration of advanced software tools. These technologies enable the simulation, analysis, and optimization of prostheses before their fabrication, improving mechanical performance, biocompatibility, and interaction with biological tissues[33]. Through the use of computational fluid dynamics (CFD), finite element modeling (FEM), and 3D printing, it is possible to study prosthesis behavior under realistic conditions, reducing the risk of clinical failures and increasing the effectiveness of surgical treatments. Future research should focus on implementing even more advanced biomaterials and integrating artificial intelligence to further optimize the personalization and effectiveness of vascular prostheses[34].

- *Computational fluid dynamics (CFD) for blood flow analysis*

  One of the fundamental aspects of vascular prosthesis design is evaluating blood flow within the implanted device. CFD simulations allow the analysis of critical parameters such as velocity distribution, pressure, wall shear stress (WSS), and stagnation zones that may promote thrombus formation. Recent studies have shown that optimized prosthesis geometries, based on CFD models, can reduce the risk of occlusion and improve long-term patency.

- *Finite element analysis (FEM) for structural evaluation)*

  Finite element analysis (FEM) enables the assessment of the mechanical response of prostheses under various physiological loads. This methodology allows for the prediction of material deformation, wear over time, and behavior under dynamic stresses, such as those generated by the heartbeat. FEM modeling is essential for optimizing prosthesis compliance characteristics, reducing the risk of complications such as intimal hyperplasia and the formation of false aneurysms.

- *Personalized design and 3D printing*

  With the advent of 3D printing, it is now possible to create custom-made prostheses for each patient. This approach, combined with medical imaging

techniques such as magnetic resonance imaging (MRI) and computed tomography (CT), enables the creation of highly accurate digital models of an individual's vascular system. These models are then used to produce personalized scaffolds that faithfully replicate the biomechanical characteristics of native vessels. The use of innovative 3D-printable biomaterials, such as thermoplastic polyurethane (TPU) and polycaprolactone (PCL), has facilitated the development of prostheses with improved elasticity and tissue compatibility. Studies have shown that prostheses fabricated using this technology exhibit higher endothelialization rates, enhancing their long-term functionality.

One of the most important challenges for vascular prostheses is their integration with surrounding tissues. The use of advanced tissue modeling algorithms allows for the prediction of the biological response to the prosthesis and the optimization of surfaces to reduce the risk of thrombosis. Recent studies have demonstrated that bioactive materials and controlled-release coatings with anticoagulant drugs can significantly mitigate the inflammatory response post-implantation. Prosthesis compliance, defined as the ability of the material to adapt to pressure variations during the cardiac cycle, is a crucial parameter for their effectiveness. FEM and CFD simulations have identified optimal structures to minimize compliance mismatch between the prosthesis and the native vessel. Compliance loss has been identified as a significant issue in polyethylene terephthalate (PET) prostheses, with a reduction of up to 60% observed within 24 hours of use[35].

2.6 Biodegradable prostheses

An important area of research in vascular prostheses focuses on biodegradable materials, which are designed to gradually degrade and be replaced by the patient's natural tissue. Unlike permanent synthetic grafts, these prostheses aim to provide temporary structural support while facilitating the regeneration of functional blood vessels. Among the most commonly used biodegradable polymers, polyglycolic acid (PGA) and polylactic acid (PLA) have attracted significant attention due to their controlled degradation rates. These materials are often combined with stem cells or bioactive compounds to stimulate endothelialization and improve integration within the vascular system[35]. In recent years, researchers have explored hybrid prostheses, which integrate synthetic polymers with biolog-

ical components such as collagen, elastin, and chitosan. This approach seeks to enhance biocompatibility and promote the formation of a natural endothelial layer on the graft's inner surface, reducing the risk of thrombosis and improving long-term function. The development of these bioengineered vascular grafts represents a promising step towards personalized medicine, where prostheses can be tailored to the specific physiological needs of each patient. Despite these advancements, the clinical application of biodegradable vascular grafts remains challenging, as the rate of material degradation should be carefully balanced with the pace of new tissue formation. Achieving this balance is essential to prevent complications such as premature graft failure or aneurysm formation, highlighting the need for further research in this field [15].

2.7 Bioprostheses

Bioprostheses represent a class of medical devices designed to replace or support damaged tissues and organs in the human body. Compared to traditional prostheses, bioprostheses are made from biological or biomimetic materials to enhance integration with host tissues and minimize adverse reactions. The use of biomaterials in regenerative medicine has undergone significant evolution throughout history. Early attempts at tissue replacement using natural materials date back to the early 20th century, with the use of chemically treated animal tissues to prevent immune rejection. During the 1960s and 1970s, the development of biocompatible polymers and tissue decellularization techniques led to the creation of modern bioprostheses, particularly in the cardiovascular and orthopedic fields. Bioprostheses can be manufactured using biological tissues of animal or human origin, subjected to decellularization and chemical stabilization processes to ensure durability and biocompatibility[21]. The most commonly used materials include:

- *Xenogeneic tissues*

  Derived from animal species, such as bovine or porcine cardiac valves

- *Allogeneic tissues*

  Obtained from human donors, such as homologous vascular grafts.

- *Synthetic biopolymers*

Engineered to mimic the biomechanical properties of natural tissues and support cellular regeneration.

Bioprostheses are medical devices specifically designed to replace or support compromised biological structures, ensuring the restoration of their physiological functions. Their versatility allows them to be used in various medical fields, as they can interact safely and effectively with biological tissues. One of the primary applications of bioprostheses is in cardiovascular surgery, where they are employed for the replacement of heart valves, blood vessels, and other essential anatomical structures required for proper circulatory function. In this context, bioprostheses must ensure high biocompatibility, mechanical resistance, and optimal interaction with biological fluids, minimizing the risk of thrombosis or inflammatory reactions. The continuous evolution of biomaterials and manufacturing techniques allows for the development of highly customized devices, capable of adapting perfectly to individual patient needs and significantly improving clinical outcomes[32]. Bioprostheses therefore represent a crucial technological advancement in modern medicine, providing innovative solutions for the treatment of a wide range of conditions and contributing to improved patient quality of life. The use of bioprostheses in vascular systems has become increasingly common for the treatment of diseases that impair blood vessel functionality. Various clinical conditions, such as arterial stenosis, aneurysms, thrombosis, and post-traumatic vascular damage, can lead to altered blood flow and loss of vascular function. In these cases, the replacement or support through bioprostheses is essential to restore circulation and prevent severe complications. One of the primary reasons for using vascular bioprostheses is the inability of damaged blood vessels to regenerate effectively on their own. While the human body has intrinsic tissue repair mechanisms, such as endothelial proliferation and vascular remodeling, extensive damage or specific pathological conditions may render the healing process insufficient. Additionally, even when autologous bypass surgery is an option, the availability of suitable donor vessels may be limited, or harvesting procedures may lead to additional complications. Bioprostheses therefore provide an effective alternative, restoring the hemodynamic function of blood vessels by ensuring adequate blood flow dynamics. Their design takes into account critical factors such as biocompatibility, mechanical resistance, and long-term durability, which are essential for reducing the risk of thrombosis, inflammation, or rejection. Furthermore, depending on the materials used and the manufacturing techniques applied, bioprostheses can

be tailored to different vascular districts, ranging from large arteries to smaller capillaries[23]. Another crucial aspect is the role of bioprostheses in cardiovascular surgery and minimally invasive therapies. The use of synthetic or biological grafts has significantly expanded treatment options, improving clinical outcomes and reducing post-operative recovery times. For patients suffering from chronic vascular diseases, such as advanced atherosclerosis, bioprosthetic implantation may be the only viable option to prevent ischemic events and organ damage. The future of vascular bioprostheses is continuously evolving thanks to advancements in bioengineering and biomaterials. Emerging technologies, such as 3D printing and electrospinning, are enabling the development of increasingly personalized prostheses, capable of replicating the biomechanical properties of natural vessels and integrating more efficiently with surrounding tissues. Additionally, research in biomaterials is leading to the creation of bioactive and resorbable scaffolds, which promote endothelial regeneration and enhance implant longevity. The integration of vascular bioprostheses into medical practice represents an essential therapeutic strategy for numerous cardiovascular diseases. Their ongoing evolution not only improves patient survival rates but also enhances quality of life, opening new frontiers in regenerative medicine and advanced vascular surgery[35].

The production of vascular bioprostheses follows advanced processes that ensure the quality of the implanted material. Some of the most widely used methods include[15]:

- *Decellularization*

  Removal of cells from the tissue to minimize immune response.

- *Chemical crosslinking*

  Stabilization of structural proteins to increase mechanical resistance and durability.

- *Tissue engineering*

  Development of three-dimensional structures with mechanical properties similar to natural vessels, including scaffolds and biomimetic matrices to guide tissue regeneration.

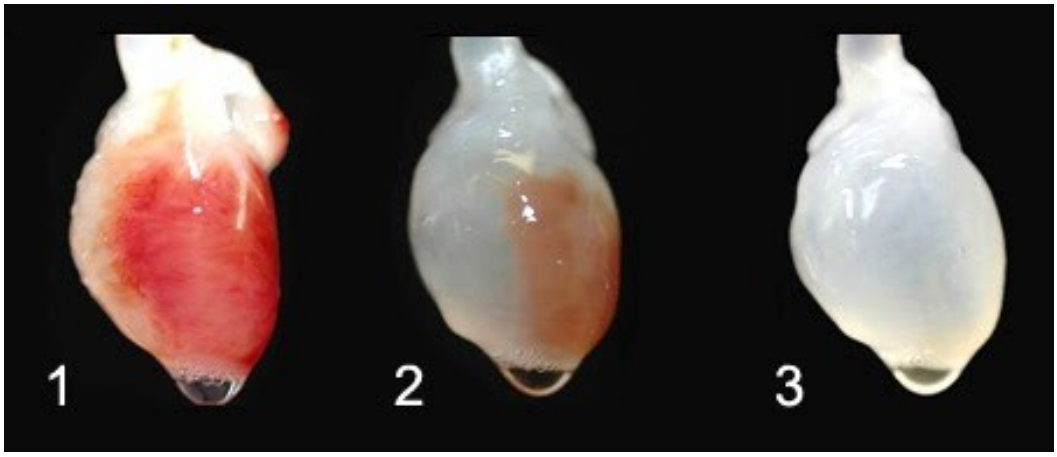

Figure 2.5: *Different stage of decellularization.*

The integration of bioprostheses into the circulatory system is a complex challenge that requires careful design to ensure compatibility with biological tissues and proper hemodynamic function. Once implanted, the bioprosthesis must interact with blood flow without altering its dynamics, preventing complications such as turbulence, intimal hyperplasia, or thrombosis. To achieve this, the prosthetic material must possess biomechanical properties similar to natural vascular tissues, adapting to vascular compliance without creating structural discontinuities or localized rigidity that could compromise blood flow[23]. One of the most critical aspects is the interface between the bioprosthesis and the vascular endothelium. To reduce the risk of thrombogenesis and inflammatory response, it is essential that the internal surface of the bioprosthesis promotes endothelial cell adhesion and proliferation. In this regard, bioactive coatings and functionalized scaffolds are often employed, incorporating biomolecules that enhance cellular recolonization and improve tissue integration. Another key factor is the mechanical response of the bioprosthesis to hemodynamic loads. The artificial vessel must withstand mechanical stresses imposed by arterial pressure and pulsatile blood flow, preventing wear and structural deformation over time. The design of optimized geometries and the use of high-performance materials improve the mechanical resistance and durability of the implant, reducing the need for long-term surgical revisions. Successful integration of bioprostheses into the circulatory system requires a multidisciplinary approach, combining expertise in materials engineering, fluid dynamics, and cellular biology to develop increasingly efficient and safe implants for patients[35].

Chapter 3

Polymers

3.1 Introduction to polymers

Polymers represent a class of materials of extraordinary importance, utilized across a wide range of sectors, from industrial production to biomedical applications. They are composed of macromolecules formed by repeating units, known as monomers, which are covalently bonded together. Their chemical structure and the arrangement of polymer chains confer specific properties that determine their physical, chemical, and mechanical behavio[36]r. Scientific interest in polymers has grown exponentially over the past decades, as their characteristics can be modified to meet specific needs. In the biomedical field, polymers are particularly studied for their ability to interact with biological tissues without inducing adverse reactions, enabling the development of implantable devices, scaffolds for tissue engineering, and controlled drug delivery systems[37]. The evolution of polymers has followed a developmental trajectory that has transitioned from rudimentary natural materials to synthetic polymers with precisely engineered properties, designed to optimize performance in biomedical applications. Advances in polymer chemistry and materials science have made it possible to create polymeric structures with well-defined mechanical, rheological, and biological characteristics, making these materials increasingly suitable for interaction with the human body. Their versatility makes them suitable not only for implantable devices but also for applications in tissue engineering, regenerative medicine, and controlled drug release, significantly impacting medical research and advanced therapies[38].

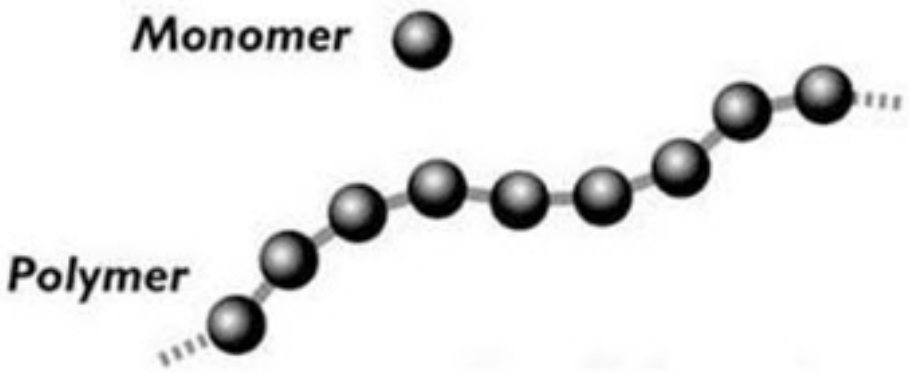

Figure 3.1: *Chemical structure of a generic polymer.*

3.2 Synthetic polymers

Synthetic polymers are artificially created materials produced through chemical polymerization processes. Their development has revolutionized numerous industries, as their properties can be modified to adapt to specific application contexts[39]. One of the key aspects of synthetic polymer design is the ability to control their morphology, which can range from amorphous to semicrystalline structures, thus influencing their flexibility, mechanical strength, and thermal stability. Additionally, their chemical reactivity can be modulated through functionalization processes, allowing for optimized interactions with biological materials. In the biomedical sector, some of the most commonly used synthetic polymers include[37]:

- *Polyethylene (PE)*

  Known for its high chemical resistance and biocompatibility, it is widely used in joint prostheses and implant materials.

- *Polymethyl methacrylate (PMMA)*

  Primarily utilized in dentistry and ophthalmology, it is valued for its transparency and mechanical stability.

- *Polytetrafluoroethylene (PTFE)*

  Commonly known as Teflon, it is employed in vascular prostheses due to its chemical inertness and reduced plasma protein adhesion.

- *Polyurethanes*

  Elastomeric materials with excellent mechanical strength, often used for cardiovascular devices and implant coatings.

Recent research is focusing on the use of functionalized polymers, which are chemically modified materials designed to enhance cell adhesion and biological compatibility. Functionalized polymers can incorporate specific chemical groups that promote cell interaction, enable controlled drug release, or facilitate programmed degradation over time. Among the most widely used functionalization techniques are graft polymerization, plasma treatment, and biomolecule modification. These innovative polymers are being employed in the design of advanced medical devices, such as artificial heart valves, resorbable sutures, and antibacterial coatings for orthopedic implants. Furthermore, the use of functionalized polymers has enabled the development of smart biomaterials, capable of responding to external stimuli such as temperature, pH, and mechanical stress, opening new frontiers in biomedical applications[40].

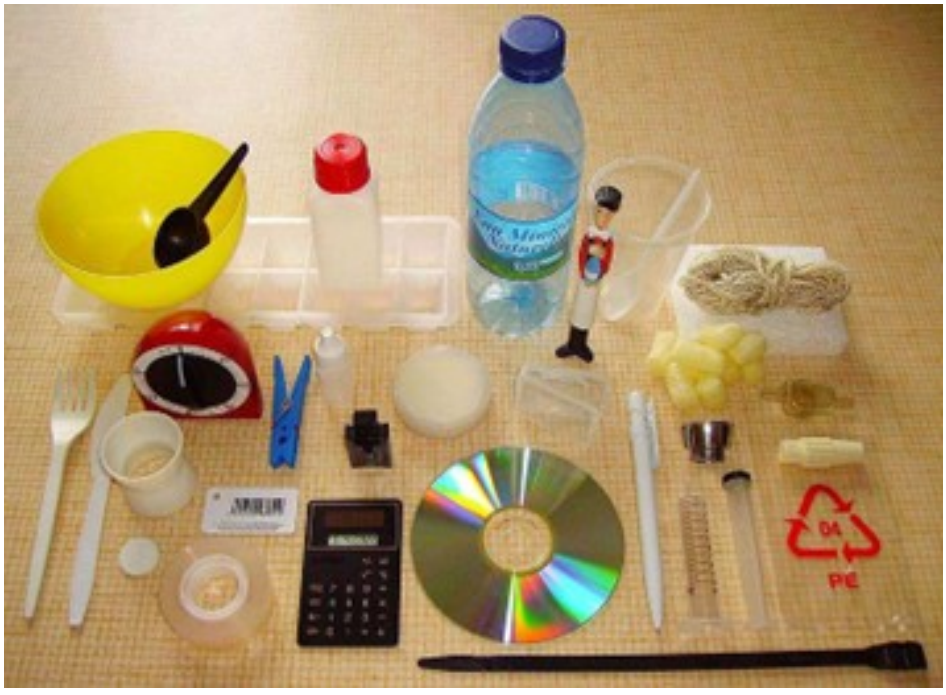

Figure 3.2: *Everyday objects made from polymers: a variety of plastic-based items used in daily life, including packaging, utensils, electronics, and medical tools.*

Figure 3.3: *Colorful polymer granules sorted by hue, ready for industrial processing and manufacturing applications.*

3.3 Natural polymers

Natural polymers have emerged as promising biomaterials for vascular prostheses due to their superior biocompatibility, biodegradability, and ability to support cell integration. These materials, often derived from animal or plant sources, closely mimic the extracellular matrix (ECM), making them ideal candidates for vascular grafts. Among the most widely studied natural polymers are collagen, elastin, chitosan, silk fibroin, and bacterial cellulose, each offering unique advantages in vascular tissue engineering. Collagen, the most abundant structural protein in mammalian connective tissues, plays a critical role in providing mechanical strength and cell adhesion sites for endothelial cells. Due to its bioactivity, collagen has been extensively used in the fabrication of vascular grafts, either alone or in combination with synthetic polymers to enhance durability. However, collagen-only grafts tend to lack mechanical stability and degrade rapidly, making crosslinking techniques or hybrid scaffolds essential for improving their long-term performance[41]. Elastin is another key component of natural blood vessels, contributing to their elasticity and compliance. It plays a crucial role in regulating vascular smooth muscle cell (SMC) activity and preventing excessive cell proliferation, which can lead to intimal hyperplasia. Despite its functional advantages,

elastin is challenging to isolate in large quantities, and its integration into vascular prostheses often requires recombinant production or blending with other biopolymers. Chitosan, a polysaccharide derived from chitin, has gained attention in vascular applications due to its antimicrobial properties, biodegradability, and hemocompatibility. It has been explored as a coating for vascular grafts to improve endothelialization while reducing thrombogenicity. However, its mechanical properties are insufficient for use as a standalone vascular graft material, necessitating reinforcement with synthetic polymers such as poly(caprolactone) (PCL). Silk fibroin, extracted from silk, has demonstrated excellent biocompatibility and mechanical strength, making it a viable material for small-diameter vascular grafts. Unlike synthetic polymers such as expanded polytetrafluoroethylene (ePTFE), silk fibroin has been shown to promote faster endothelialization and superior cell attachment, reducing the risk of thrombosis. Research has focused on electrospinning silk fibroin into nanofibrous scaffolds, mimicking the architecture of natural blood vessels[42]. Another promising natural polymer is bacterial cellulose (BC), a polysaccharide produced by Komagataeibacter xylinus. BC offers high mechanical strength, water retention, and excellent biocompatibility, making it a strong candidate for vascular grafts. Unlike other natural polymers, BC is resistant to enzymatic degradation in the human body, ensuring longer graft patency. Preclinical studies have demonstrated the long-term stability of BC-based vascular grafts, with evidence of sustained patency and endothelialization in animal models. Despite these advantages, the clinical application of natural polymer-based vascular prostheses remains limited by their mechanical weakness, inconsistent degradation rates, and complex fabrication requirements. Hybrid approaches that combine natural polymers with synthetic materials or bioprinting techniques are being actively explored to overcome these challenges. Future research aims to enhance the mechanical and biological properties of natural polymer grafts, paving the way for their broader clinical adoption in vascular surgery[43].

Figure 3.4: *In this figure, we can see different sources of natural polymers: in the top left, the latex from the rubber tree; in the top right, crustacean shells rich in chitin; in the bottom left, starch extracted from corn and potatoes; in the bottom right, silkworm cocoons.*

3.4 Biocompatible polymers and biopolymers

The concept of a biocompatible polymer refers to a material that, once introduced into the body, does not trigger adverse reactions such as inflammation, rejection, or toxicity. Biocompatibility depends on the chemical structure of the polymer, its interaction with proteins and biological cells, and its ability to resist enzymatic or hydrolytic degradation. Biopolymers, on the other hand, represent a subclass of polymers that are derived from natural sources or produced through biological processes. Many biopolymers are also biodegradable, making them ideal for applications that require gradual dissolution over time, such as scaffolds for tissue engineering and controlled drug delivery devices [41].

3.5 Biopolymers

3.5.1 Introduction to biopolymers

Biopolymers represent a class of materials of growing interest in scientific research and industry due to their natural origin, biocompatibility, and biodegradability. Unlike synthetic polymers, biopolymers are produced by living organisms or derived from renewable raw materials. Their chemical structure varies depending on their source and the biological function for which they have been evolutionarily selected, making them highly versatile in multiple applications. In recent years, biopolymers have seen widespread use in biomedical applications due to their ability to integrate with human tissues without triggering adverse immune responses. They are employed in the production of implantable devices, scaffolds for tissue engineering, controlled drug delivery systems, and advanced biomaterials[44].

3.5.2 Types of biopolymers

Biopolymers can be classified into different categories based on their chemical structure and biological function. Among the most extensively studied biopolymers are polysaccharides, polypeptides, and natural polyesters. Polysaccharides are biopolymers composed of complex sugars and are particularly valued for their hydrophilicity and ability to form protective films. Due to their high biocompatibility, they are widely used in biomedical applications, such as controlled drug release systems and advanced wound dressing materials[21]. Polypeptides and proteins, on the other hand, are biopolymers made up of long chains of amino acids and play a fundamental role in the structure of biological tissues. They are extensively utilized in the production of scaffolds for regenerative medicine, as they support cell adhesion and proliferation. Collagen and fibrin are examples of polypeptides with well-established clinical applications. Another important class is natural polyesters, which are biosynthesized by microorganisms or extracted from plants. These polymers are distinguished by their excellent biodegradability and bioabsorption properties, making them particularly suitable for the production of resorbable implantable devices. A significant example is polyhydroxyalkanoates (PHA), a family of biodegradable polyesters produced by bacteria, widely studied for advanced biomedical applications. Finally, biopolymers can be com-

bined to form hybrid materials, known as composite biopolymers. These materials integrate multiple types of biopolymers to enhance their mechanical and biological properties, providing innovative solutions for the fabrication of implants, sutures, and tissue engineering materials[45].

3.5.3 Properties of biopolymers

The properties of biopolymers depend on their chemical composition and molecular structure. Some of the key characteristics that determine their applicability include[41]:

- *Biodegradability*

  The ability to degrade into non-toxic byproducts through enzymatic or hydrolytic processes.

- *Biocompatibility*

  Favorable interaction with biological tissues without inducing inflammatory or immune reactions.

- *Structural flexibility*

  The capability to be processed into various forms, such as films, hydrogels, fibers, and three-dimensional scaffolds.

- *Customizable mechanical properties*

  The ability to modulate elasticity, strength, and hardness to meet specific requirements in medical and industrial applications.

3.5.4 Applications of biopolymers

Thanks to their unique properties, biopolymers have a wide range of applications in the biomedical field. Biopolymers are extensively used in the fabrication of three-dimensional scaffolds that support cell growth and tissue regeneration. Materials such as collagen, poly(lactic acid) (PLA), and poly(caprolactone) (PCL) are employed to construct biomimetic structures capable of replicating the architecture of biological tissues. The integration of biopolymers into drug delivery systems enables the controlled and targeted release of pharmaceuticals, enhancing therapeutic efficacy while minimizing side effects. Polymeric nanoparticles and

biopolymer-based hydrogels are currently among the most promising technologies for the treatment of chronic diseases and cancer. Biopolymers are also utilized in the manufacturing of vascular prostheses, artificial heart valves, biodegradable sutures, and orthopedic implants. Their ability to integrate with host tissues and biodegrade over time makes them ideal for long-term implantable applications. Additionally, advanced wound dressings made from biopolymers, such as bioactive bandages and antimicrobial hydrogels, accelerate wound healing and reduce the risk of infections. Materials like chitosan and alginate are widely used in the treatment of burns and chronic ulcers, offering significant advancements in regenerative medicine and wound care[46].

3.5.5 Future developments

The evolution of biopolymer research is focusing on new strategies to enhance their properties and expand their biomedical applications[40][42][31]. Some of the major emerging trends include:

- *Smart biopolymers*

  Materials capable of responding to environmental stimuli such as temperature, pH, and biological signals, enabling personalized drug release or controlled tissue regeneration.

- *Biofabrication technologies*

  The use of 3D printing and bioprinting facilitates the creation of complex structures with optimized mechanical and biological properties.

- *Nanotechnology applied to biopolymers*

  The integration of nanoparticles into biopolymer matrices enhances their mechanical strength, bioactivity, and interaction with cells.

- *Sustainability and production from renewable sources*

  Research is increasingly focused on developing biopolymers derived from agricultural waste and renewable resources, thereby reducing environmental impact and production costs.

Chapter 4

Poly(caprolactone) and poly(glycerol sebacate)

4.1 Poly(caprolactone) (PCL)

4.1.1 Chemical structure and properties

Poly(caprolactone) (PCL) is a semicrystalline aliphatic polymer belonging to the polyester family. It is well known for its biocompatibility, biodegradability, and workability, which make it a strategic material for numerous applications in the biomedical field. Due to its easy processing and controlled degradation, PCL is widely used in tissue regeneration, drug delivery systems, and vascular prostheses fabrication. PCL is a linear polyester derived from the polymerization of ϵ-caprolactone, a six-membered lactone. Its repeating unit is represented by the following structure[36]:

$$-[O-(CH_2)_5-CO]_n-$$

Each monomeric unit consists of six carbon atoms, an ester group (-COO-), and an oxygen atom.

Figure 4.1: *Chemical structure of PCL.*

This configuration provides PCL with the following properties:

- *Good flexibility and mechanical strength*

  Due to the presence of long aliphatic chains that allow high conformational mobility.

- *Hydrophobicity*

  Resulting from the absence of free polar groups along the polymer backbone, which limits water absorption and affects cell adhesion.

- *Moderate crystallinity (45-50%)*

  Contributing to its structural resistance and influencing its degradation rate.

- *Hydrophobicity*

From a thermal perspective, PCL has a relatively low melting temperature (60 °C), making it easily processable through melting, molding, and advanced techniques such as electrospinning (which will be discussed later).

The biodegradation of PCL primarily occurs through hydrolysis of ester bonds in aqueous environments. This process is catalyzed by environmental factors such as temperature, pH, and enzyme activity, making PCL particularly suitable for long-term applications, such as tissue engineering scaffolds. Compared to other biodegradable polyesters, such as poly(lactic acid) (PLA) and poly(glycolic acid)

(PGA), PCL degrades at a significantly slower rate, with a resorption time ranging from months to several years. This makes it ideal for implants requiring gradual replacement by native biological tissue. Biologically, PCL exhibits high biocompatibility, meaning it does not elicit significant immune responses upon implantation. However, its poor hydrophilicity may limit cell adhesion, a drawback often addressed through chemical modifications or blending with more hydrophilic polymers[47].

Figure 4.2: *Granules of PCL.*

4.1.2 Applications

PCL is extensively documented for its biomedical applications, particularly in tissue engineering and regenerative medicine. One of its most relevant applications is in the field of vascular prostheses, where it is employed in the fabrication of scaffolds for blood vessel regeneration. In this context, it is often combined with more elastic polymers such as poly(glycerol sebacate) (PGS) to enhance its mechanical performance and reduce thrombogenicity. In the area of bone and cartilage regeneration, PCL is used to develop scaffolds capable of supporting the repair of these tissues. Its slow degradation rate ensures that the material provides structural support while allowing gradual cellular infiltration and tissue remodeling[48]. Another significant application of PCL is in the development of controlled drug delivery systems. Its biodegradable nature enables the encapsu-

lation and progressive release of pharmaceuticals, making it suitable for treating chronic diseases or enabling localized administration of bioactive agents. Beyond these applications, PCL is also utilized in the production of resorbable sutures and orthopedic devices. Biodegradable sutures made from PCL gradually dissolve in the body, reducing the need for additional surgical procedures for removal. Similarly, orthopedic plates and fixation devices composed of PCL provide temporary mechanical support before being naturally resorbed over time. Despite its advantages, PCL has some inherent limitations, particularly its low hydrophilicity and relatively low elastic modulus. These factors can restrict its applications in areas requiring high mechanical performance and optimal cell adhesion. To overcome these limitations, PCL is often blended with other polymers to enhance its mechanical and biological properties. The combination with poly(lactic-co-glycolic acid) (PLGA) accelerates degradation and improves cellular support, while the incorporation of poly(glycerol sebacate) (PGS) increases elasticity and reduces thrombosis risk in vascular applications. Furthermore, PCL is frequently combined with natural polymers such as collagen and gelatin, which significantly enhance cell adhesion and promote neotissue formation. Electrospinning is an extremely effective technique for obtaining micrometric PCL fibers used in scaffold production for tissue engineering and other biomedical applications. The choice of solvents plays a fundamental role in ensuring a stable process and accurate control of fiber morphology. Chloroform is the most commonly used solvent for PCL electrospinning, but in recent years, alternative mixtures such as formic acid and acetic acid have been explored, allowing the production of nanometric fibers[49].

4.2 Poly(glycerol sebacate) (PGS)

4.2.1 Chemical structure and properties

Polyglycerol sebacate (PGS) is a biodegradable polymer belonging to the class of synthetic polyesters. It was developed to provide an elastomeric, biocompatible material with mechanical properties suitable for various applications in regenerative medicine and tissue engineering. PGS is distinguished by its elasticity, high hydrophilicity, and ability to support cell adhesion, making it particularly suitable for the fabrication of scaffolds for soft tissue and vascular regeneration. Its controlled degradability further enhances its suitability for applications requiring

the gradual replacement of the material with newly formed tissue[50]. PGS is a crosslinked polyester synthesized via the polycondensation of glycerol and sebacic acid. Glycerol, a tri-hydroxylated molecule, contributes to the formation of a three-dimensional network, while sebacic acid, a long-chain aliphatic diacid, imparts flexibility and elasticity to the polymer. The synthesis of PGS occurs through a two-step process. Initially, a prepolymer is formed via controlled-temperature reaction under vacuum conditions. This is followed by a thermal curing step that induces crosslinking, thereby defining the final properties of the material. The degree of crosslinking directly influences the polymer's stiffness and degradation rate, allowing its characteristics to be tailored to specific applications. Physically, PGS exhibits a rubbery and flexible nature, with tensile strength that varies according to its crosslinking density. Its inherent hydrophilicity facilitates interaction with biological fluids, making it an excellent candidate for vascular and cardiac applications [51]. A key feature of PGS is its controlled biodegradability, which can be adjusted by modifying its polymeric network density and the environmental conditions in which it is placed. The degradation mechanism primarily involves hydrolysis of ester bonds, leading to the breakdown of the material into biocompatible byproducts such as glycerol and sebacic acid, both of which are metabolized by the body without toxic effects. Compared to other biodegradable polyesters, PGS degrades more rapidly than polycaprolactone (PCL) but more slowly than poly(lactic-co-glycolic acid) (PLGA). This intermediate degradation rate makes it highly adaptable for applications requiring specific resorption times[52].

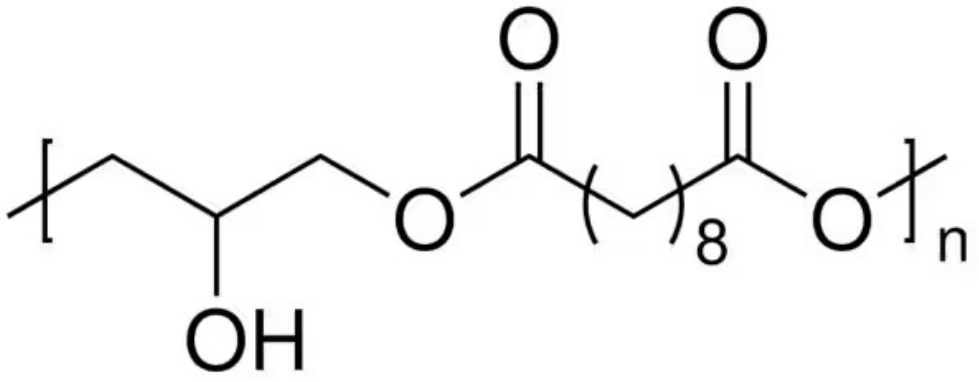

Figure 4.3: *Chemical structure of PGS.*

4.2.2 Applications

From a biological perspective, PGS has demonstrated high biocompatibility, eliciting minimal inflammatory response while supporting cell adhesion and proliferation. In vitro and in vivo studies have shown strong attachment of endothelial cells, fibroblasts, and myocytes on PGS surfaces, suggesting its suitability for soft tissue and vascular regeneration. Due to its elasticity, biocompatibility, and controlled degradability, PGS has been extensively explored for various applications in tissue engineering. One of its most promising uses is in the fabrication of scaffolds for blood vessel regeneration. PGS, owing to its high elasticity, can replicate the biomechanical properties of arteries and provide a favorable environment for endothelial cell growth. Unlike other synthetic materials that may exhibit thrombogenicity or excessive stiffness, PGS offers mechanical properties closer to those of native tissue, making it a superior alternative for vascular grafts. Beyond vascular engineering, PGS has also been successfully employed in cardiac and muscle tissue regeneration, where an elastic and biocompatible material is essential. Additionally, its use extends to cartilage repair and scaffold fabrication for skin and soft tissue regeneration, where its hydrophilic nature facilitates nutrient diffusion and cellular colonization[53]. Another significant area of development for PGS is in controlled drug delivery, where its adjustable degradability allows for the gradual release of therapeutic agents in specific biological environments. This feature makes it particularly suitable for long-term drug delivery systems, useful for chronic therapies or localized treatment of injuries. PGS can be processed into various forms using advanced fabrication techniques. Among these, electrospinning is widely used to produce ultrafine fibers for three-dimensional scaffold fabrication, enabling high porosity and structural biomimicry. Electrospinning of PGS, often combined with other polymers such as PCL, allows for the development of fibrous structures with tunable mechanical properties, enhancing cell interaction and tissue regeneration capabilities. This topic will be discussed in greater detail later, as it represents one of the most promising approaches for biomedical applications of PGS[54].

Chapter 5

Electrospinning

5.1 Overview

Electrospinning is a versatile and efficient technique for the production of polymer fibers with diameters ranging from the micrometer scale down to a few nanometers. The process utilizes electrostatic forces to generate a jet of polymer solution or molten polymer, which is progressively stretched and dried, forming continuous and highly porous fibers[55]. The fundamental principle of electrospinning is based on applying a high-voltage electric field to a polymer solution contained in a syringe with a thin needle. The needle is connected to a high-voltage electrode, while a grounded collector, usually metallic, serves as the surface where the fibers are deposited. When the applied voltage exceeds a critical threshold, electrostatic repulsion forces within the polymer solution overcome the liquid's surface tension, leading to the formation of the so-called Taylor cone. From this cone, a polymer jet emerges, which, due to solvent evaporation and electrostatic forces, thins down to form continuous fibers. As the polymer jet develops, electrostatic forces cause it to oscillate and stretch irregularly. This effect results in the formation of extremely thin fibers, which deposit to create a porous network [14].

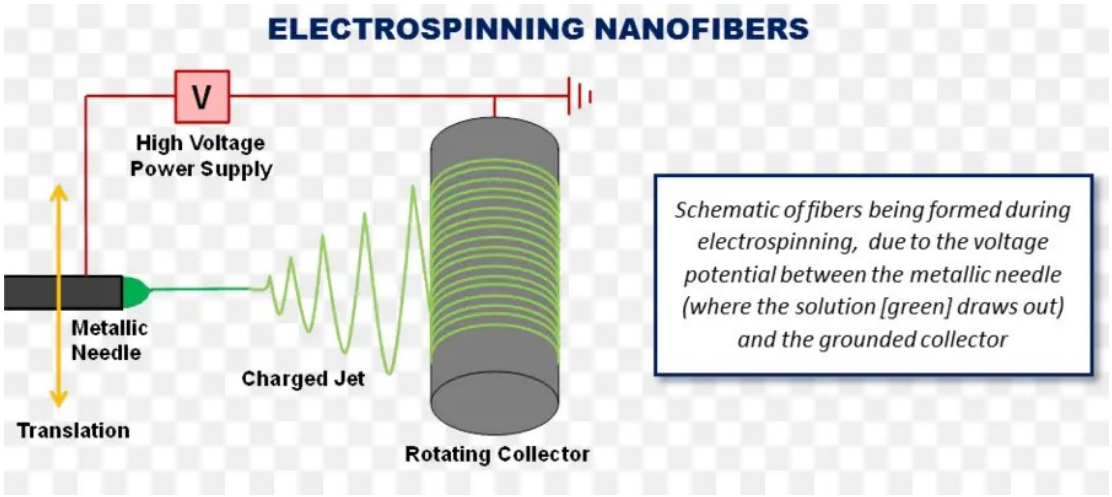

Figure 5.1: *Schematic representation of electrospinning nanofibers. The process involves a high-voltage power supply that creates a potential difference between the metallic needle and the grounded rotating collector, resulting in the formation of charged polymer jets that solidify into nanofibers.*

The success of electrospinning depends on several parameters that influence the morphology and properties of the produced fibers. These parameters include[56]:

- *Polymer solution properties*

  Such as viscosity, electrical conductivity, and surface tension. A viscosity that is too low may lead to droplet formation instead of continuous fibers, while excessive viscosity may hinder jet formation.

- *Electrical parameters*

  Including the applied voltage and the distance between the needle and the collector. A voltage that is too low may be insufficient to overcome the liquid's surface tension, while an excessive voltage may cause uncontrolled material deposition.

- *Environmental conditions*

  Such as humidity and temperature, which influence the solvent evaporation rate and fiber formation.

The type of collector used to gather the fibers directly affects their morphology. Stationary flat collectors lead to the formation of randomly oriented, nonwoven

structures, whereas high-speed rotating collectors promote fiber alignment, generating more ordered structures with superior mechanical properties[57]. Additionally, there are variations of the traditional technique, such as coaxial electrospinning, which enables the production of core-shell fibers, and melt electrospinning, which eliminates the use of toxic solvents by utilizing molten polymer instead of a polymer solution. Thanks to its ability to produce nanofibers with controlled porosity and high surface area, electrospinning is employed in numerous fields, including[58]:

- *Tissue engineering*

  For the fabrication of biomimetic scaffolds that support cell growth.

- *Controlled drug delivery systems*

  Leveraging the capability to encapsulate active ingredients and release them in a controlled manner.

- *Filtration and biosensors*

  Utilizing the high surface area and permeability of nanofibers.

Figure 5.2: *Electrospinning machine.*

Electrospinning, therefore, represents an innovative and highly versatile technology for the production of polymer nanofibers. Its ability to control fiber morphology and properties through process parameter optimization continues to drive new biomedical and industrial applications. Although challenges remain, such as industrial scalability and improved fiber reproducibility, ongoing research in this field is leading to increasingly efficient and widely applicable solutions[59].

5.2 Electrospinning in vascular tissues engineering

5.2.1 Introduction

Electrospinning has emerged as one of the most promising techniques for fabricating biomimetic scaffolds for vascular tissue engineering. Due to its ability to generate nanometer- and micrometer-scale fibers, this technique enables the high-fidelity reproduction of the extracellular matrix (ECM) structure, promoting cell adhesion and proliferation. As discussed in the previous chapter, the process involves applying a high-voltage electric field to a polymer solution, inducing the formation of a jet that solidifies into ultrafine fibers, which are deposited onto a collector to form a three-dimensional porous structure. This configuration allows for the production of scaffolds with highly controllable morphology and optimal parameters for tissue engineering[16]. The primary advantage of electrospinning lies in its ability to create structures that replicate the mechanical and biochemical characteristics of the native ECM. In particular, fibers can be aligned to mimic the anisotropic organization of biological tissues, a crucial aspect of vascular engineering. Recent studies have demonstrated that by adjusting the rotation speed of the mandrel on which the fibers are deposited, a highly aligned arrangement of collagen fibers can be achieved, thereby enhancing interactions with endothelial cells. Despite these advantages, electrospinning still presents some limitations, including poor cell infiltration in thicker tissues due to small pore sizes and the need to optimize the degradation of the polymers used. To overcome these challenges, various strategies are being developed, including combined techniques such as merging electrospinning with melt spinning and incorporating bioactive materials to enhance cell integration[6].

5.2.2 Research and contributions of different study groups

1. Duan et al. (2016) Research Group

Duan et al. developed vascular scaffolds with a core-shell structure using coaxial electrospinning. The fiber core was composed of poly(ϵ-caprolactone) (PCL), chosen for its mechanical stability, while the coating was made of collagen to enhance biocompatibility and promote cell adhesion. The results showed excellent endothelial cell proliferation and good mechanical resistance of the material. However, the degradation of PCL remains relatively slow, which could hinder full integration with native tissue in the long term. The study utilized scanning electron microscopy (SEM) and transmission electron microscopy (TEM) to confirm the core-shell structure of the fibers, while thermogravimetric analysis (TGA) and UV-spectrophotometry were used to assess the scaffold's mechanical and biochemical properties [60].

2. Boland et al. (2004)

Electrospinning of collagen and elastin: Another significant contribution comes from the group of Boland et al., who studied the electrospinning of collagen and elastin for the creation of biomimetic vascular substitutes. Their research demonstrated that the addition of elastin improves the mechanical compliance of the scaffold, making it more similar to that of natural arteries. However, the fibers proved to be fragile in humid environments and required cross-linking treatments to ensure adequate stability. The group employed Fourier-transform infrared spectroscopy (FTIR) and mechanical tensile testing to evaluate the stability and mechanical performance of the scaffolds [26].

3. Chung et al. (2010)

Chung et al. adopted an innovative approach by combining electrospinning and melt spinning to create multilayer structures with adjustable porosity. Their scaffold consisted of macro- and nanometric fibers of poly(L-lactide-co-ϵ-caprolactone) (PLCL), a bioabsorbable elastomeric material. The results highlighted good cell proliferation capacity and mechanical behavior comparable to that of native arteries. However, the combination of two fabrication techniques made the process more complex and less scalable for clinical applications. The study employed scanning electron microscopy (SEM) to analyze fiber morphology and mechanical testing (MTS ReNew Model 1122) to evaluate tensile strength and elongation [61].

4. Fu et al. (2014)

Fu et al. explored the use of hybrid scaffolds composed of gelatin/PCL and collagen/PLCL for applications in vascular tissue engineering. Their research demonstrated that combining natural and synthetic polymers improves both the biocompatibility and mechanical properties of the material. In particular, scaffolds made of collagen/PLCL exhibited greater elasticity compared to gelatin/PCL scaffolds. However, variability in fabrication methods could affect the reproducibility of results. The study utilized X-ray diffraction (XRD) and mechanical tensile testing to analyze the crystalline structure and mechanical properties of the scaffolds [62]. Electrospinning represents an extremely versatile and promising technology for the creation of vascular scaffolds. Studies conducted to date have demonstrated that combining synthetic and natural polymers is essential for obtaining materials with good mechanical properties and adequate biocompatibility. However, some challenges remain to be addressed, including controlling material degradation, optimizing porosity to promote revascularization, and ensuring long-term mechanical stability. Future research should focus on integrating biofunctionalization techniques and validating them in preclinical models to bring these solutions closer to clinical application[5].

Materials and methods

Chapter 6

Blend production

6.1 Polymeric blend

This research employs a polymeric blend of poly(caprolactone) (PCL) and poly(glycerol sebacate) (PGS), a combination of materials that has gained increasing interest in the field of bioengineering. The research group at the Department of Civil, Chemical and Environmental Engineering Department (University of Genoa) and that at IRCCS Policlinico San Martino Hospital have already optimized the electrospinning process for the fabrication of small-caliber vascular prostheses using this polymeric mixture, demonstrating the feasibility of the technology and the potential clinical applicability of the material. Studies conducted so far have shown that the PCL:PGS blend meets the requirements for the development of vascular grafts, complying with industry standards. One of the innovative aspects of this combination is its bioresorbability, which differentiates it from other biopolymeric blends currently under investigation for vascular applications. While several bioengineered materials being studied for vascular bioprostheses share key properties such as elasticity, biocompatibility, and biodegradability, the PCL:PGS blend stands out for its ability to be completely resorbed and replaced by native tissue over time. This characteristic represents a major advantage over other experimental bioprostheses, which, despite being degradable, often exhibit significantly slower degradation rates or lack the controlled resorption necessary for effective tissue regeneration. The ability of a prosthesis to degrade in a controlled manner, synchronizing with tissue remodeling, is a key aspect in regenerative medicine. A resorbable vascular graft could significantly reduce the risks associated with long-term complications, such as chronic inflammation, fibrosis, or late-stage throm-

bosis, which remain critical challenges in the development of bioprostheses. By allowing gradual tissue integration and replacement, the PCL:PGS blend offers a pathway toward functional vascular regeneration, rather than merely providing a passive conduit for blood flow[63]. The use of this polymeric blend is supported by recent research, which has demonstrated the material's favorable performance in terms of biological compatibility and mechanical properties. Although preliminary results are promising, the PCL:PGS blend remains in an experimental phase and is not yet commercially available. Ongoing research aims to further consolidate knowledge on this biomaterial and assess its actual applicability in clinical settings. As previously discussed, the prosthesis production process has already been optimized, which demonstrated the feasibility of using a PCL:PGS blend for manufacturing small-caliber vascular grafts. However, the focus of this study is not the production of the prosthesis itself but rather the analysis of the internal conditions within the vessel made from this specific material, with particular attention to thermal, fluid dynamics, and structural aspects[64]. The primary objective is to understand the fluid behavior within the prosthesis, investigating potential temperature variations, thermal gradients, and interactions with blood flow to assess the impact of the blend on vascular functionality. These data are crucial for improving the design and performance of the device, ensuring that the material properties not only meet mechanical and biological requirements but are also optimized in terms of fluid dynamics and heat transfer. This study, therefore, contributes to an advanced optimization framework, aiming to further validate the blend's behavior not only in terms of fabrication but also in terms of biomechanical and thermal response under realistic operating conditions.

6.2 Sample production

The sample production follows a standardized laboratory protocol to ensure the reproducibility and consistency of the process. For the preparation of the polymer blend, two distinct solutions are prepared: one based on poly(caprolactone) (PCL) and one based on poly(glycerol sebacate) (PGS), both at a 20% (w/v) concentration. As solvents, a mixture of chloroform and ethanol in a 9:1 (v/v) is used. This combination was selected as it allows for complete polymer solubilization, while preserving their chemical-physical properties and optimizing the solution viscosity for the subsequent electrospinning process. For each polymer,

5.0 mL of solution is prepared by dissolving 1.0 g of polymer in 4.5 mL of chloroform and 0.5 mL of ethanol. The solutions are left under magnetic stirring for 24 hours to ensure homogeneous polymer chain dispersion and complete dissolution of the material[65]. After the stirring period, the two solutions are combined in a 1:1 (v/v). Specifically, PGS is added to the PCL solution, as the latter exhibits significantly higher viscosity. This approach facilitates better miscibility between the two components and prevents the formation of non-homogeneous aggregates. The mixture is then subjected to an additional magnetic stirring phase for approximately 3 hours, after which a uniform polymer solution is obtained, suitable for further processing.

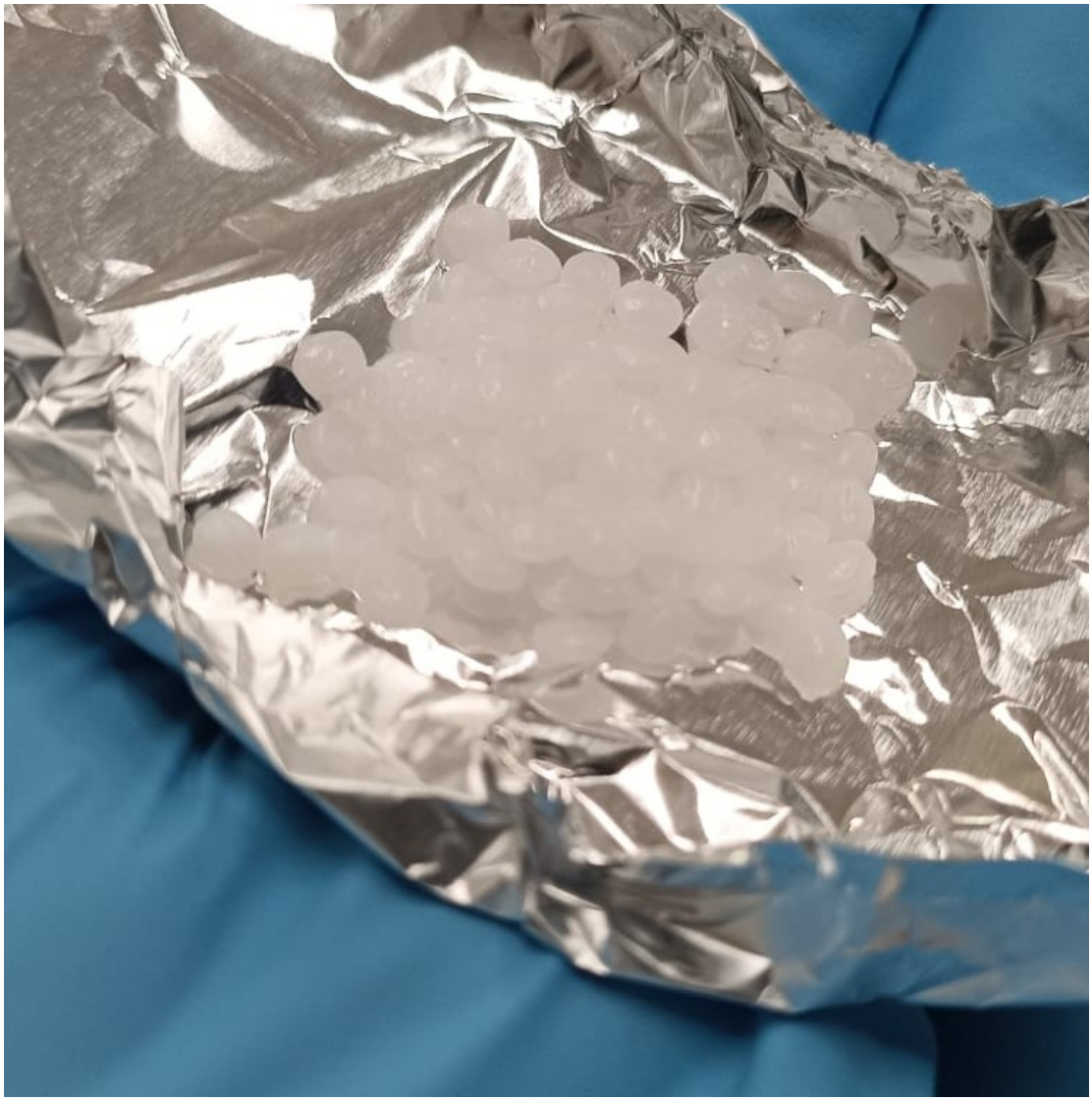

Figure 6.1: *PCL used for sample production.*

Figure 6.2: *PGS used for sample production.*

6.3 Electrospinning and study objectives

Once the polymeric mixture is obtained, it is loaded into the electrospinning machine, allowing for the fabrication of a fibrous structure intended for the production of a vascular bioprosthesis. Electrospinning is a fundamental technique for developing three-dimensional scaffolds with optimized morphological and mechanical properties for tissue engineering applications.

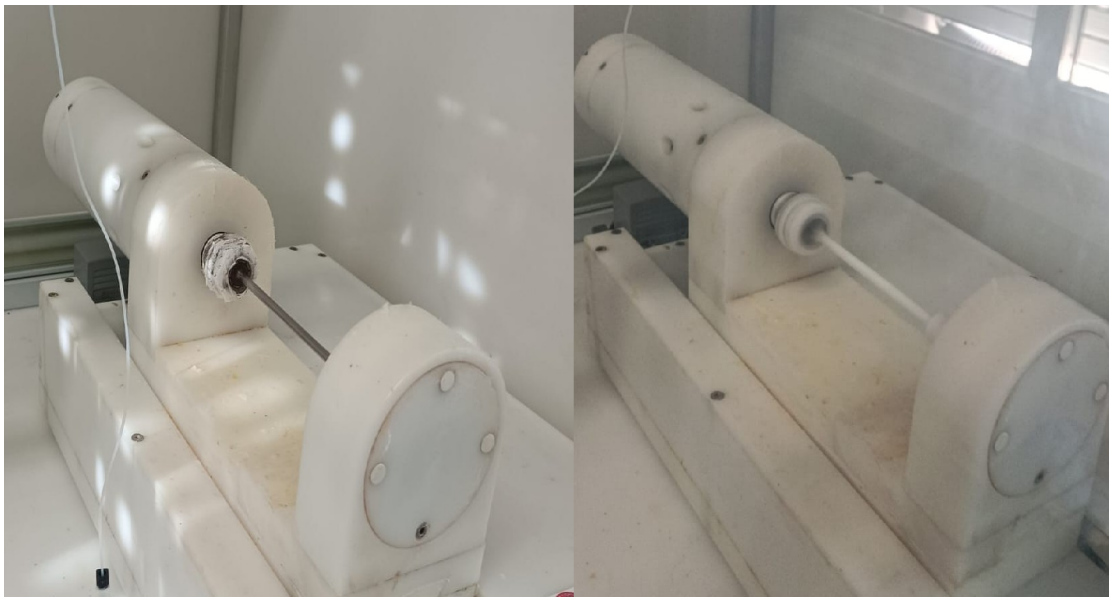

Figure 6.3: *Electrospinning machine used for sample production. On the left, the machine is idle before production. On the right, the machine is in operation, halfway through the sample production process.*

The production of scaffolds through electrospinning is a highly parameter-dependent process, as the correct configuration directly influences the morphology, structure, and mechanical properties of the fibers obtained. In this study, the sample was produced using a set of optimized parameters to ensure the formation of a small-caliber vascular bioprosthesis, with a diameter suitable for vascular applications[63].

1. Generator Voltage: 17 kV

The applied voltage during the electrospinning process is a critical parameter, as

it determines the formation of the polymer jet and the subsequent fiber deposition onto the collector surface. In this case, the voltage was set at 17 kV, an appropriate value to ensure the correct formation of the Taylor cone, which is the point where the polymer is accelerated and transformed into fibers under the influence of the electric field. A voltage that is too low may prevent jet formation, while an excessively high voltage may lead to process instability and an uneven fiber distribution.

2. Collector Translation Limits: 21 mm (left) and 115 mm (right)

The movement of the collection system, represented in this case by the rotating collector, is regulated by two translation limits: 21 mm for the left limit and 115 mm for the right limit. This motion determines the deposition area and directly affects the uniformity of the scaffold. A controlled translation mechanism prevents excessive fiber accumulation in specific areas and ensures a homogeneous distribution of material across the collector surface.

3. Translation Speed: 600 mm/min

The translation speed of the deposition system was set at 600 mm/min, a value chosen to maintain a balanced fiber distribution on the collector surface. A speed that is too slow could lead to excessive fiber density in certain regions, whereas an excessively high speed could disrupt fiber continuity and introduce structural defects.

4. Collector Diameter: 5 mm

One of the key aspects of this study is the investigation of small-caliber vascular scaffolds, where the diameter of the collection collector plays a fundamental role. In this case, a 5 mm diameter was chosen, which allows for the fabrication of a device suitable for the replacement of small-diameter blood vessels. This value falls within the physiological range of peripheral or coronary arteries. The selection of this parameter is therefore strategic for designing a functional and biomechanically adequate bioprosthesis.

5. Generator Current: 3 mA

The current supplied by the generator was set at 3 mA, ensuring a stable electric flow throughout the electrospinning process. The current level influences the stability of the polymer jet and fiber formation, preventing undesirable effects

such as droplet formation (electrospraying) or jet breakage.

6. Collector Rotation Speed: 500 rpm

The rotation speed of the collector influences fiber morphology and alignment within the scaffold. In this study, the collector was set to rotate at 500 revolutions per minute (rpm), an optimal speed for obtaining well-aligned and uniformly distributed fibers. A higher rotation speed promotes the formation of oriented fibers along the collector axis, improving the mechanical resistance of the material in the direction of blood flow[64].

The optimization of electrospinning parameters is essential to obtain vascular scaffolds with suitable biomechanical and morphological characteristics. The selected values in this study were chosen based on previous experimental experience and are considered ideal for fabricating small-caliber vascular bioprostheses. Among the analyzed parameters, the 5 mm collector diameter is of particular interest, as it corresponds to the dimensions of the small-diameter blood vessels studied in this thesis. This selection enables the development of devices applicable to real vascular scenarios, particularly for peripheral or coronary artery replacement[48]. This study is part of a broader framework aimed at optimizing the electrospinning process, with the objective of obtaining bioprostheses with high mechanical performance and functional properties, capable of replicating the characteristics of native blood vessels and ensuring seamless integration with surrounding biological tissue.

Figure 6.4: *The 5 mm vessel fabricated in this study according to the aforementioned parameters.*

6.4 Criteria for the selection of vessels and their parameters for numerical modeling

The selection of arteries in this study was conducted with the aim of representing a wide range of vascular conditions in terms of diameter, anatomical position, and function. Four arteries were chosen: the coronary, femoral, carotid, and radial arteries. In order to cover both small-caliber vessels, which are more clinically critical and still under investigation, and larger-caliber vessels, which are useful for broader comparisons in fluid dynamics. The selection was guided by the intention to analyze arteries from different anatomical districts, including both the upper limbs (radial artery) and lower limbs (femoral artery), as well as a central region represented by the carotid and coronary arteries. This diversity allows for the exploration of fluid dynamic scenarios characterized by distinct physiological conditions, variations in pressure and flow, and differences in interactions with the vascular wall. The selected arteries have diameters of 2.5, 3.5, 5, and 7 mm, as shown in Table 6.1, enabling the study of both small and large vessels to assess the applicability of models across all types of prostheses used in vascular surgery. Indeed, for small-caliber vessels, as previously analyzed, research is still ongoing, making it essential to optimize solutions for the design of bioprostheses. Conversely, in large-caliber vessels, fluid dynamic interactions can provide valuable insights for validating computational models on more stable structures that are already well-established in the medical field.

Each artery exhibits specific hemodynamic characteristics influenced by parameters such as age, sex, weight, pathological conditions, physical activity status, and numerous other factors. Moreover, the literature indicates that blood flow varies significantly among individuals, and available data represent average values obtained from large population studies. Since this thesis does not focus on a specific patient category, intermediate parameters were considered to ensure adaptable results. The analysis of these arteries allows for the evaluation of fluid dynamic behavior under different conditions, with the aim of developing simulation tools that can assist surgeons in personalizing interventions. The objective is not to examine a single clinical scenario or conduct an accurate numerical analysis for a medical study, but rather to establish a methodological framework for adapting models to specific cases, thereby enabling surgeons to conduct targeted studies based on their individual needs. The investigation of vessels with different char-

acteristics facilitates the identification of key parameters for the design of vascular bioprostheses, improving the understanding of hemodynamic conditions and potential clinical implications. The adopted approach lays the groundwork for future optimizations, aiming to make numerical simulations increasingly precise tools for surgical practice. Although this study aims to analyze and establish the foundation for optimizing the PCL:PGS blend, its potential also lies in the ability to optimize other bioprostheses by appropriately modifying the computational model based on the chemical-physical parameters of the specific bioprosthesis under consideration.

The 1 mm thickness of the bioprosthesis wall, as reported in Table 6.1, was determined experimentally. Unlike other parameters for which consolidated data can be found in the literature, there are currently no known experimental values for a vascular prosthesis made of poly(caprolactone) (PCL) and poly(glycerol sebacate) (PGS). This lack of data is due to the fact that the PCL:PGS blend has never been studied before, and its characterization is being carried out for the first time through the present thesis work. The innovative nature of this material necessitated a direct experimental approach to determine the prosthetic wall thickness, providing a realistic parameter for numerical simulations. To this end, several vascular bioprostheses were fabricated through electrospinning, with a diameter of 5 mm, corresponding to the only dimension available in the university's laboratory facilities. The thickness of the obtained prostheses was subsequently measured using a caliper to derive a representative average value. In addition to serving as a reference for the numerical model, this operation allowed for the practical verification of the feasibility of producing the bioprosthesis with such a thickness. The experimental validation of the thickness was particularly significant for two reasons. First, it confirmed that the electrospinning process could generate structures free of significant discontinuities, meaning no defects or voids within the fibrous matrix. The presence of structural defects would have compromised both the effectiveness of the prosthesis and its reproducibility. Second, the thickness needed to be sufficiently small to ensure adequate elasticity of the device. Excessive thickness could have rendered the structure too rigid, limiting its ability to adapt to the mechanical stresses typical of the vascular environment. It is important to emphasize that the 1 mm value does not represent a fixed standard, but rather an average value obtained from the measurements conducted. The experimental variability was not considered in the numerical simulations, as

this study does not aim to establish a definitive thickness for the prosthesis but to provide a reference useful for modeling. Consequently, the standard deviation or a specific margin of error was not taken into account, as these factors do not critically impact the objectives of the computational analysis. Looking ahead, once the feasibility of implanting bioprostheses made from the PCL:PGS blend has been verified, it will be up to manufacturers to optimize the constructive parameters according to specific clinical needs. The final determination of the prosthesis thickness for medical applications will depend on several factors, including the patient's physiological conditions and the characteristics of the vascular district in which it will be implanted. Therefore, this study provides a methodological basis for future optimizations, without constraining the design of bioprostheses to an absolute thickness value.

	Diameter *[mm]*	**Blood Flow** *[mL/min]*	**Thickness** *[mm]*
Femoral	7[66]	350[67]	1
Carotid	5[68]	500[69]	1
Coronary	3.5[70]	150[71]	1
Radial	2.5[72]	6.7[72]	1

Table 6.1: *The table presents a summary of the diameter, blood flow, and thickness of the four different arteries: femoral, carotid, coronary, and radial. The first column specifies the arterial type, while the second column provides the diameter of each artery in millimeters (mm). The third column reports the blood flow measured in milliliters per minute (mL/min). The final column presents the thickness of the arterial wall. This table provides a structured overview of key vascular parameters that are essential for fluid dynamics analysis and computational modeling in vascular research.*

The parameters reported in Table 6.2 are additional parameters employed in the simulations. Unlike others that may vary depending on vascular geometry or the location of arteries within the human body, these parameters are intrinsic to the materials and fluids considered. This characteristic grants them a universal value within the context of numerical simulations, making them applicable in fu-

ture studies regardless of the specific anatomical configuration. In other words, they do not depend on the selection of the analyzed arteries or their location in different body districts but rather on the physical and chemical properties of the constituent materials and fluids under examination. Such independence is a key aspect, as it allows the simulation results to be extended to different scenarios without requiring a redefinition of these parameters based on the vascular structure analyzed. The choice to adopt realistic and non-averaged parameters, detached from the specificity of the considered arteries, represents a strategic approach to ensuring greater flexibility and reproducibility in future scientific and engineering applications.

PARAMETER	**SYMBOL**	**VALUE**	**UNIT**
Dynamic viscosity of blood[73]	ν	$\mathbf{3.5}\times10^{-3}$	Pa·s
Specific heat capacity of blood[74]	c_p	3.65	J/(kg·K)
Molecular weight of blood[75]	MW	64.5	kDa
Density of blood[76]	ρ	1060	kg/m^3
Thermal conductivity of blood[77]	k	0.5	W/(m·K)
Thermal conductivity of real vessel[77]	k	0.5	W/(m·K)
Thermal conductivity of blend[78]	k	0.05	W/(m·K)
Temperature of blood[1]	Tb	311	K
Temperature of human body[1]	Thb	309.5	K

Table 6.2: *Summary of the main physical properties of blood and the materials used in this study. The table includes dynamic viscosity, specific heat capacity, molecular weight, density, and thermal conductivity for both blood and the studied vascular materials. These parameters are fundamental for computational modeling and numerical simulations.*

Chapter 7

Governing equations

Modeling of conjugate forced convection using effective boundary conditions

7.1 Navier-Stokes equations

The Navier-Stokes equations are fundamental in fluid dynamics as they describe the behavior of real fluids by considering the forces acting on them. In the field of bioengineering combined with fluid dynamics, these equations are crucial for modeling and analyzing blood flow within vascular bioprostheses. Blood can be considered an incompressible and viscous fluid, whose motion is governed by the Navier-Stokes equations. The correct application of these equations allows for precise prediction of blood flow behavior, providing essential information for the design and optimization of vascular bioprostheses. The objective of this chapter is to provide an overview of the Navier-Stokes equations, emphasizing their application in blood flow modeling and their significance in the design and evaluation of bioprostheses[34]. Laminar flow is a condition in which a fluid moves in parallel layers without turbulence. In the human circulatory system, blood generally flows in a laminar regime within blood vessels, particularly in medium and large arteries and veins. The characteristics of laminar flow are:

- *Reynolds Number*

  The flow regime (laminar or turbulent) is determined by the Reynolds number (Re), a dimensionless parameter that evaluates the ratio between inertial and viscous forces in a fluid. In the context of blood flow, an Re value lower than 2000 indicates a laminar flow.

- *Velocity Profile*

  In laminar flow, blood velocity is highest at the center of the vessel and gradually decreases towards the vessel walls, creating a parabolic velocity profile across the vessel's cross-section.

Understanding laminar flow is crucial in the design of medical devices, such as stents and vascular prostheses, to ensure that blood flow remains smooth and to minimize turbulence, which could lead to complications. In Computational Fluid Dynamics (CFD), assuming a laminar flow regime simplifies mathematical models, reducing computational time and resources required for simulations.

7.2 Problem definition and homogenization procedure

The hydrodynamic and thermal interactions occurring within a fluid flowing through a channel, subjected to an external force in the $\hat{x}$ direction, are analyzed in this study, as depicted in Figure 7.1(a). This problem is addressed in the context of conjugate heat transfer (CHT), where the interplay between thermal conduction within the stationary walls and forced convection in the fluid phase is examined numerically. To describe the system, the governing equations for mass, momentum, and energy conservation are formulated under the assumptions of steady-state, incompressible, and Newtonian flow conditions. These equations, expressed in dimensional form, define the behavior of the system at any given point $(\hat{x}_1, \hat{x}_2, \hat{x}_3) = (\hat{x}, \hat{y}, \hat{z})$ within the fluid domain (β). The mathematical formulation governing this problem is presented below:

$$\frac{\partial \hat{u}_i}{\partial \hat{x}_i} = 0, \tag{7.1}$$

$$\rho\, \hat{u}_j \frac{\partial \hat{u}_i}{\partial \hat{x}_j} = -\frac{\partial \hat{P}}{\partial \hat{x}_i} + \mu\, \frac{\partial^2 \hat{u}_i}{\partial \hat{x}_j^2}, \tag{7.2}$$

$$\hat{u}_j \frac{\partial \hat{T}}{\partial \hat{x}_j} = \left(\frac{k_f}{\rho c_p}\right) \frac{\partial^2 \hat{T}}{\partial \hat{x}_j^2}, \tag{7.3}$$

Here, $\hat{\mathbf{u}}$ represents the velocity vector, while $\hat{P}$ and $\hat{T}$ denote the pressure and temperature, respectively. The physical properties of the fluid, including density

(ρ), dynamic viscosity (μ), thermal conductivity (k_f), and specific heat capacity (c_p), are assumed to be constant, meaning that their variations with temperature along and across the channel are neglected. For the solid bounding layers (σ), the thermal field is governed by steady-state conduction, which is described by Laplace's equation. This equation characterizes the spatial distribution of temperature $\hat{\mathcal{T}}$ within the solid domain, ensuring a proper formulation of the heat transfer problem:

$$\frac{\partial^2 \hat{\mathcal{T}}}{\partial \hat{x}_j^2} = 0. \tag{7.4}$$

A uniformly prescribed temperature $\hat{\mathcal{T}}_C$ is applied at the outer surfaces ($\mathcal{I}_C$) of the bounding plates. Specifically, this condition is imposed at $\hat{x}_2 = -e$ for the lower boundary and at $\hat{x}_2 = H + e'$ for the upper boundary. The side surfaces of the plates, which are perpendicular to $\hat{x}_1 = \hat{x}$ and correspond to the channel inlet and outlet (denoted as $\mathcal{I}_{ad}$), are considered adiabatic, meaning that no heat transfer occurs through these boundaries. At the solid-fluid interfaces ($\mathcal{I}_{\sigma\beta}$), both temperature continuity and heat flux conservation must be satisfied. These conditions ensure a consistent heat transfer mechanism across the fluid-solid domain. The complete set of boundary conditions governing the system is mathematically expressed as follows:

$$\begin{cases} \hat{\mathcal{T}} = \hat{\mathcal{T}}_C & \text{at } \mathcal{I}_C, \\ \dfrac{\partial \hat{\mathcal{T}}}{\partial \hat{x}_1} = 0 & \text{at } \mathcal{I}_{ad}, \\ \hat{T} = \hat{\mathcal{T}}, \ \dfrac{\partial \hat{T}}{\partial \hat{n}} = \kappa \dfrac{\partial \hat{\mathcal{T}}}{\partial \hat{n}} & \text{at } \mathcal{I}_{\sigma\beta}, \end{cases} \tag{7.5}$$

Here, $\kappa = \dfrac{k_s}{k_f}$ represents the solid-to-fluid thermal conductivity ratio, while $\hat{n}$ denotes the dimensional distance measured along the direction normal to $\mathcal{I}_{\sigma\beta}$ at any given point. Additionally, the fluid enters the channel with a uniform velocity $\hat{u}_1 \big| \hat{x}_1 = 0 = \hat{u}inlet$ and a uniform temperature $\hat{T} \big| \hat{x}_1 = 0 = \hat{T}inlet$. At the solid-fluid interface ($\mathcal{I}_{\sigma\beta}$), a no-slip velocity condition is imposed, ensuring that the fluid adheres to the bounding surfaces. At the channel outlet, the static pressure is set to zero, serving as a reference condition. Furthermore, all flow and thermal fields are periodic in the spanwise direction, denoted as $\hat{x}_3 = \hat{z}$.

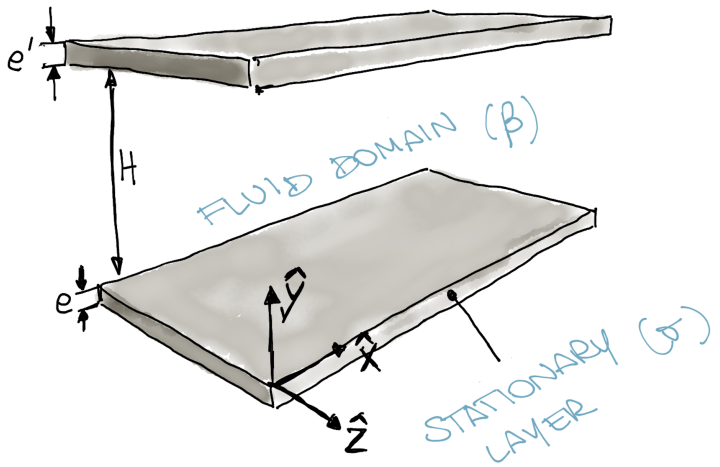

Figure 7.1: Sketch of the problem under consideration. The plane interfaces delimited by $\hat{y} = 0$ and $\hat{y} = H$ constitute the *virtual boundaries* where effective conditions are to be enforced.

7.2.1 The homogenization-based upscaling

The previously described analysis provides a detailed resolution of both the fluid and solid domains, capturing the complete thermal and hydrodynamic interactions. However, when the focus shifts towards the macroscale behavior of the channel flow, a computationally efficient approach is preferable. In such cases, an upscaling strategy can be employed to replicate the effects of wall roughness by introducing effective velocity and temperature boundary conditions at fictitious plane interfaces positioned near the actual physical boundaries. In this work, a multiscale homogenization approach is adopted, closely following the methodology previously derived, validated, and refined in [79, 80, 81]. The main difference is that, while the original studies focused on natural convection, the present analysis considers forced convection, meaning that buoyancy effects are not included in the formulation. In the limiting case of a channel flow confined by a smooth wall with a finite thickness e and a finite thermal conductivity k_s, it is possible to derive analytical solutions for the temperature boundary conditions, expressed as follows:

$$T\Big|_{\hat{n}=0} \approx \hat{\mathcal{T}}_C + \frac{e}{\kappa} \times \frac{\partial T}{\partial \hat{n}}\Big|_{\hat{n}=0}, \tag{7.6}$$

This formulation implies that the temperature at the inner surface of the wall, $T\big|_{\hat{n}=0}$, deviates from the reference uniform value $\hat{\mathcal{T}}_C$ prescribed at the outer surface. In the previous equation, $\hat{n}$ represents the dimensional distance measured along the direction normal to the solid-fluid interface, where $\hat{n}$ increases as one moves towards the fluid region. More specifically, if the condition is applied at the lower (or alternatively the upper) smooth wall, the gradient $\dfrac{\partial T}{\partial \hat{n}}$ corresponds to $\dfrac{\partial T}{\partial \hat{x_2}}$ for the lower boundary, and to $-\dfrac{\partial T}{\partial \hat{x_2}}$ for the upper boundary, following the coordinate system adopted in Figure 7.1.

Chapter 8

Onshape

8.1 Overview

As can be found on the official website, Onshape is a cloud-based CAD platform that enables 3D modeling, simulation, and data management. Unlike traditional CAD software, Onshape does not require installation on local computers since all operations are performed directly in the browser, allowing for real-time access independent of location. One of Onshape's distinguishing features is the ability to collaborate in real time with other team members. Multiple users can work simultaneously on the same model, making modifications and instantly viewing changes made by others. It is a software that uses parametric modeling within a defined virtual space, allowing users to define dimensions and geometric relationships between different parts of a model, even for the creation of highly complex models. This methodology makes it much easier to modify the design, as it is sufficient to change constraints and basic parameters (such as length, width, angles) to automatically update the entire model while maintaining good control over the model's geometry. The platform supports a wide range of file formats for importing and exporting data, such as STEP, IGES, STL, and DXF, ensuring compatibility with other CAD systems and facilitating collaboration between different platforms. The software supports a range of features, such as direct modeling and editing, and includes advanced capabilities for simulation and rendering. The intuitive interface allows users to quickly learn how to create and modify models, making the software accessible to both beginners and professionals. In this thesis, Onshape was used to design and model vascular bioprostheses, adapting parameters for specific cases based on the requirements of each design[82].

Figure 8.1: *Onshape software logo.*

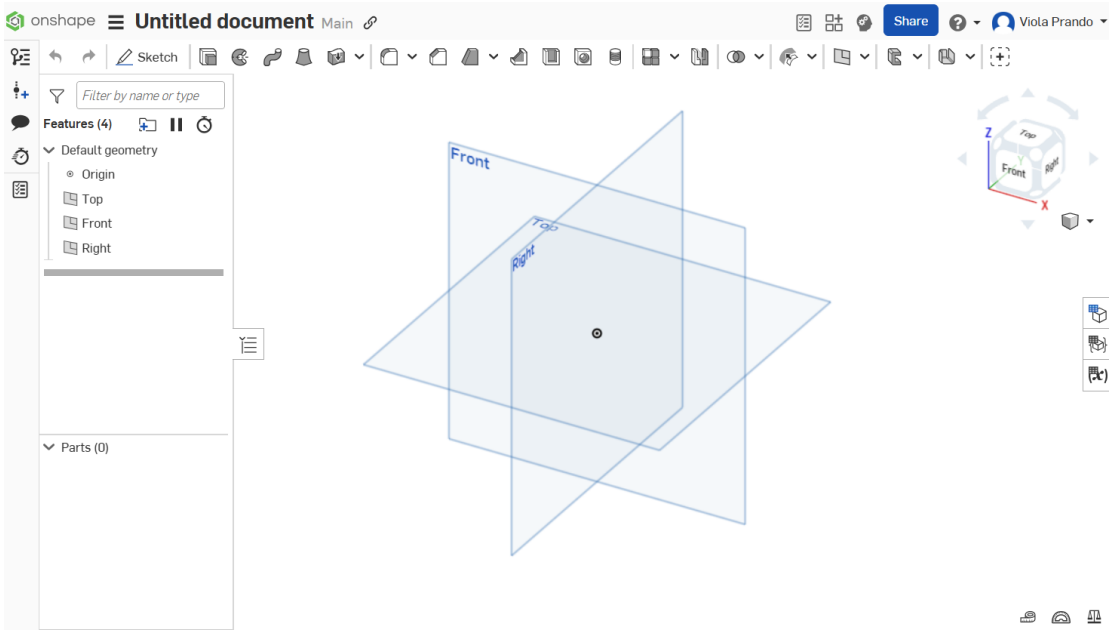

Figure 8.2: *Onshape software interface.*

8.2 Geometry

As discussed in Chapter 6, we examined four different type of arteries: coronary, carotid, femoral, and radial. Accordingly, vascular geometries have been developed to conform to the anatomical structure of the human circulatory system in the analyzed regions. This approach ensures results that closely approximate real

physiological values, providing an accurate foundation for future studies aimed at optimizing bioprostheses based on this specific blend. It is important to note that this study does not consider vessel replacement through bypass procedures, as these involve numerous variables that are not functional to the objectives of this research. Each vessel has been designed with the diameters previously presented, resulting in four different size variations for each geometry. All other parameters remain unchanged. The length values do not correspond to a specific vessel; instead, an extended terminal section has been employed to facilitate convergence in numerical calculations within the software. The geometries considered in this study are:

- *Linear vessel*

  The blood vessel shown in Figure 8.3 can exist in both vertical and horizontal orientations. The vertical configuration is of particular interest due to the significant influence of gravitational force as a parameter. The vessel has a simple cylindrical shape, with the scaffold positioned in the central section. As we can see in Figure 8.3, there is an initial section, colored in blue, which represents the vessel before the insertion of the scaffold and has a length of 10 cm. The orange section represents the placement of the scaffold and has a length of 15 cm. The silver section represents the vessel after the scaffold and has a length of 25 cm. The different colors serve to distinguish the regions, as the boundary conditions vary, along with the simulation parameters. The linear geometry is presented with the same dimensions in the various sections, incorporating the four previously mentioned diameters: 2.5 mm, 3.5 mm, 5 mm, and 7 mm.

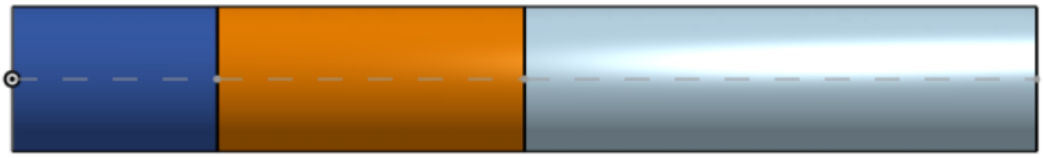

Figure 8.3: *Geometric representation of the linear vessel using Onshape software. The blue section refers to the vessel before the scaffold, with a length of 10 cm. The orange section represents the scaffold, with a length of 15 cm, while the silver section corresponds to the vessel after the scaffold, with a length of 25 cm.*

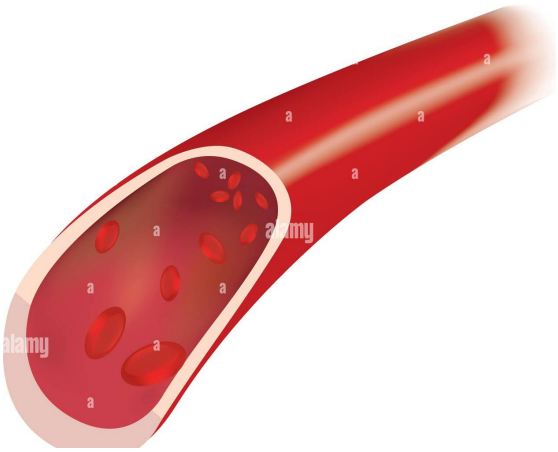

Figure 8.4: *3D representation of a section of a linear vessel from the human circulatory system.*

- *Curved vessel*

  This type of blood vessel can also be represented in a vertical orientation; however, it would not introduce a study significantly different from the one previously analyzed. The vessel retains a cylindrical shape, but unlike the linear vessel, it features a curvature in the central section where the scaffold is positioned. This curvature influences the variation in flow velocity. As we can see in Figure 8.5, there is an initial section, colored in blue, which represents the vessel before the insertion of the scaffold and has a length of 10 cm. The grey section represents the placement of the scaffold and has a length of 15 cm. The silver section represents the vessel after the scaffold and has a length of 25 cm. The different colors serve to distinguish the regions, as the boundary conditions vary, along with the simulation parameters. The curved geometry is presented with the same dimensions in the various sections, incorporating the four previously mentioned diameters: 2.5 mm, 3.5 mm, 5 mm, and 7 mm.

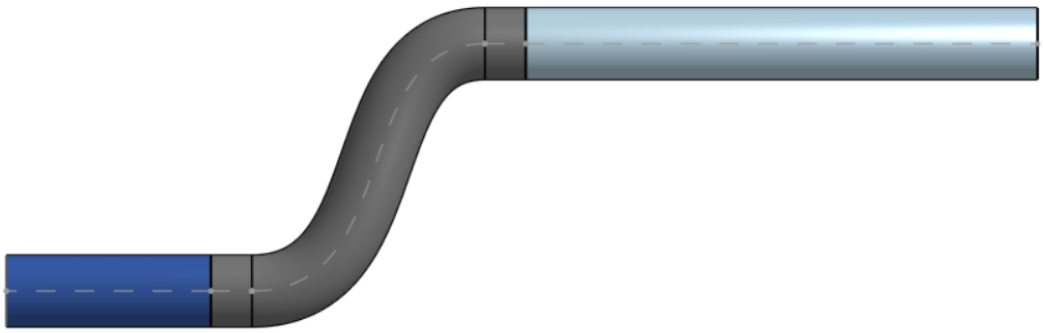

Figure 8.5: *Geometric representation of the curved vessel using Onshape software. The blue section refers to the vessel before the scaffold, with a length of 10 cm. The grey section represents the scaffold, with a length of 15 cm, while the silver section corresponds to the vessel after the scaffold, with a length of 25 cm.*

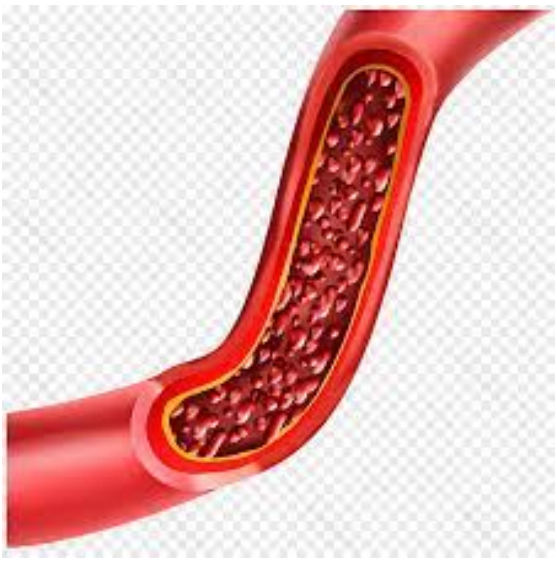

Figure 8.6: *3D representation of a section of a curved vessel from the human circulatory system.*

- *Bifurcated vessel*

  This vessel is more complex, and given human anatomy, it can only be represented in a vertical orientation with the bifurcation directed downward. Starting from a cylindrical structure, it features a bifurcation after the scaffold placement. This configuration demonstrates how temperature variation

stabilizes differently when distributed across multiple sections. The presence of the scaffold in the bifurcated section would not result in a case significantly different from the one previously analyzed. As we can see in Figure 8.7, there is an initial section, colored in blue, which represents the vessel before the insertion of the scaffold and has a length of 10 cm. The light grey section, represents the placement of the scaffold and has a length of 15 cm. The section following, represented by the dark grey, yellow, orange, and silver colors, represents the vessel after the scaffold and has a length of 43 cm. The bifurcated geometry is presented with the same dimensions in the various sections, incorporating the four previously mentioned diameters: 2.5 mm, 3.5 mm, 5 mm, and 7 mm. To achieve thermal stability, it was necessary to significantly increase the length of the section following the scaffold, as thermal stability had not yet been reached in the bifurcation area. The different colors serve to distinguish the regions, as the boundary conditions vary, along with the simulation parameters. In this specific case, the section following the scaffold is characterized by different colorations. However, this chromatic differentiation holds no significance from either an anatomical or computational perspective. It is merely a result of the way the software handles the geometry construction, distinguishing the various parts as separate entities. In the numerical computation, however, all these sections share the same boundary conditions and are therefore considered as a single entity.

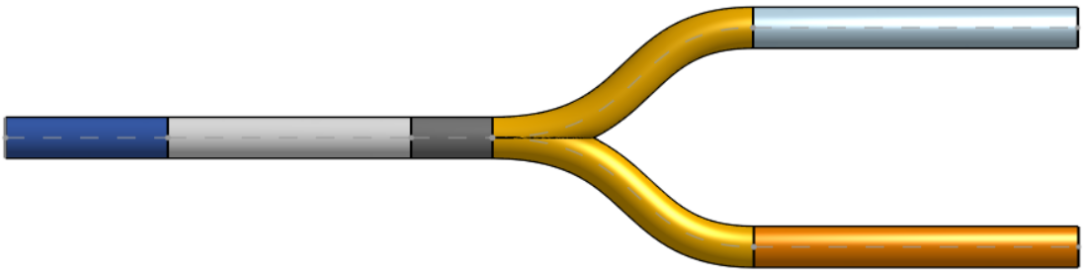

Figure 8.7: *Geometric representation of the bifurcated vessel using Onshape software. The blue section refers to the vessel before the scaffold, with a length of 10 cm. The light grey section represents the scaffold, with a length of 15 cm. The section represented by the dark grey, yellow, orange, and silver colors, corresponds to the vessel after the scaffold, with a length of 43 cm.*

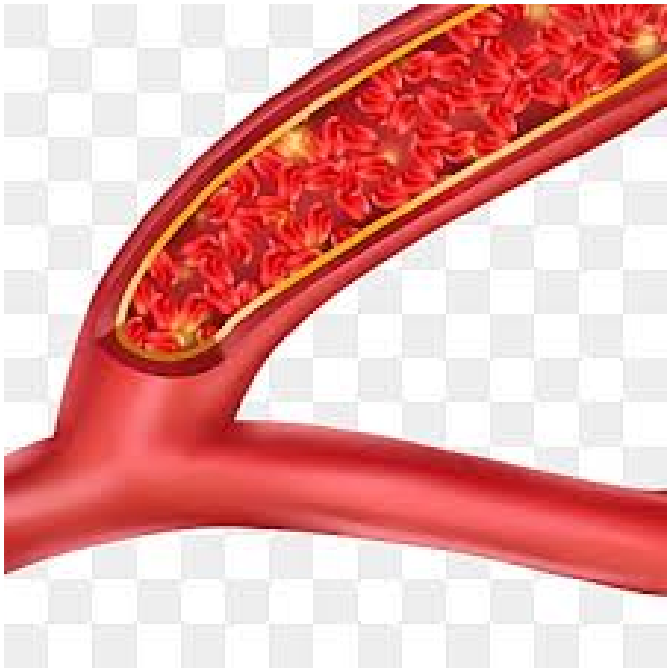

Figure 8.8: *3D representation of a section of a curved vessel from the human circulatory system.*

Chapter 9

OpenFoam

9.1 Overview

As can be found on the official website, OpenFOAM (Open Source Field Operation And Manipulation) is an open-source software for computational fluid dynamics (CFD), widely used for the numerical simulation of complex physical phenomena in continuum mechanics[83]. Based on the C++ programming language, OpenFOAM enables the resolution of problems related to fluid dynamics, heat transfer, and fluid-structure interactions, making it an ideal tool for analyzing thermal behavior within a vascular bioprosthesis[84]. The software employs the finite volume method (FVM) to discretize the governing equations, including the Navier-Stokes equations, which describe the behavior of blood flow, and the energy equation, which governs heat transfer. This combination provides a detailed representation of the temperature distribution and thermal variations occurring within the examined prosthetic blood vessel[33].

Figure 9.1: *OpenFoam software logo.*

As can be found on the official website, the graphical interface of OpenFOAM is

represented by the ParaView software, a powerful open-source post-processing tool widely used for visualizing and analyzing numerical simulation results. ParaView allows graphical representation of simulated data, offering a wide range of tools for three-dimensional analysis, data manipulation, and animation generation[83]. One of ParaView's key features is its ability to visualize the temporal evolution of simulations, enabling the analysis of dynamic and transient phenomena through an intuitive interface. The software supports a variety of file formats and is capable of handling large datasets thanks to its scalable architecture, which allows processing both on local workstations and on high-performance computing clusters[85]. In the context of this thesis, ParaView is crucial for analyzing the temperature profile within the vascular bioprosthesis, as it allows for a detailed visualization of heat distribution within the simulated model. Through its post-processing tools, it is possible to evaluate the spatial and temporal variation of temperature, identifying potential thermal gradients that may be critical for the bioprosthesis' functionality. Moreover, the integration with OpenFOAM enables the extraction and analysis of numerical data related to temperature, velocity, and pressure fields, facilitating the comparison between different geometric configurations and boundary conditions. The ability to generate thermal maps, cross-sectional views, and animations makes ParaView an essential tool for interpreting simulation results and validating the developed models[84].

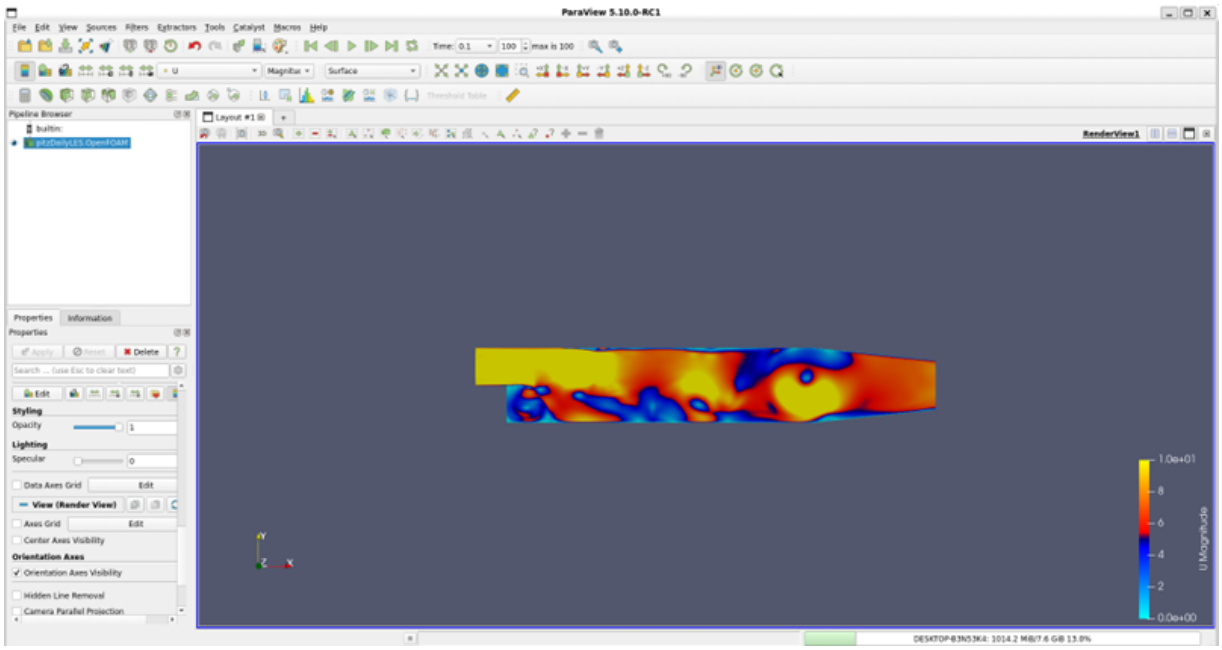

Figure 9.2: *ParaView software interface with a generic time-dependent simulation example, aimed at illustrating the graphical representation of the results.*

9.2 Structure

OpenFOAM is structured into a set of software tools categorized into three main components:

- *Solvers*

  Programs or numerical algorithms that solve a set of mathematical equations associated with a specific physical problem. In OpenFOAM solvers are designed to handle various types of simulations in computational fluid dynamics (CFD). Each solver employs methods based on the discretization of differential equations, enabling the computation of physical variable evolution within the simulation domain.

- *Utilities*

  Tools for data processing and management, used for mesh generation, boundary condition definition, and result analysis.

- *Core Libraries*

  Modules responsible for managing interactions between mesh elements, implementing physical equations, and performing numerical discretization.

OpenFOAM provides dedicated environments for both pre-processing and post-processing of data. The interface for these operations consists of built-in utilities, ensuring uniform and consistent data management throughout all phases of the simulation process. At the core of its structure lies a set of object-oriented classes that allow users to manipulate meshes, geometries, and discretization techniques with a high level of abstraction in the code[83]. These classes serve as fundamental building blocks for the development of OpenFOAM-based applications and tools, facilitating the construction of new algorithms and promoting extensive code reuse. Thanks to its numerous capabilities, OpenFOAM enables the simulation of a wide range of physical phenomena and supports the generation of meshes even for highly complex geometries. Another key advantage of OpenFOAM is its ability to execute most operations in parallel, fully leveraging the capabilities of modern multi-core processors and multi-processor systems. This significantly enhances computational efficiency and reduces simulation times, making it particularly suitable for complex numerical analyses[84].

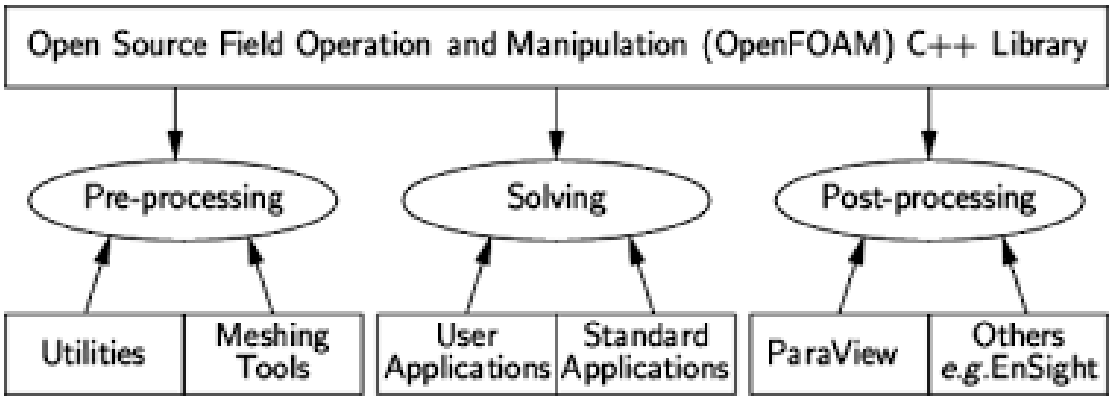

Figure 9.3: *Diagram of the OpenFOAM software structure.*

- **Fluid Dynamics Physical Modelling**
  - Turbulence modelling

  - Thermophysical modelling
  - Multiphase flows
  - Rotating flows with multiple reference frames (MRF)
  - Dynamic meshes
  - Compressible/thermal flows
  - Conjugate heat transfer
  - Lagrangian particle tracking
  - Reaction kinetics / chemistry
- **Geometry And Meshing**
  - Mesh generation for complex geometries with **snappyHexMesh**
  - Mesh generation for simple geometries with **blockMesh**
  - Mesh conversion tools
  - Mesh manipulation tools
- **Data Analysis**
  - ParaView post-processing
  - Post-processing command line interface (CLI)
  - Graphs and data monitoring
- **Numerical Solution**
  - Numerical method
  - Linear system solvers
  - ODE system solvers
- **Computing And Programming**
  - Equation syntax
  - Libraries of functionality
  - Parallel computing

9.3 Settings

In this study, OpenFOAM was employed to generate CFD simulations that model the thermal behavior of blood within the vascular bioprosthesis. The solver *rhoSimpleFoam* was used to solve the fluid dynamics and heat conduction in the presence of forced convection. Various vascular geometries (linear, curved, and bifurcated) were considered to assess the effect of vessel shape on temperature distribution. The parallel computing capabilities of the software allowed for a significant reduction in simulation time, enabling efficient handling of detailed meshes and long-time-scale analyses. The use of OpenFOAM in this study enabled:

- Modeling heat transfer within the bioprosthesis by reproducing blood flow dynamics throughout the cardiac cycle.
- Analyzing the influence of vessel geometry on temperature distribution, identifying potential areas of heat accumulation or dissipation.
- Validating results through comparison with experimental data and simplified models based on analytical equations.

The ability to modify and customize OpenFOAM solvers made it possible to implement realistic boundary conditions based on physiological data related to blood flow and the thermal properties of the prosthetic material used.

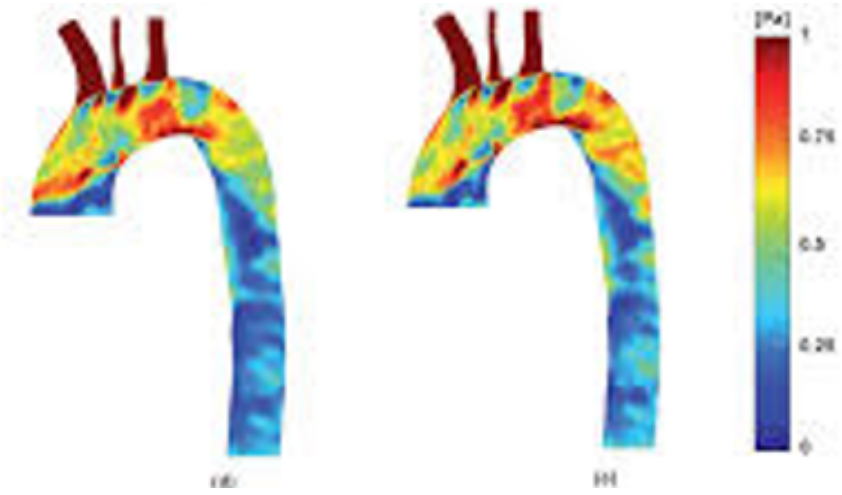

Figure 9.4: *Example of simulation with OpenFoam on ParaView's interface.*

The management of a case in OpenFOAM follows a modular organizational structure, allowing for flexible definition and control of simulation parameters.

9.4 Case's structure

A case in OpenFOAM is divided into three main directories[83]:

- **System**: This folder contains the essential configuration files for controlling the execution of the simulation. Specifically:
  - *controlDict* defines the control parameters, such as the simulation start and end times, time step size, and data output settings.
  - *fvSchemes* specifies the discretization schemes used to solve the differential equations.
  - *fvSolution* sets the tolerances and numerical methods related to the solvers used. These files enable the configuration of solution parameters in accordance with the physiological conditions of blood flow, which are fundamental for studying heat transfer within bioprostheses.
- **Constant**: This directory includes the complete mesh description, stored in the polyMesh folder, and gathers the physical properties of the system (e.g., gravity, turbulence properties, etc.). Accurate mesh definition is crucial for realistically replicating vascular geometries and ensuring that the computed temperature profile reflects real-world conditions.
- **Time directories**: These folders store data for each simulated time step. The data include initial values, boundary conditions, and computational results for physical fields such as temperature, velocity, and pressure. This system allows for tracking the temporal evolution of parameters, which is essential for analyzing how blood flow influences the thermal profile of the bioprosthesis.

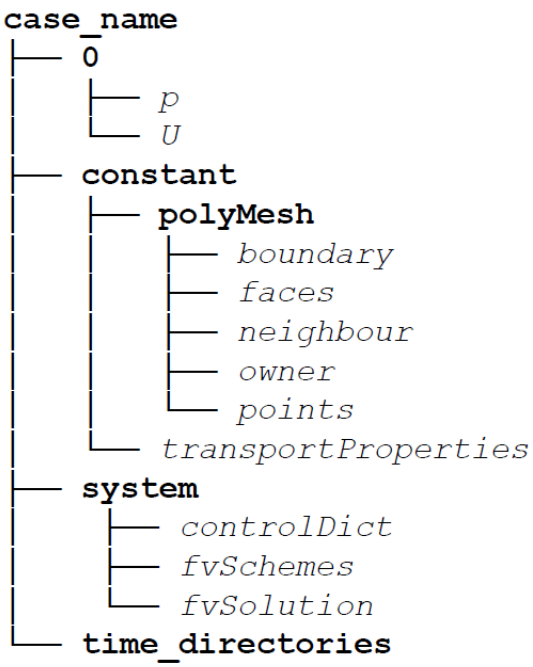

Figure 9.5: *Structure of OpenFoam's directory for a generic case study.*

The hierarchical structure of a case in OpenFOAM facilitates modular simulation management, enabling independent modification of parameters and configurations. In this study, this organization allowed the replication of specific conditions of the human circulatory system and the comparison of results obtained from different prosthetic geometries. This approach aimed to optimize bioprosthesis design concerning heat transfer efficiency.

9.5 Implementation and setup in our solver

From a computational perspective, modeling the problem requires the adoption of specific simplifying assumptions and boundary conditions. In Chapter 6, the numerical selection of parameters was determined based on the physical characteristics of the system and the available data. However, it is also necessary to define the implementation aspects required for the simulation. Blood is known to be a non-Newtonian fluid, meaning that its viscosity depends on the velocity gradient. However, for the specific purpose of this simulation, the approximation of a Newtonian fluid has been adopted. This simplification is justified by the fact that, in the context of heat exchange analysis, the non-Newtonian behavior of blood

does not introduce significant variations in the results. Conversely, this characteristic would be crucial in rheological studies, where the viscoelastic properties of the fluid strongly influence flow dynamics. The assumption of Newtonian blood therefore allows for simplified calculations without introducing significant errors in heat transfer phenomena. Another assumption made is that blood is considered an incompressible fluid, which is consistent with the literature and the physiological conditions of the circulatory system. This assumption allows for the application of the Navier-Stokes equations in their classical formulation for low-velocity flows, avoiding complications related to compressibility effects. From a fluid dynamics perspective, laminar flow is assumed, a condition that depends on the Reynolds number, which must be below 2000 for the hypothesis to be valid. However, the Reynolds number is not a fixed value, as it depends on the blood velocity and the vessel diameter. Therefore, this assumption will be verified in the simulation results to confirm that the calculated values comply with the laminar regime. Furthermore, the no-slip condition is considered, meaning that the velocity of the fluid in proximity to the vessel wall is zero. This assumption is consistent with the physiological conditions of the vascular system and represents a fundamental constraint in numerical fluid simulations. Regarding the treatment of vascular walls, an equivalent boundary condition has been adopted, as described in Chapter 7, which replaces the vessel wall thickness with a simplified condition. This approach allows for avoiding direct modeling of the wall, reducing computational complexity while preserving the accurate representation of thermal and fluid dynamic phenomena. The boundary conditions imposed in the simulation domain require specifying velocity and pressure values at both the inlet and outlet of the vessel. However, to ensure simulation stability, it is not possible to assign both variables simultaneously at the inlet and outlet. Consequently, a velocity value at the inlet was assigned, calculated based on the considered volumetric flow rate, while at the outlet, a zero-pressure condition was imposed. This approach allows for numerically determining the outlet velocity and the inlet pressure, thereby providing a comprehensive representation of flow conditions. Furthermore, each imposed flow rate generates a pressure variation along the vessel. Thus, it is possible to calculate the pressure gradient as a function of the inlet velocity, providing an additional verification of the coherence of the simulation assumptions.

Results

Chapter 10

Results

As previously introduced in the preceding chapters, this study aims to analyze the temperature profile within a vascular bioprosthesis made from a polycaprolactone (PCL) and polyglycerol sebacate (PGS) blend, evaluating its thermal and fluid dynamic behavior through numerical simulations in OpenFOAM. The simulations were conducted within the framework of computational fluid dynamics (CFD) by solving the Navier-Stokes equations under the assumption of laminar, incompressible flow. Three different vascular geometries were considered: a straight vessel, a curved vessel, and a bifurcated vessel, to assess the influence of conduit morphology on heat transfer conditions. The key parameters in this study are vessel geometry and, most importantly, the presence of the PCL-PGS blend, which represents the most innovative aspect of this work. Additionally, flow conditions play a significant role, although they exhibit considerable variability depending on the individual, patient category, and pathological conditions. Consequently, while the flow values used in the simulations provide a reference, they cannot be considered representative of a specific clinical scenario. To ensure the generalizability of the study, the physical and chemical properties of blood and the bioprosthetic material were selected based on established data. Moreover, to avoid explicitly modeling heat transfer within the vessel wall, a boundary condition presented in Chapter 7 was adopted. This approach accounts for wall thickness and thermal conductivity without directly incorporating the wall into the simulation. Table 10.1 provides a comprehensive summary of the parameters implemented in the software for the execution of the simulations, including both established values and averaged parameters to support a generalized analysis.

Parameter	Value	Unit
Femoral artery	7[66]	mm
	350[67]	mL/min
Carotid artery	5[68]	mm
	500[69]	mL/min
Coronary artery	3.5[70]	mm
	150[71]	mL/min
Radial artery	2.5[72]	mm
	6.7[72]	mL/min
Wall Thickness	1	mm
***Dynamic viscosity of blood*[73]**	$\mathbf{3.5}\times10^{-3}$	Pa·s
***Specific heat capacity of blood*[74]**	3.65	J/(kg·K)
***Molecular weight of blood*[75]**	64.5	kDa
***Density of blood*[76]**	1060	kg/m^3
***Thermal conductivity of blood*[77]**	0.5	W/(m·K)
***Thermal conductivity of real vessel*[77]**	0.5	W/(m·K)
***Thermal conductivity of blend*[78]**	0.05	W/(m·K)
***Temperature of blood*[1]**	311	K
***Temperature of human body*[1]**	309.5	K

Table 10.1: *Summary of vascular and physical parameters used in the simulation.*

10.1 Case-specific analysis of thermal and flow dynamics

The analysis of results focuses on the variation of temperature within the considered vascular configurations, evaluating how vessel geometry and the presence of the scaffold influence heat transport. The objective of this section is to examine the temperature distribution along the longitudinal axis of the vessel and compare different geometric configurations to highlight differences in heat dissipation mechanisms. To achieve this, the data have been represented using two main visualization methods: temperature graphs along the vessel axis and cross-sectional views of the simulation domain. The former illustrates temperature variation along the vessel length, distinguishing the temperature distribution at the center of the lumen and near the vessel wall. In the linear cases, both profiles are presented to demonstrate the constancy of temperature at the center of the vessel, as predicted by theoretical assumptions. However, in curved and bifurcated configurations, the temperature graph is shown only near the wall, as this is where the most significant thermal variations occur and represents the most relevant aspect for this study. Cross-sectional views, on the other hand, allow for direct observation of local temperature variations, highlighting the thermal gradient generated by blood flow and the potential influence of vessel geometry. The analysis was conducted on three different vascular configurations: a straight vessel, a curved vessel, and a bifurcated vessel. For each configuration, temperature profiles obtained from the simulations were examined, and the results were compared to assess the impact of vessel morphology on heat transfer conditions. In addition to the case-by-case analysis, three reference elements are also presented to support the interpretation of the overall results. The first concerns the temperature behavior in a vessel without scaffold, which is useful for highlighting differences in thermal profiles compared to the bioprostheses under investigation. The second element consists of a representative case showing the velocity distribution in a linear vessel. Although this is not the primary focus of the thermal analysis, examining the velocity profile allows for verification of the assumptions formulated in the numerical model, particularly the presence of laminar flow and adherence to the vessel wall according to the no-slip condition. Finally, an exploratory case is introduced involving a linear configuration with the same diameters as those used in the previous cases, but with a significantly greater length. While the ge-

ometries analyzed in the other simulations represent vascular segments of realistic dimensions, this extended configuration is designed to conceptually represent the continuity of the human circulatory system, which has no defined beginning or end. The aim is to observe the evolution of the thermal profile under prolonged conditions, simulating a virtually infinite vessel segment in order to evaluate temperature behavior over extended lengths and in the absence of major geometric discontinuities.

10.2 Linear vessel geometry

The linear vessel configuration serves as the reference case for this study, allowing the analysis of temperature variation in a simplified system, free from curvatures or bifurcations that could influence thermal distribution. Four different geometries were considered, characterized by internal diameters of 2.5 mm, 3.5 mm, 5 mm, and 7 mm. The objective of this section is to evaluate the influence of diameter on temperature variation along the vessel length, both at the center and at the wall.

10.2.1 Case without scaffold

To understand the effect of the scaffold on thermal distribution, the temperature variation in a vessel without a scaffold was initially analyzed (Figure 10.1). The temperature profile shows a progressive decrease along the vessel axis, confirming the expected behavior. Blood enters the system at a temperature of approximately 38°C, while the external wall of the vessel is at body temperature, approximated to 36.5°C. This heat exchange leads to a gradual cooling of the fluid, with a more pronounced decrease near the wall compared to the central region. The observed linear trend is consistent with literature findings for similar conditions, highlighting the role of the thermal gradient between blood and surrounding tissues.

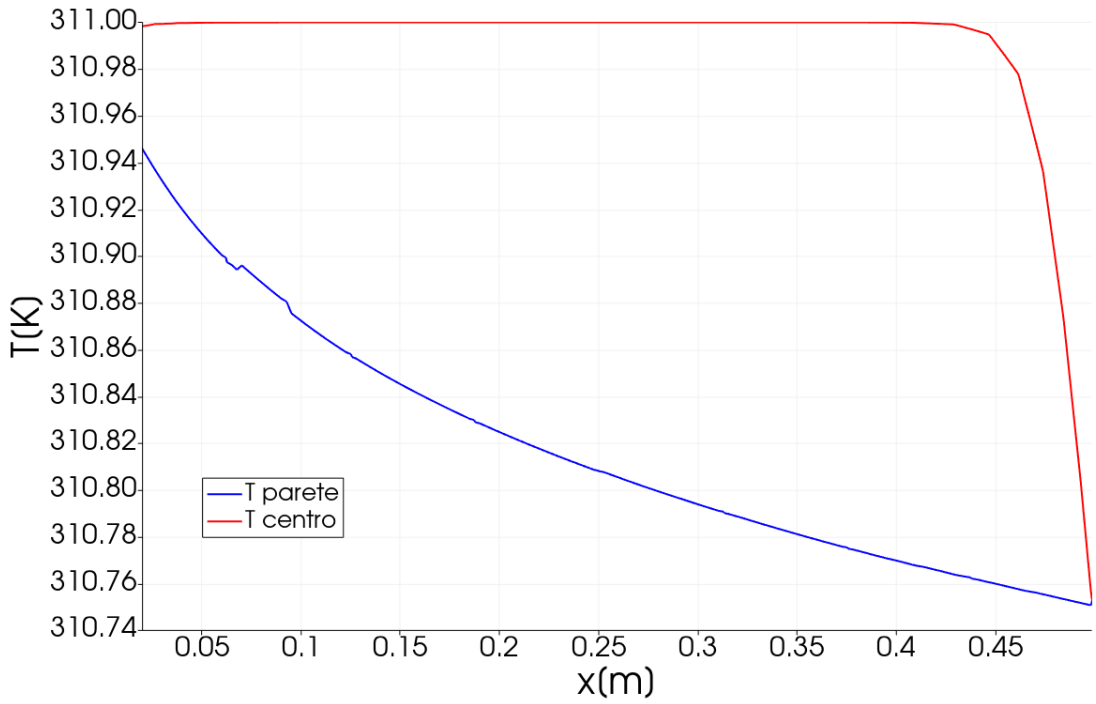

Figure 10.1: *Temperature profile along the axis of the linear vessel with a diameter of 3.5 mm, without the presence of a scaffold. The central temperature remains constant along the entire length of the vessel, consistent with theoretical expectations. In contrast, the wall temperature exhibits a progressive decrease due to heat exchange with the external environment. This trend is expected, as the external vessel wall temperature is approximately 36.5°C, while the blood temperature is around 38°C, leading to a thermal gradient that drives heat dissipation.*

The thermal distribution observed in the cross-sectional plane of the linear vessel (Figure 10.2) highlights a clear difference between the central and peripheral regions of the vessel. Specifically, a pronounced radial thermal gradient is evident, with higher temperatures concentrated along the central axis of the vessel and progressively lower values towards the outer walls. This distribution confirms the expected behavior of blood flow, which maintains higher temperatures in the central region due to the reduced influence of thermal exchange with the surrounding environment. The presence of axial symmetry in the observed thermal distribution confirms the stability of the flow and aligns with the expected physical behavior for steady-state conditions in the absence of a scaffold. These observations provide an essential reference for understanding the subsequent effect introduced by the addition of the scaffold device on the overall thermal distribution within the

vessel.

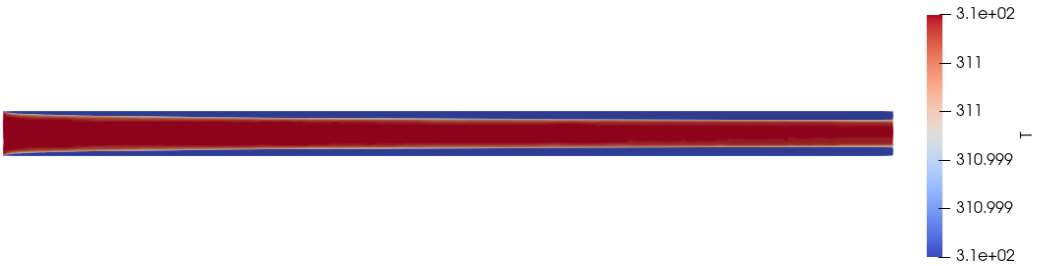

Figure 10.2: *Cross-sectional temperature distribution in the linear vessel model without scaffold, highlighting the radial temperature gradient and axial symmetry indicative of stable, laminar flow conditions.*

10.2.2 Temperature profile along the vessel axis

Regarding the cross-sectional analysis of vessel models equipped with scaffolds of varying diameters, additional thermal distribution images have not been included. This decision stems from the observation that cross-sectional views of vessels with scaffolds are perfectly comparable to the one previously presented for the scaffold-free model, exhibiting no visually discernible differences. Although the axial temperature profiles subsequently discussed indicate that slight thermal variations indeed exist, such variations are minimal enough to remain imperceptible in cross-sectional representations. Therefore, to avoid redundancy and maintain clarity in the discussion, it was deemed appropriate to omit these additional images. The variation in temperature was analyzed through the representation of thermal profiles for each diameter, as shown in the following graphs.

The temperature distribution along the axis of the vessel with a 2.5 mm diameter is presented in Figure 10.3. It can be observed that the central temperature (T center) remains constant throughout the entire vessel length, consistent with what was observed in the case without a scaffold and with the theoretical predictions for this type of flow. Conversely, the temperature at the vessel wall (T wall) exhibits a progressive decrease along the vessel axis. However, in the region occupied by the scaffold, a partial increase in temperature is observed. This behavior can be attributed to the different thermal conductivity of the scaffold

compared to natural vascular tissue: while the wall of a biological vessel allows continuous heat exchange with the surrounding environment, the scaffold limits heat transfer between the blood and the external medium. As a result, there is reduced thermal dissipation and a consequent localized increase in temperature. The overall temperature trend along the wall, characterized by a gradual decrease interrupted by a local increase in correspondence with the scaffold, confirms the role of the scaffold in altering the thermal balance of blood flow.

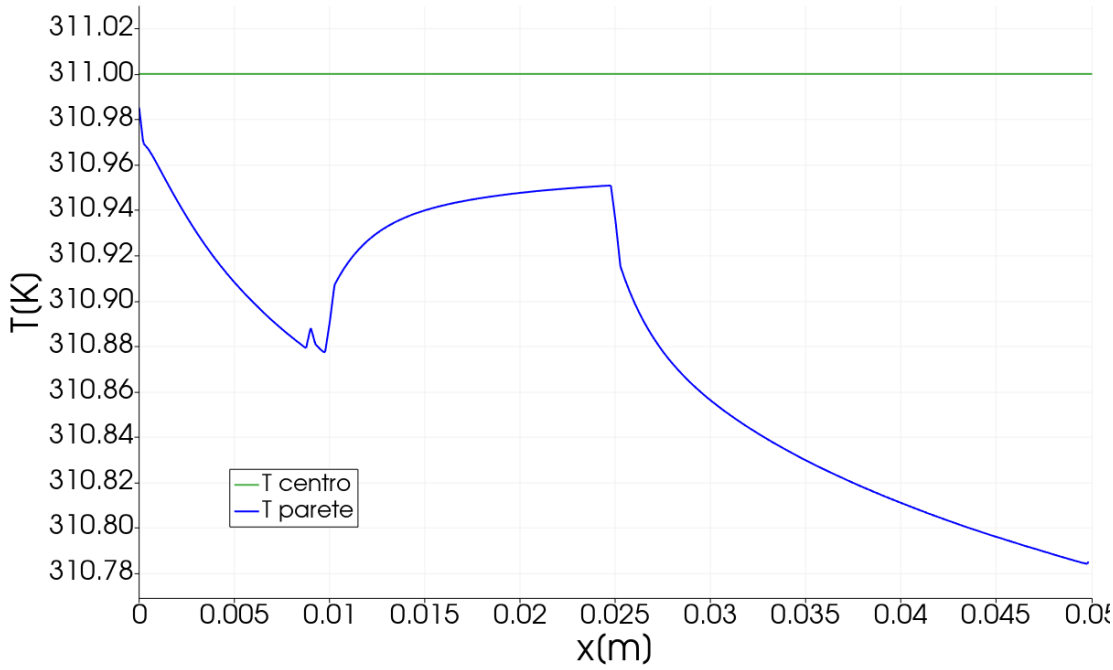

Figure 10.3: *Temperature profile along the axis of the linear vessel with a diameter of 2.5 mm. The central temperature remains constant along the length of the vessel, while the wall temperature shows a progressive decrease, with a rise in correspondence with the scaffold. This behavior is attributable to the scaffold's lower heat exchange capacity compared to the natural vascular wall, which leads to reduced heat dissipation in this region.*

Figure 10.4 illustrates the temperature distribution along the axis of the vessel with a 3.5 mm diameter. Once again confirming the trends observed in previous cases and aligning with theoretical expectations. Compared to the 2.5 mm diameter case, the temperature increase in the region occupied by the scaffold appears less pronounced. This behavior may be attributed to the greater thermal capacity of the fluid, which facilitates a more uniform heat distribution and mitigates the

localized effect of the scaffold on temperature variation.

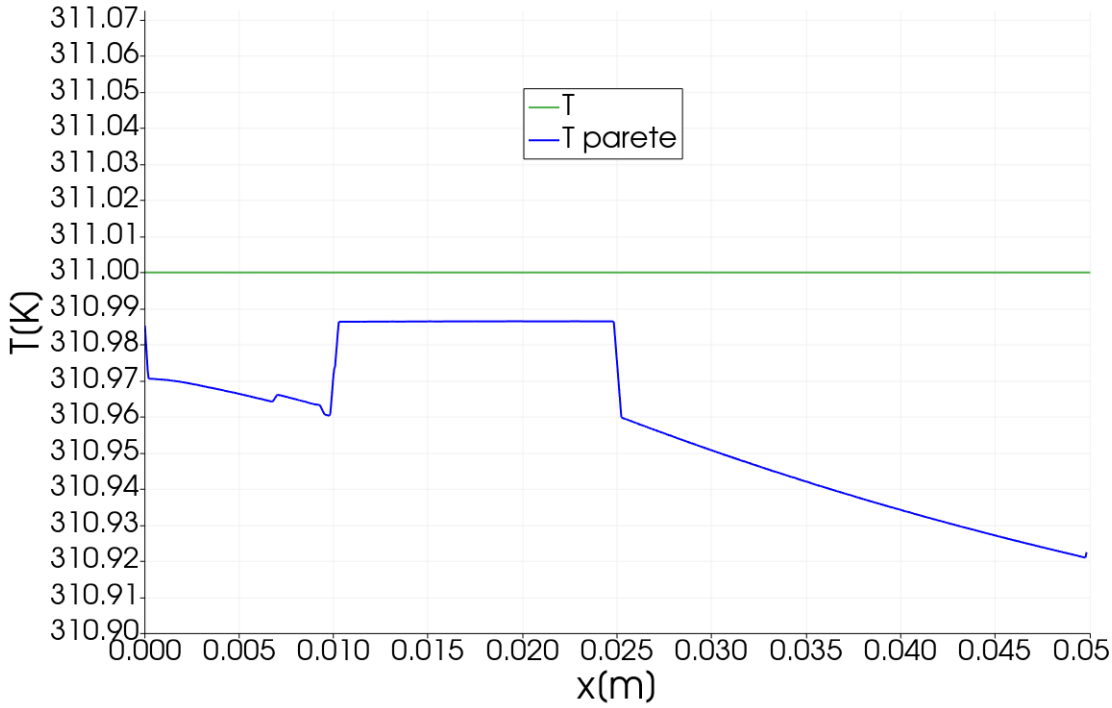

Figure 10.4: *Temperature distribution along the axis of the linear vessel with a diameter of 3.5 mm. The central temperature remains constant, while the temperature at the vessel wall progressively decreases. Compared to the 2.5 mm diameter case, more abrupt temperature variations are observed along the vessel, and the final temperature is slightly higher. The temperature increase near the scaffold is less pronounced, suggesting a reduced local effect of the structure on heat distribution.*

Figure10.5 presents the temperature distribution along the axis of the vessel with a 5 mm diameter. Compared to smaller-diameter vessels, a more pronounced stabilization of the wall temperature is observed, although a thermal gradient is still present. The difference between the central and peripheral temperatures is reduced, indicating an improved retention of heat within the vascular lumen.

Figure 10.5: *Temperature distribution along the axis of the linear vessel with a 5 mm diameter. Compared to smaller vessels, the temperature at the wall exhibits greater stability, with a reduced thermal gradient. The difference between the core and wall temperatures is lower, indicating enhanced heat retention within the vascular lumen and reduced heat dissipation at the boundary.*

Finally, Figure 10.6 illustrates the thermal profile for the vessel with a diameter of 7 mm. The increase in vessel diameter further reduces heat loss along the vessel wall. This observation suggests that, as the vascular caliber increases, the thermal gradient becomes less pronounced, thereby preserving blood temperature more effectively compared to smaller-diameter vessels.

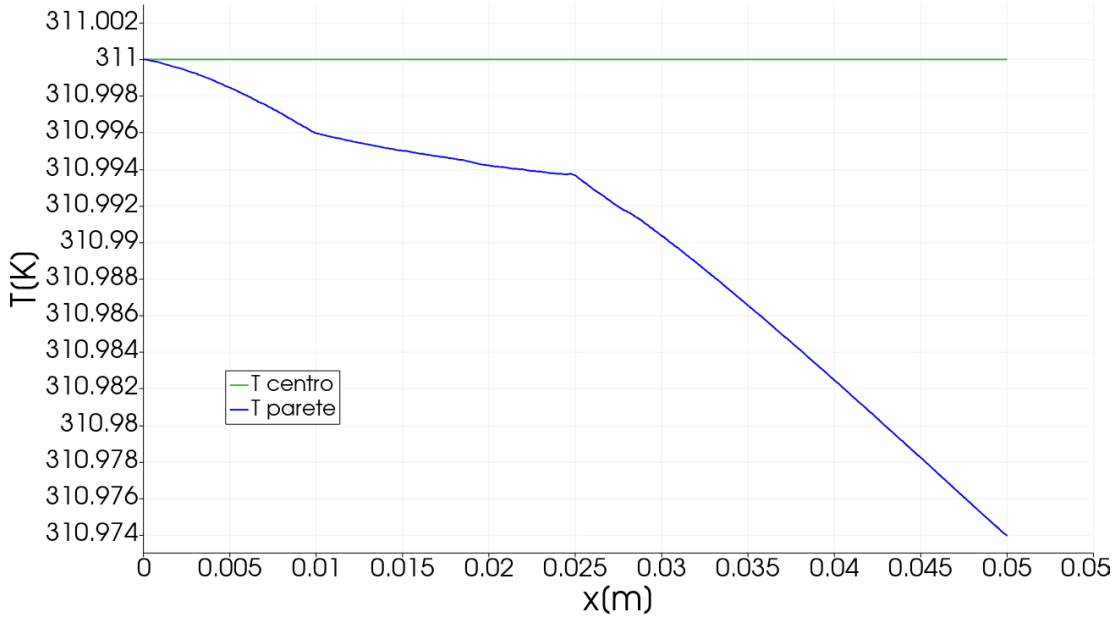

Figure 10.6: *Temperature distribution along the axis of the linear vessel with a diameter of 7 mm. The thermal profile shows a further reduction in temperature loss along the vessel wall compared to smaller diameters. The central temperature remains nearly constant, while the wall temperature exhibits a more gradual decline. This trend indicates that larger vessel diameters contribute to better thermal retention within the lumen, minimizing heat dissipation and reducing the temperature gradient between the core and the periphery.*

Comparison of all diameters

The graph in Figure 10.7 presents the temperature profiles along the vessel wall for all considered diameters (2.5 mm, 3.5 mm, 5 mm, and 7 mm), enabling a direct comparison of how the vascular caliber influences thermal variation. The expected trend is confirmed: in vessels with larger diameters, the temperature along the wall decreases more gradually, approaching the ideal linear decline observed in the case without a scaffold. Conversely, smaller diameters exhibit a more pronounced deviation from this behavior, with sharper variations in the temperature profile. A key observation is the localized temperature increase in correspondence with the scaffold region, which is most evident in the smallest diameter (2.5 mm) and becomes progressively less pronounced as the diameter increases. This effect results from the scaffold's lower thermal conductivity compared to the natural vessel

wall, which limits heat dissipation to the external environment. Consequently, in narrower vessels, where the surface-to-volume ratio is higher, the scaffold has a stronger influence on the overall thermal balance. For the larger diameters (5 mm and 7 mm), the temperature profile more closely follows the expected linear trend, indicating that in these cases, the scaffold has a reduced impact on thermal dissipation. This suggests that, for vessels of greater caliber, the presence of the scaffold does not significantly alter the expected thermal gradient along the wall, preserving a temperature decrease more similar to that of a natural vessel.

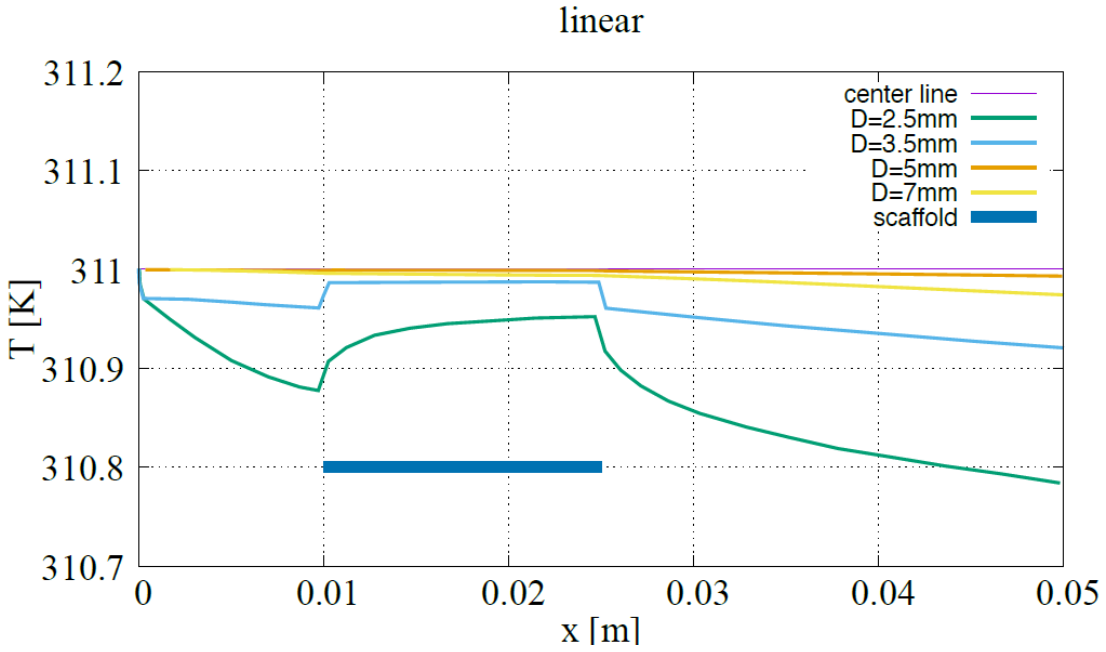

Figure 10.7: *Temperature profiles along the vessel wall for all considered diameters (2.5 mm, 3.5 mm, 5 mm, and 7 mm). The graph highlights the influence of vessel caliber on thermal variation, showing that larger diameters exhibit a more gradual temperature decrease, approaching the linear decline observed in the case without a scaffold. In contrast, smaller diameters display more pronounced deviations, particularly in the scaffold region, where a localized temperature increase is evident. This effect is attributed to the scaffold's lower thermal conductivity, which reduces heat dissipation to the external environment. As the diameter increases, the scaffold's influence diminishes, allowing the thermal profile to more closely resemble that of a natural vessel.*

10.2.3 Analysis of velocity distribution in extended configurations

This exploratory study focuses on a significantly longer linear vascular configuration compared to previously analyzed cases, aiming to clearly observe the evolution of the fluid dynamic profile. This analysis conceptually represents the continuity of the human circulatory system and assesses blood flow velocity behavior under prolonged conditions without significant geometric discontinuities. As illustrated in Figures 10.8 and 10.9, increasing vessel length allows the complete development of the velocity profile to be clearly visualized, revealing the characteristic parabolic distribution typical of steady laminar flows. In the limited-length geometry (Figure 10.8), the velocity profile appears incomplete and nearly uniform in the central region. Conversely, in the extended model (Figure 10.9), a fully developed fluid dynamic regime is distinctly evident, confirming theoretical predictions associated with stabilized laminar flows.

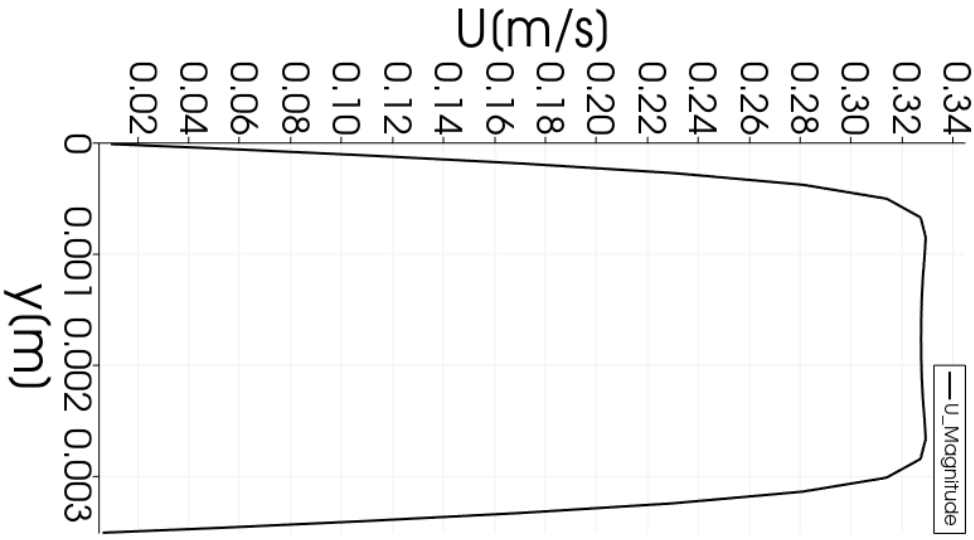

Figure 10.8: *Velocity profile along a short linear vascular segment. The graph illustrates an incomplete velocity distribution characterized by an almost uniform central region, indicating that the flow has not yet reached a fully developed laminar regime due to the limited vessel length.*

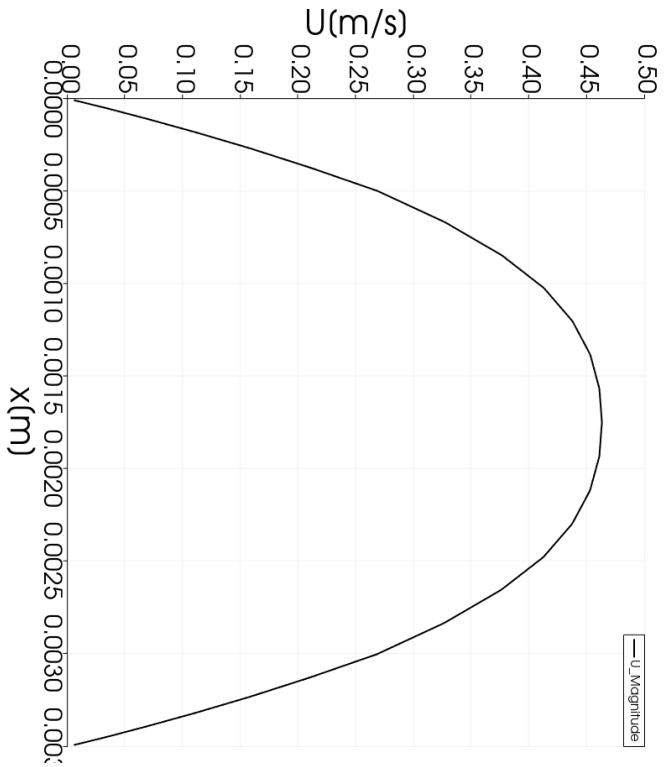

Figure 10.9: *Velocity profile in an extended linear vascular configuration. The clearly parabolic shape of the velocity distribution demonstrates the achievement of a fully developed, stabilized laminar flow, validating theoretical expectations for long vessels without geometric discontinuities.*

10.3 Curved vessel geometry

The next step of the analysis involves the study of curved vessel configurations. This scenario presents increased complexity compared to the previously examined linear cases due to the presence of curvature, which introduces additional fluid-dynamic and thermal phenomena. The diameters considered for these vessels remain consistent with previous cases, allowing direct comparison. In this analysis, particular emphasis will be placed on cross-sectional studies, as these provide critical insights into the flow behavior and thermal distribution influenced by curvature effects.

10.3.1 Temperature and velocity fields along the vessel axis

Temperature fields In the curved vessel configurations showed in Figures 10.10, 10.11, 10.12 and 10.13 the temperature fields reveal significant deviations from the linear case due to curvature-induced complexities. Although turbulence cannot be explicitly discussed, given the low Reynolds numbers (well below the typical turbulent threshold of approximately Re = 2000), significant flow unsteadiness is clearly observable. Starting with the smallest diameter configuration (Figure 10.10, Re = 17.22), minimal unsteadiness is present, with a generally smooth temperature distribution that closely resembles a stable laminar profile. As the diameter and corresponding Reynolds number increase, particularly evident in Figures 10.11 (Re = 275.388), 10.13 (Re = 321.392), and 10.12 (Re = 642.66), significant unsteady flow patterns emerge. These instabilities are generated as fluid particles fail to follow the curved geometry precisely, resulting in regions of flow separation and uneven temperature distribution. The presence of these regions can potentially create localized areas of reduced thermal and fluid-dynamic efficiency, with possible medical implications. Since the solver employed for these simulations computes flow fields transiently, the images represent a snapshot at a particular instant in time, capturing the dynamic nature of the flow. Flow instabilities lead to vortex formation, consequently enhancing heat transfer within the fluid. However, direct visual comparisons between these cases remain challenging, as variations in vessel diameter and fluid velocity are simultaneously introduced. To effectively isolate and compare the specific impacts of individual parameters, a dedicated study varying only one parameter at a time would be required.

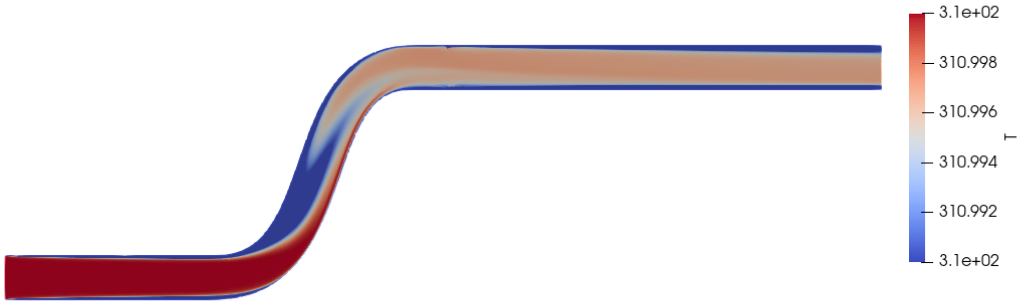

Figure 10.10: *Temperature distribution in the curved vessel configuration with Re = 17.22. The thermal profile appears stable and symmetric, indicating minimal flow unsteadiness due to the low Reynolds number and moderate curvature effects.*

Figure 10.11: *Temperature distribution in the curved vessel configuration with Re = 275.388. The thermal profile appears stable and symmetric, indicating minimal flow unsteadiness due to the low Reynolds number and moderate curvature effects.*

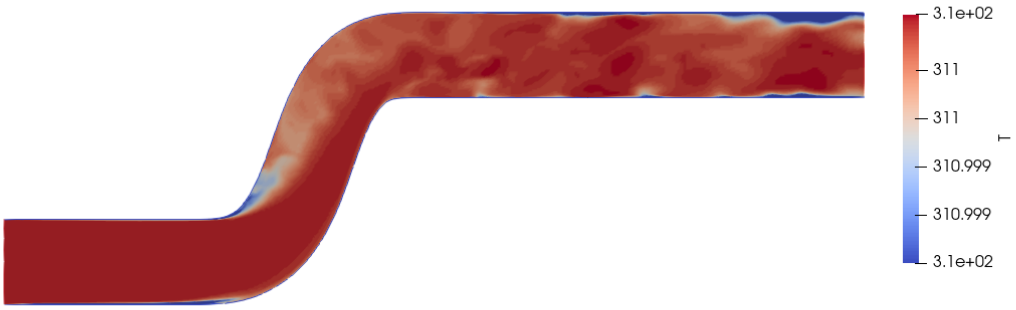

Figure 10.12: *Temperature distribution in the curved vessel configuration with Re = 642.66. The thermal profile appears stable and symmetric, indicating minimal flow unsteadiness due to the low Reynolds number and moderate curvature effects.*

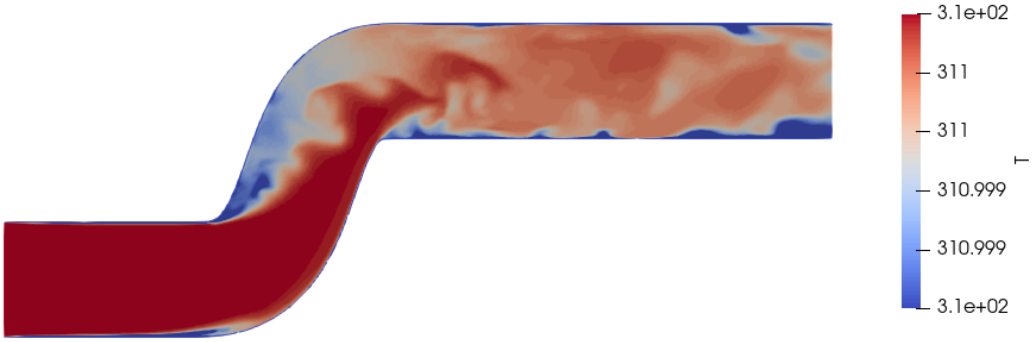

Figure 10.13: *Temperature distribution in the curved vessel configuration with Re = 321.392. The thermal profile appears stable and symmetric, indicating minimal flow unsteadiness due to the low Reynolds number and moderate curvature effects.*

Velocity fields Examining the velocity fields in curved vessel configurations Figure 10.14, 10.15, 10.16 and 10.17, substantial differences from the linear scenario are again observed, consistent with the thermal analysis previously discussed. Starting with the smallest Reynolds number case (Figure 10.14, Re = 17.22), the flow remains relatively stable and exhibits a symmetric and stream-

lined velocity distribution, closely following the vessel's geometry. As the Reynolds number increases, flow complexity and unsteadiness become progressively pronounced. For instance, Figure 10.15 (Re = 275.388) displays initial signs of secondary flows and regions of velocity variations caused by curvature-induced flow separation. This phenomenon intensifies further at higher Reynolds numbers, as clearly depicted in Figures 10.17 (Re = 321.392) and 10.16 (Re = 642.66). In these cases, significant flow instability is apparent, characterized by intricate velocity patterns and clearly visible vortices. These flow disturbances indicate that particles increasingly fail to adhere strictly to the vessel contours, creating regions of low velocity and potential stagnation. Such conditions are medically significant, as these low-velocity regions might lead to reduced efficiency in transport processes and could favor adverse physiological conditions. The presented snapshots represent instantaneous velocity distributions captured from transient simulations, reflecting the dynamic and evolving nature of flow instabilities. As previously noted, direct comparative analysis between different cases remains challenging since both vessel diameter and fluid velocity parameters vary simultaneously. A dedicated parametric analysis varying only one parameter at a time would be essential for more precise quantitative comparisons.

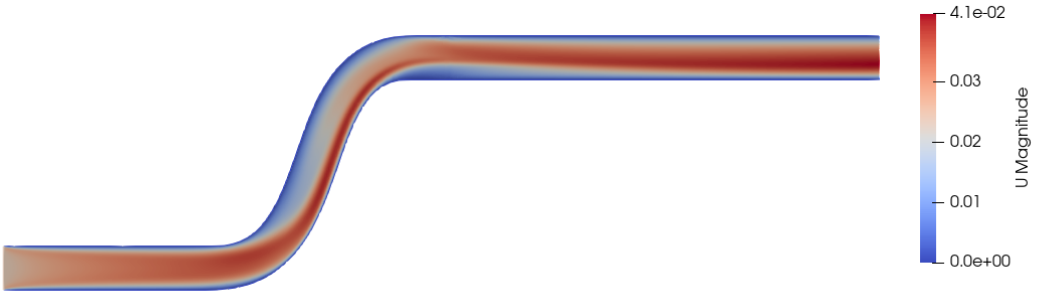

Figure 10.14: *Velocity distribution in the curved vessel configuration with Re = 17.22. The velocity field remains streamlined and symmetric, closely following the geometry of the vessel, demonstrating laminar and stable flow conditions at this low Reynolds number.*

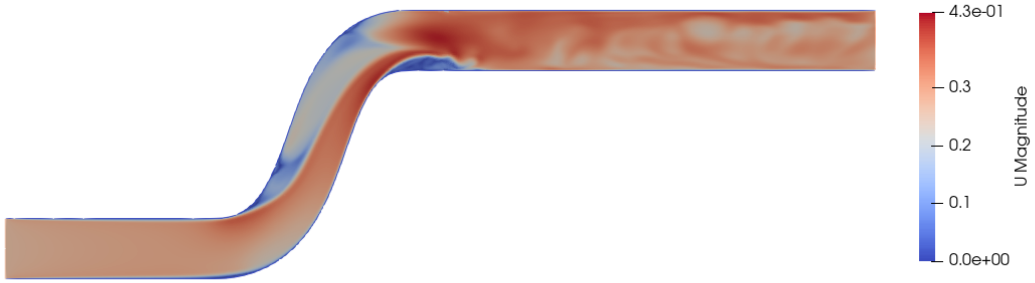

Figure 10.15: *Velocity distribution in the curved vessel configuration with Re = 275.388. The velocity field remains streamlined and symmetric, closely following the geometry of the vessel, demonstrating laminar and stable flow conditions at this low Reynolds number.*

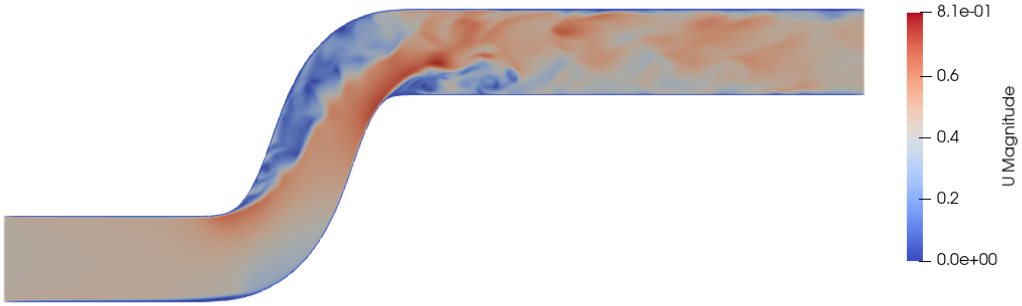

Figure 10.16: *Velocity distribution in the curved vessel configuration with Re = 642.66. The velocity field remains streamlined and symmetric, closely following the geometry of the vessel, demonstrating laminar and stable flow conditions at this low Reynolds number.*

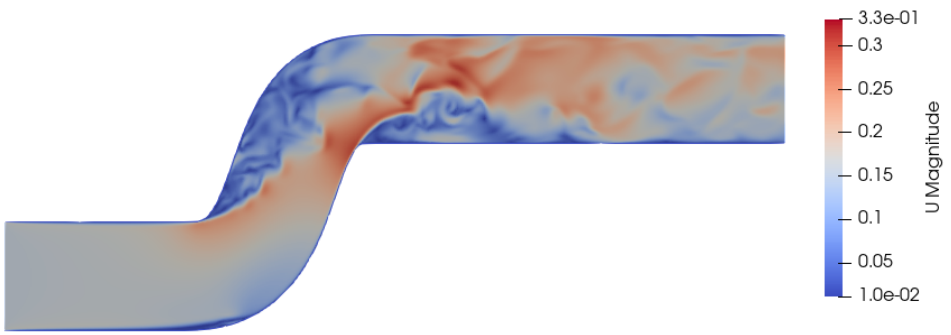

Figure 10.17: *Velocity distribution in the curved vessel configuration with Re = 321.392. The velocity field remains streamlined and symmetric, closely following the geometry of the vessel, demonstrating laminar and stable flow conditions at this low Reynolds number.*

10.3.2 Temperature profile along the vessel axis

The numerical temperature graphs for curved vessel configurations are presented in Figures 10.18, 10.19, 10.20, and 10.21. Central temperature values are omitted since previous linear vessel analyses demonstrated negligible central temperature variation; this omission simplifies graph interpretation for the more complex curved geometries. As previously observed in cross-sectional analyses, the temperature profiles for curved vessels exhibit notably less stable and more irregular behaviors compared to linear cases, reflecting the complex and unstable fluid dynamics induced by curvature. Specifically, temperature fluctuations become more prominent downstream of the curvature, evidencing regions of variable heat transfer efficiency. Nonetheless, each graph consistently highlights a distinct temperature increase near the scaffold region, indicating locally enhanced heat transfer phenomena induced by flow disturbances associated with curvature and scaffold interaction.

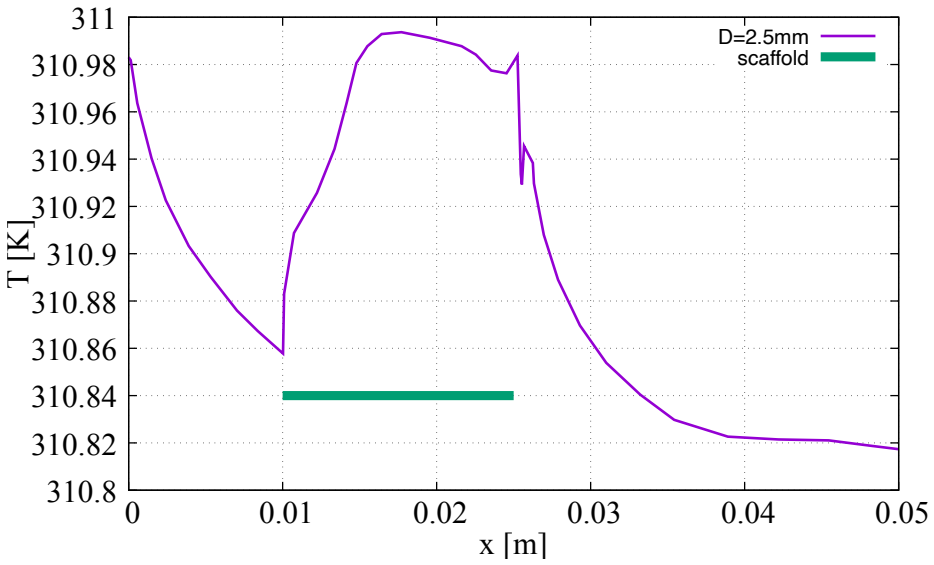

Figure 10.18: *Temperature profile along selected segments in the curved vessel with diameter of 2.5 mm. The graph highlights the irregular and fluctuating behavior of the temperature distribution induced by vessel curvature, with a noticeable temperature increase near the scaffold region.*

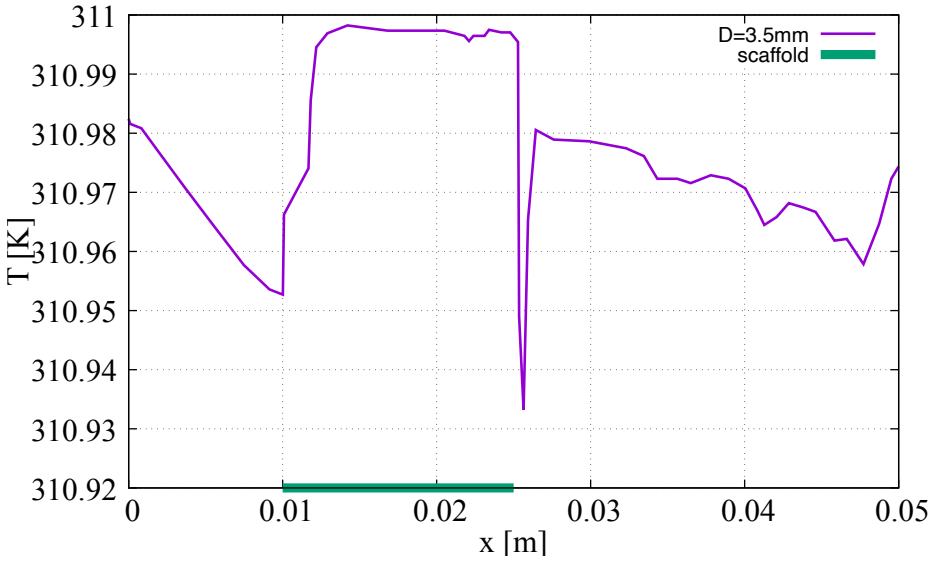

Figure 10.19: *Temperature profile along selected segments in the curved vessel with diameter of 3.5 mm. The graph highlights the irregular and fluctuating behavior of the temperature distribution induced by vessel curvature, with a noticeable temperature increase near the scaffold region.*

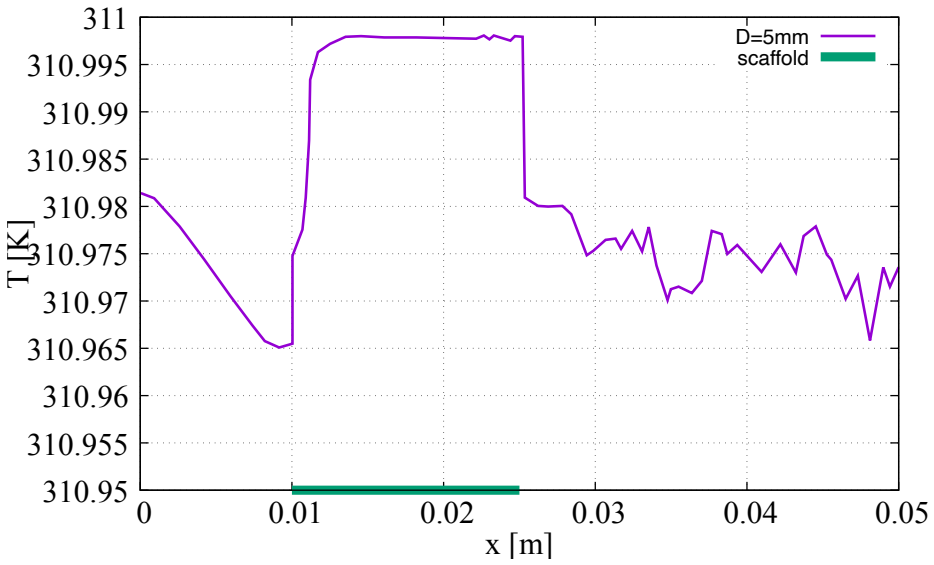

Figure 10.20: *Temperature profile along selected segments in the curved vessel with diameter of 5 mm. The graph highlights the irregular and fluctuating behavior of the temperature distribution induced by vessel curvature, with a noticeable temperature increase near the scaffold region.*

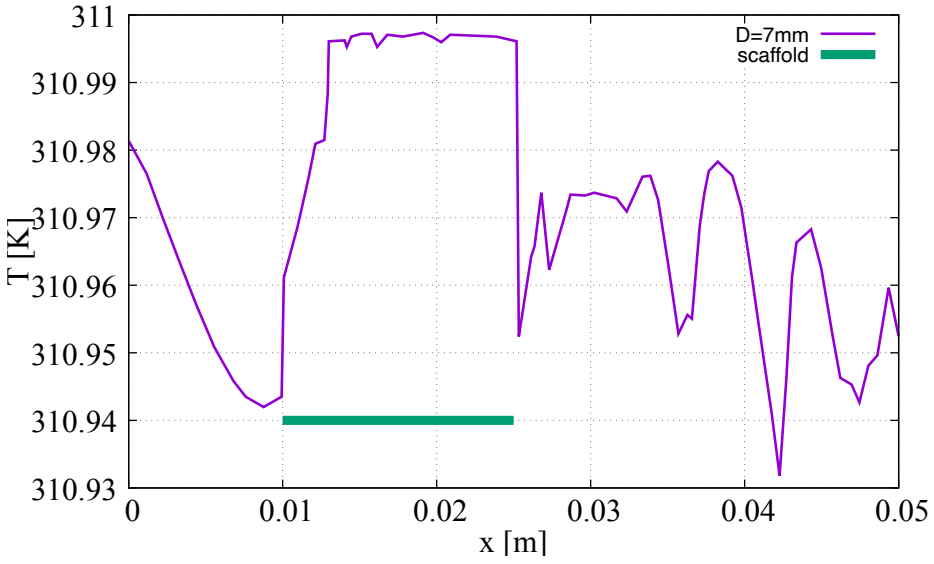

Figure 10.21: *Temperature profile along selected segments in the curved vessel with diameter of 7 mm. The graph highlights the irregular and fluctuating behavior of the temperature distribution induced by vessel curvature, with a noticeable temperature increase near the scaffold region.*

Comparison of all diameters

Examining the overlapping temperature profiles for curved vessels (Figure 10.22), significant differences in temperature distribution among the various diameters become apparent, demonstrating the pronounced influence of geometry on local heat transfer. Compared to analogous linear cases, curved configurations display greater fluctuations and intensified thermal gradients downstream of the scaffold region, underlining the increased sensitivity of curved vessels to diameter and velocity variations. These observations emphasize the complexity introduced by vessel curvature and reinforce the necessity of detailed analysis when evaluating heat transfer in curved vascular geometries.

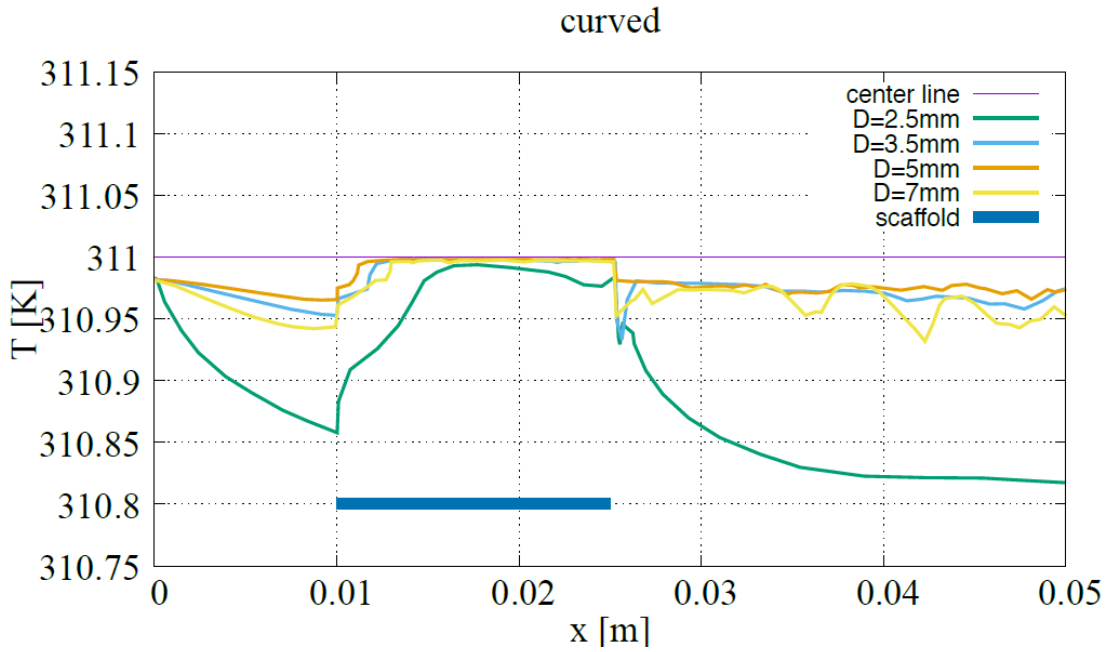

Figure 10.22: *Overlapping temperature profiles for curved vessel configurations with varying diameters. The graph illustrates significant variations and enhanced temperature fluctuations downstream of the scaffold region, underscoring the heightened influence of curvature on local thermal dynamics compared to linear configurations.*

10.4 Bifurcated vessel geometry

The analysis of bifurcated vessel configurations introduces an additional layer of complexity, as these geometries are characterized by a distinct branching structure, significantly influencing local fluid dynamics and heat transfer. The temperature distribution within bifurcated vessels holds even greater clinical and engineering relevance due to the pronounced effects of flow separation and interaction at the bifurcation.

10.4.1 Temperature and velocity fields along the vessel axis

Temperature fields Examining the temperature fields presented in Figures 10.23, 10.24, 10.25, and 10.26, a substantial increase in flow instability and irregularity is immediately noticeable downstream of the bifurcation point. The branching significantly amplifies temperature fluctuations and non-uniformities, creating regions with enhanced mixing and convective heat transfer. These irregularities are especially evident for higher Reynolds numbers, reflecting intensified disturbances within the flow. Each image clearly highlights areas where fluid particles deviate from ideal trajectories, producing localized temperature gradients. Such areas could potentially present medical challenges, including regions of disturbed physiological function. The temperature profiles of bifurcated vessels thus require meticulous consideration, reinforcing the necessity for targeted studies to address the complexities inherent in these configurations.

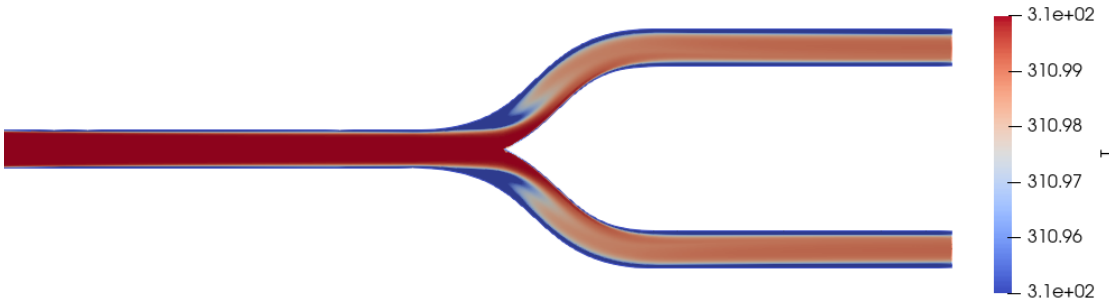

Figure 10.23: *Temperature field for the bifurcated vessel configuration with 2.5 mm diameter and Re=17.22. The presence of bifurcation significantly increases flow complexity and generates noticeable temperature fluctuations. Areas of non-stationarity, particularly around the bifurcation, indicate localized disturbances, enhancing heat transfer through vortex formation and fluid separation phenomena.*

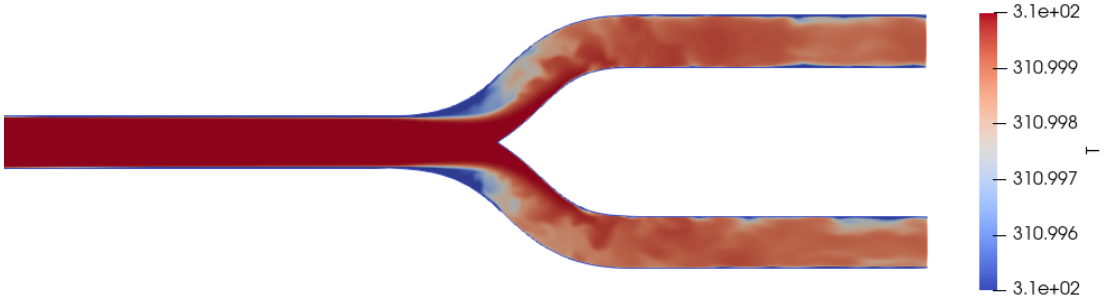

Figure 10.24: *Temperature field for the bifurcated vessel configuration with 3.5 mm diameter and Re=275.388. The presence of bifurcation significantly increases flow complexity and generates noticeable temperature fluctuations. Areas of non-stationarity, particularly around the bifurcation, indicate localized disturbances, enhancing heat transfer through vortex formation and fluid separation phenomena.*

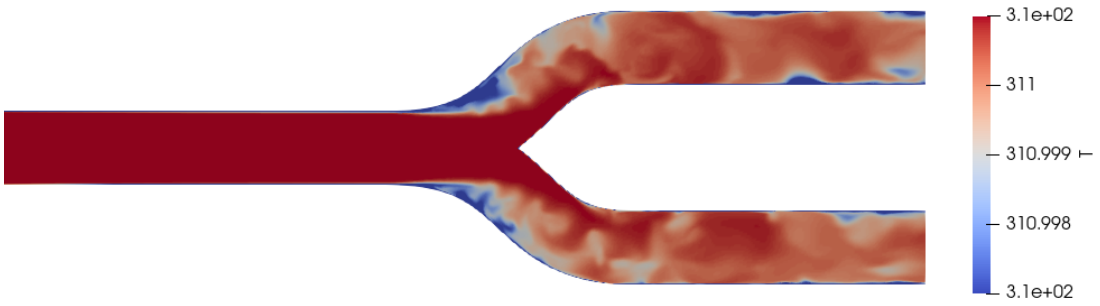

Figure 10.25: *Temperature field for the bifurcated vessel configuration with 5 mm diameter and Re=642.66. The presence of bifurcation significantly increases flow complexity and generates noticeable temperature fluctuations. Areas of non-stationarity, particularly around the bifurcation, indicate localized disturbances, enhancing heat transfer through vortex formation and fluid separation phenomena.*

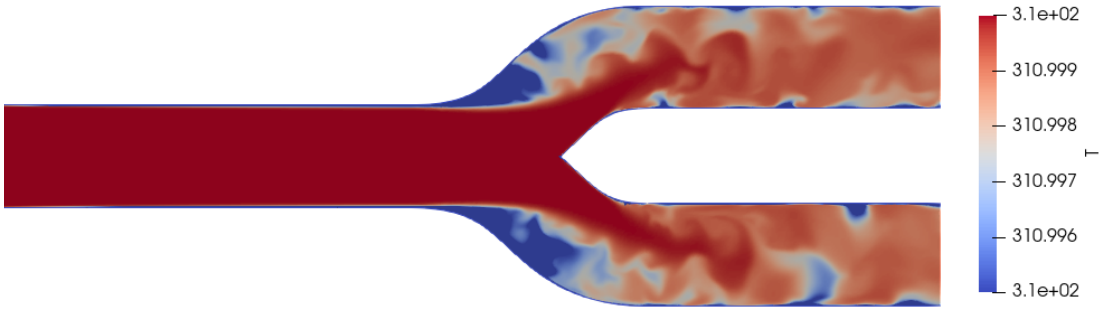

Figure 10.26: *Temperature field for the bifurcated vessel configuration with 7 mm diameter and Re=321.392. The presence of bifurcation significantly increases flow complexity and generates noticeable temperature fluctuations. Areas of non-stationarity, particularly around the bifurcation, indicate localized disturbances, enhancing heat transfer through vortex formation and fluid separation phenomena.*

Velocity fields The velocity fields in bifurcated vessels, shown in Figures 10.27, 10.28, 10.29, and 10.30, exhibit even more pronounced complexity compared to linear and curved vessels. The bifurcation induces notable flow disturbances, resulting in non-stationary flow conditions with significant velocity fluctuations, particularly around the bifurcation region. Similar to curved vessels, certain fluid particles fail to smoothly follow vessel geometry, creating regions of flow separation and recirculation. These regions, characterized by vortices and pronounced velocity gradients, substantially enhance heat transfer and underscore the potential challenges posed by bifurcations in biomedical applications, such as localized damage to vascular tissues or increased thrombosis risks.

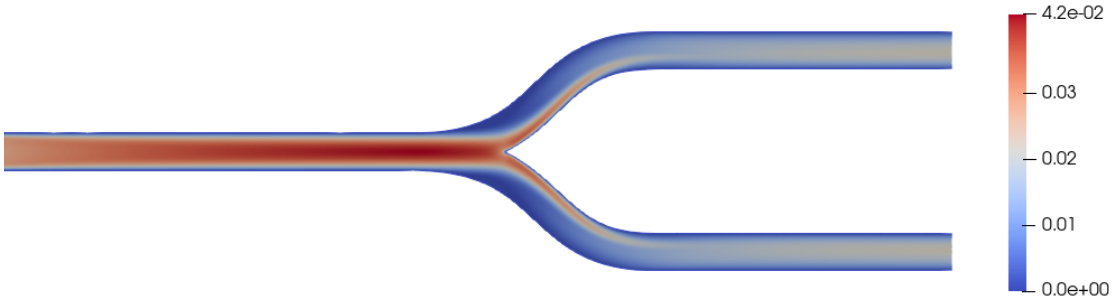

Figure 10.27: *Velocity magnitude field for the bifurcated vessel configuration with 2.5 mm diameter and Re=17.22. The bifurcation clearly induces a disturbed velocity profile, characterized by regions of flow separation and recirculation. These non-stationary flow patterns may significantly impact heat and mass transfer, potentially affecting vascular health or device performance.*

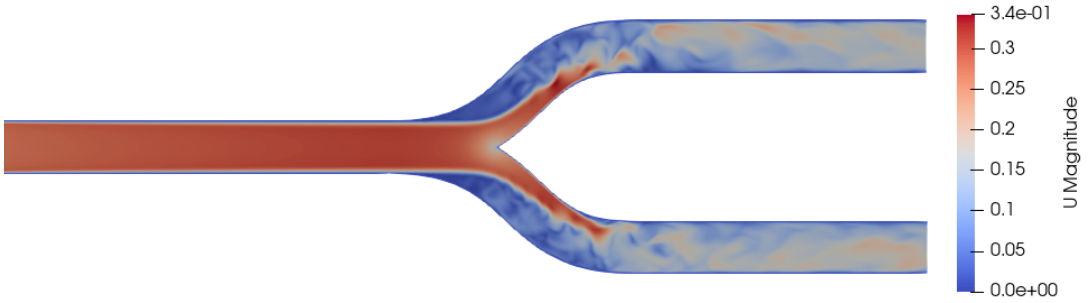

Figure 10.28: *Velocity magnitude field for the bifurcated vessel configuration with 3.5 mm diameter and Re=275.388. The bifurcation clearly induces a disturbed velocity profile, characterized by regions of flow separation and recirculation. These non-stationary flow patterns may significantly impact heat and mass transfer, potentially affecting vascular health or device performance.*

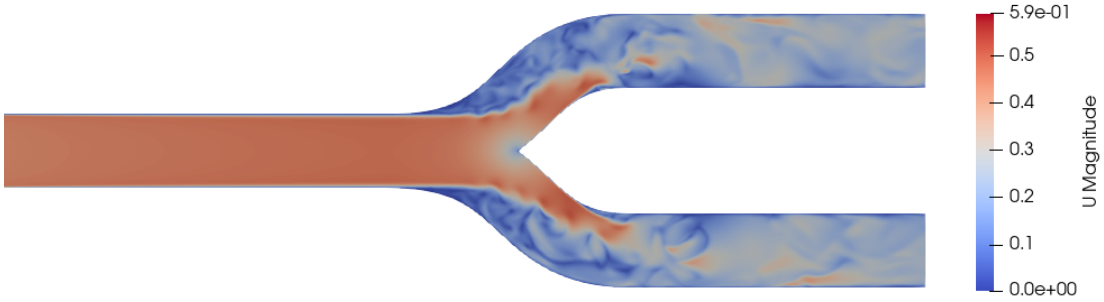

Figure 10.29: *Velocity magnitude field for the bifurcated vessel configuration with 5 mm diameter and Re=642.66. The bifurcation clearly induces a disturbed velocity profile, characterized by regions of flow separation and recirculation. These non-stationary flow patterns may significantly impact heat and mass transfer, potentially affecting vascular health or device performance.*

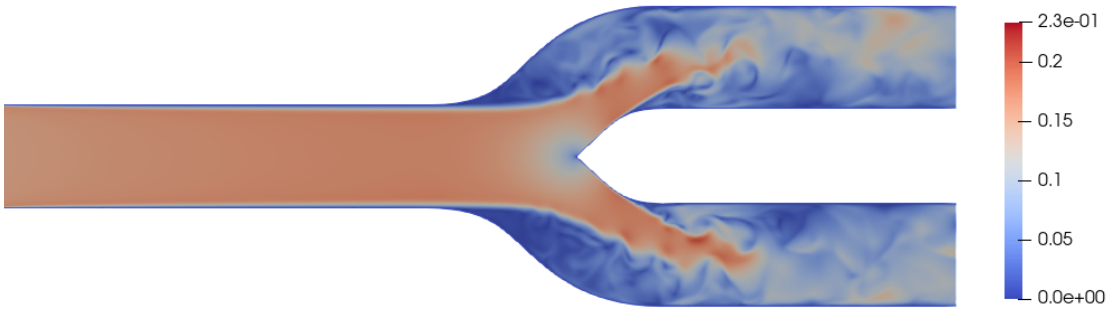

Figure 10.30: *Velocity magnitude field for the bifurcated vessel configuration with 7 mm diameter and Re=321.392. The bifurcation clearly induces a disturbed velocity profile, characterized by regions of flow separation and recirculation. These non-stationary flow patterns may significantly impact heat and mass transfer, potentially affecting vascular health or device performance.*

10.4.2 Temperature profile along the vessel axis

The numerical temperature graphs for bifurcated vessel configurations are presented in Figures 10.31, 10.32, 10.33, and 10.34. Central temperature values are omitted since previous linear vessel analyses demonstrated negligible central temperature variation; this omission simplifies graph interpretation for the more complex bifurcated geometries. As previously observed in cross-sectional analyses, the temperature profiles for bifurcated vessels exhibit notably less stable and more irregular behaviors compared to linear and curved cases, reflecting the complex and unstable fluid dynamics induced by bifurcation. Specifically, temperature fluctuations become more prominent downstream of the bifurcation, evidencing regions of variable heat transfer efficiency. Nonetheless, each graph consistently highlights a distinct temperature increase near the scaffold region, indicating locally enhanced heat transfer phenomena induced by flow disturbances associated with bifurcation and scaffold interaction. A brief overview of bifurcated vessels highlights a further complexity introduced by the geometry, as seen in Figures 10.31, 10.32, 10.33, and 10.34. Starting from the smallest diameter configuration (Figure **??**), temperature profiles display significant fluctuations immediately downstream of the bifurcation, evidencing a highly disturbed flow and variable heat transfer patterns. These fluctuations become increasingly pronounced as ves-

sel diameter increases, as clearly visible in Figure **??**. The bifurcation geometry generates regions of intense mixing and temperature irregularities, far surpassing those observed in linear and curved vessel configurations.

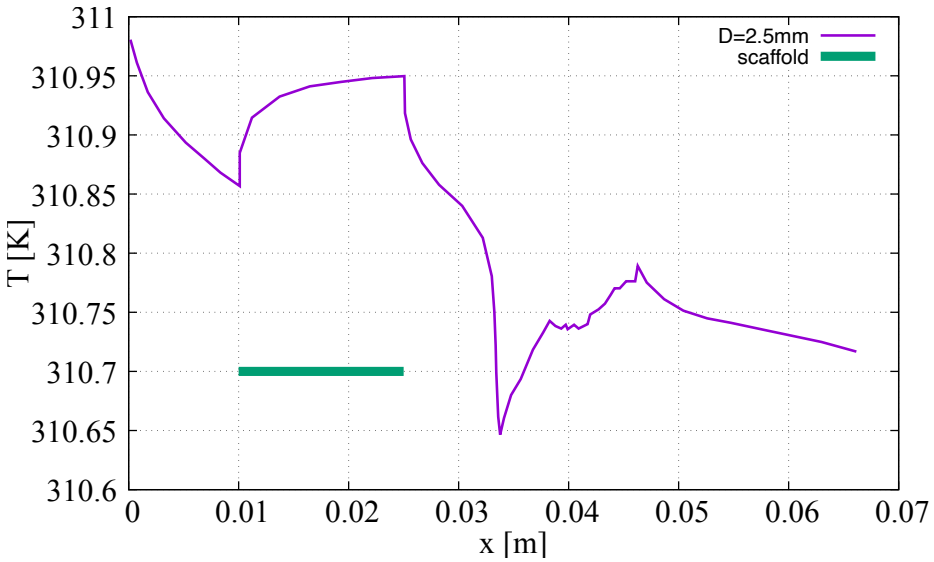

Figure 10.31: *Temperature profile along selected segments in the bifurcated vessel with diameter of 2.5 mm. The graph highlights the irregular and fluctuating behavior of the temperature distribution induced by vessel curvature, with a noticeable temperature increase near the scaffold region.*

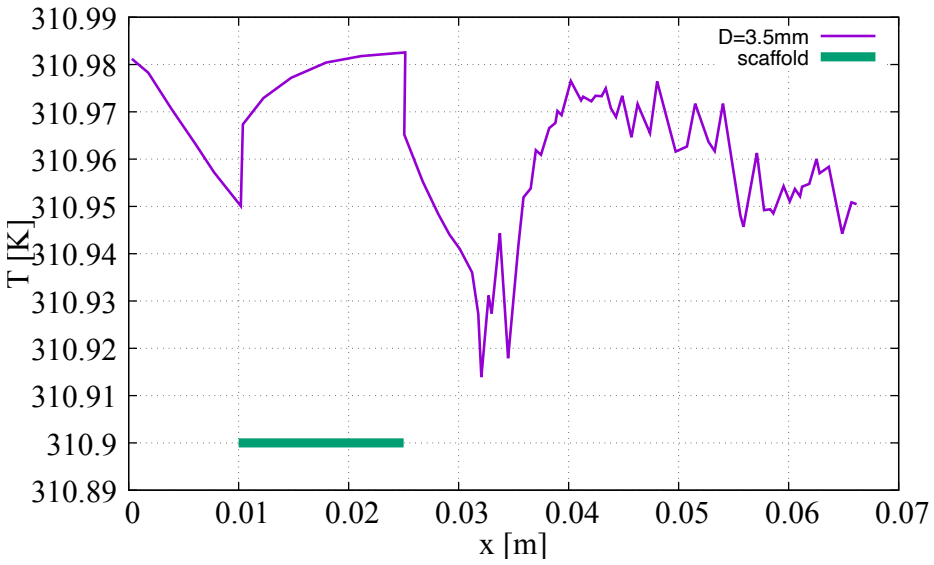

Figure 10.32: *Temperature profile along selected segments in the bifurcated vessel with diameter of 3.5 mm. The graph highlights the irregular and fluctuating behavior of the temperature distribution induced by vessel curvature, with a noticeable temperature increase near the scaffold region.*

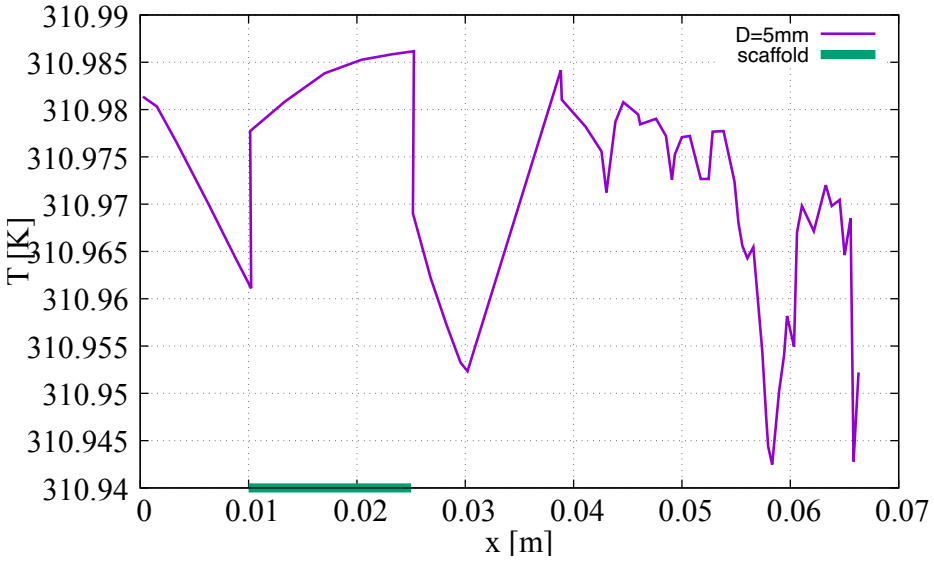

Figure 10.33: *Temperature profile along selected segments in the bifurcated vessel with diameter of 5 mm. The graph highlights the irregular and fluctuating behavior of the temperature distribution induced by vessel curvature, with a noticeable temperature increase near the scaffold region.*

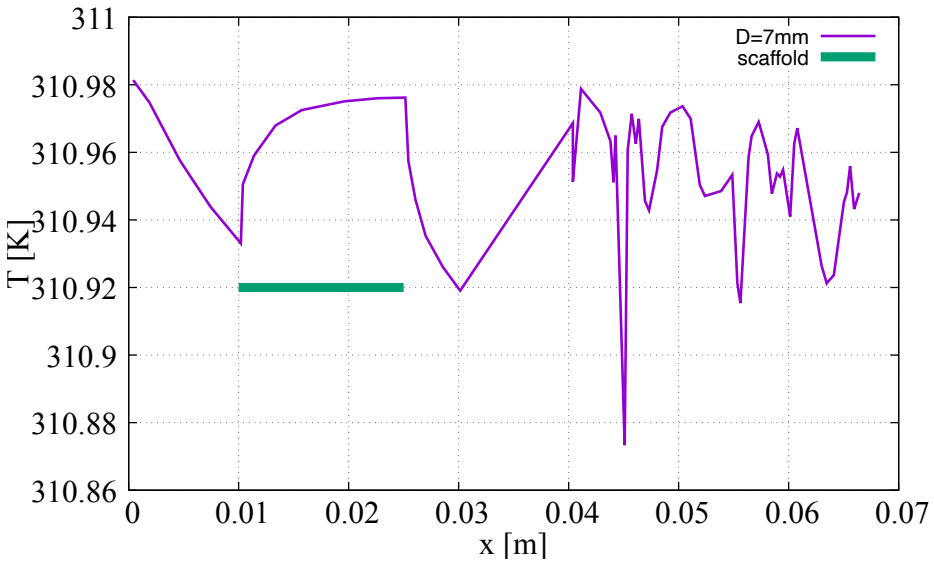

Figure 10.34: *Temperature profile along selected segments in the bifurcated vessel with diameter of 7 mm. The graph highlights the irregular and fluctuating behavior of the temperature distribution induced by vessel curvature, with a noticeable temperature increase near the scaffold region.*

Comparison of all diameters

Examining the overlapping temperature profiles for bifurcated vessels (Figure 10.35), significant differences in temperature distribution among the various diameters become apparent, demonstrating the pronounced influence of geometry on local heat transfer. Compared to analogous linear and curved cases, bifurcated configurations display greater fluctuations and intensified thermal gradients downstream of the scaffold region, underlining the increased sensitivity of bifurcated vessels to diameter and velocity variations. These observations emphasize the complexity introduced by vessel bifurcation and reinforce the necessity of detailed analysis when evaluating heat transfer in bifurcated vascular geometries. Such enhanced temperature variability underscores the critical role bifurcation geometry plays in amplifying fluid dynamics complexities and heat transfer rates, emphasizing its importance for accurate modeling and design in biomedical engineering applications.

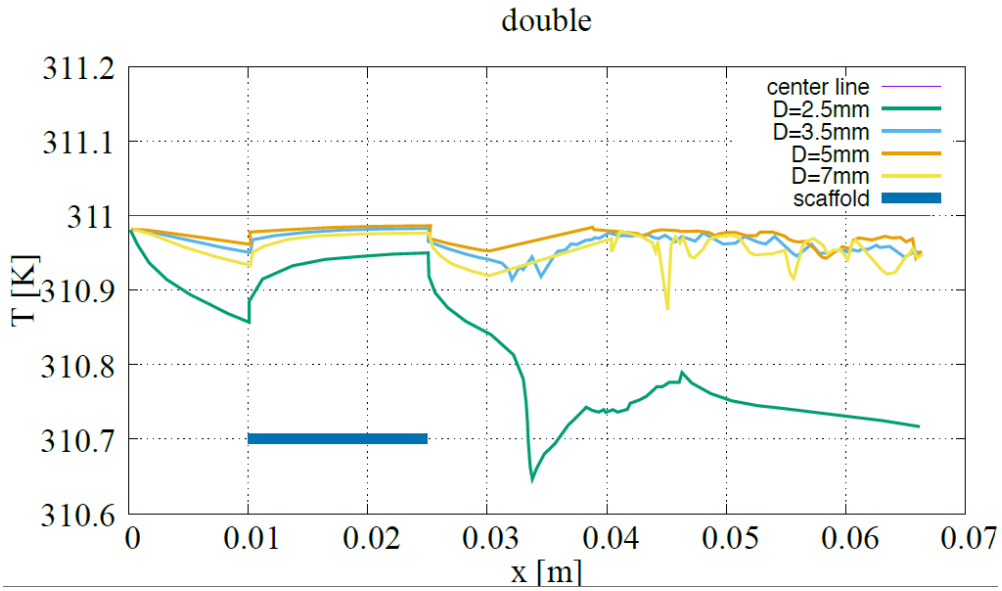

Figure 10.35: *Overlapping temperature profiles for bifurcated vessel configurations with varying diameters. The graph illustrates significant variations and enhanced temperature fluctuations downstream of the scaffold region, underscoring the heightened influence of curvature on local thermal dynamics compared to linear configurations.*

10.5 Concluding observations

The results obtained in this thesis were analyzed through two distinct approaches: temperature graphs along the vessel axis and instantaneous cross-sectional snapshots of temperature and velocity fields. These methodologies provided complementary insights into the thermal behavior of blood flow within vascular prostheses. The presence of the prosthesis was observed to influence the temperature distribution, albeit minimally. The data demonstrate that while the scaffold introduces a localized zone of elevated temperature, this increment is notably small and therefore does not represent a significant obstacle to the practical realization and clinical application of this type of prosthesis. Indeed, recognizing the existence of this region is crucial from an engineering perspective, even though its magnitude remains negligible, highlighting the safety and efficacy of the proposed solution. Further analysis revealed that vessel diameter significantly affects temperature distribution. Larger diameter vessels were consistently associated with smaller

temperature variations due to their capacity to accommodate greater volumes of warm fluid, thus enhancing heat dispersion. Conversely, smaller diameter vessels exhibited more pronounced temperature fluctuations, aligning with previous findings which identified these vessels as particularly challenging from an engineering standpoint. Fortunately, the temperature variation observed in smaller vessels, despite being comparatively larger, remains trivial enough to avoid presenting any real impediment to clinical implementation. Investigating the relationship between fluid flow and vessel diameter revealed a correlation with the Reynolds number (Re). It was observed that increased flow rates, independent of vessel diameter, led to higher Re values. However, even at the highest Re observed (approximately 650), the flow remained within the non-stationary regime, clearly below the turbulent threshold which typically starts around Re = 2000. Therefore, these fluid dynamic conditions confirm that the blood flow remains safely within a laminar or slightly non-stationary regime, rather than transitioning to turbulence. These observations hold true across all examined geometries, although more complex geometries, such as curved and bifurcated vessels, introduced additional non-linear flow characteristics. Specifically, these geometries fostered increased vortex formation and flow instabilities, thereby intensifying local temperature fluctuations. Nonetheless, these variations remained sufficiently minor and non-critical from a biomedical engineering perspective. To conclusively illustrate the minimal impact of the scaffold, a comparative analysis between scaffold-equipped and natural vessels was performed using linear geometry at a 3.5 mm diameter. Figure 10.36 clearly demonstrates that scaffold presence induces a temperature increase below 0.1 degrees, applicable to both Celsius and Kelvin scales. This minimal rise firmly establishes the vascular prosthesis as clinically viable and implantable without significant risk of thermal complications.

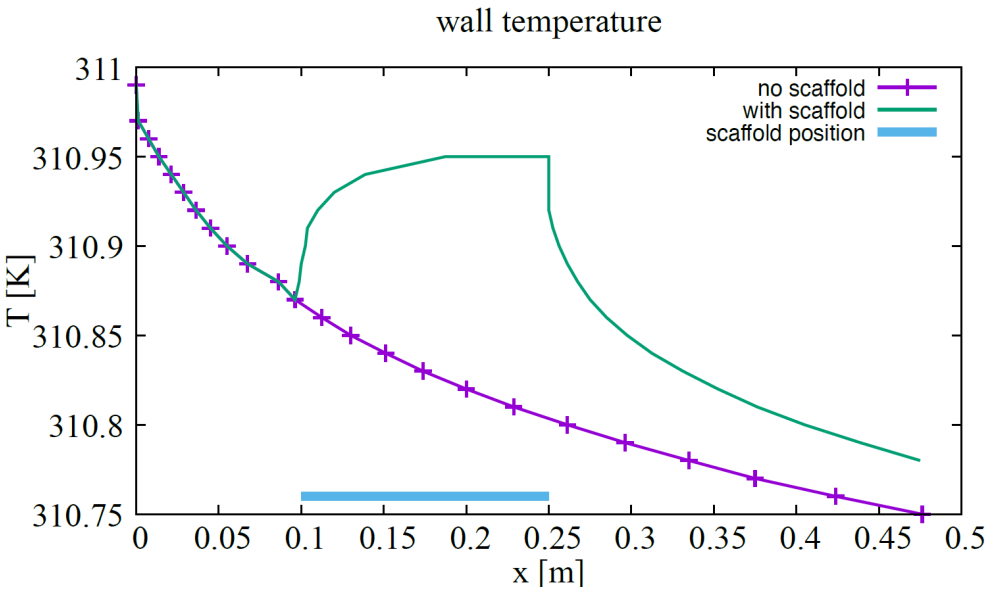

Figure 10.36: *Comparison of the wall temperature profiles along the longitudinal axis for two linear vessels (diameter = 3.5 mm): one including the scaffold (green curve) and one without it (purple curve). The position of the scaffold is indicated by the blue region. The scaffold introduces a localized region of slightly increased temperature due to altered heat transfer dynamics. However, as clearly depicted, this increase remains well below 0.1 degrees (applicable to both Kelvin and Celsius), confirming that the thermal effect of the scaffold is minimal and clinically negligible.*

Conclusions

The objective of this thesis was to analyze temperature variations within a vascular bioprosthesis composed of poly(caprolactone) (PCL) and polyglycerol sebacate (PGS). The collaborative research carried out by the Department of Civil, Chemical and Environmental Engineering at the University of Genoa and the IRCCS Policlinico San Martino Hospital has already optimized the electrospinning manufacturing process for small-caliber vascular prostheses utilizing this polymeric blend, confirming its implantability based on biological and mechanical criteria. To fully evaluate the prosthesis's implantability, my research focused specifically on thermal aspects, aiming to assess whether the presence of the prosthesis significantly impacts local temperature profiles. Through detailed computational fluid dynamics (CFD) simulations, this study demonstrated that the temperature variation induced by the prosthesis is minimal. Specifically, the presence of the scaffold introduced only a negligible local temperature increase, generally less than 0.1°C (or Kelvin), compared to the physiological state without the prosthesis. Such small thermal variations indicate no significant risk or medical contraindication associated with implanting the prosthesis from a thermal perspective, thus affirming its overall suitability for clinical applications. These results underscore that the bioprosthesis is thermally compatible, ensuring patient safety and clinical efficacy. An essential contribution of this thesis is its advancement in computational modeling methodology. The CFD model developed throughout this research offers remarkable versatility, providing a robust and highly adaptable computational framework. The primary strength of the approach lies in its flexibility and scalability; the established simulation setup and computational algorithms can easily accommodate variations in clinical parameters or changes dictated by specific patient conditions or disease pathologies. This inherent adaptability dramatically increases the model's applicability, enabling it to support a wide range of future studies within biomedical engineering and clinical research. Indeed, the

developed model can readily incorporate alterations in geometric parameters, flow conditions, or material properties by simply adjusting the input parameters. Such adaptability means the model can extend beyond standard physiological conditions to simulate scenarios representative of particular pathological conditions or to cater to unique patient cohorts. This creates opportunities to analyze and predict the prosthesis's thermal impact under extreme or specialized conditions, such as pulsatile blood flow, non-Newtonian blood behavior, or various vascular pathologies. Conducting such studies would be crucial to ensuring that the prosthesis remains thermally inert and safe under conditions significantly different from the standard scenarios explored in this work. The research presented in this thesis, therefore, not only verifies the thermal implantability of the specific vascular prosthesis under investigation but also lays a fundamental groundwork for a variety of future computational studies. Future research endeavors can leverage this validated computational framework to investigate numerous clinically relevant scenarios without extensive redevelopment of the underlying CFD infrastructure. Consequently, this methodology significantly accelerates the pace of research and development in vascular prosthetics, enabling swift and reliable evaluations across diverse medical and physiological contexts. This work constitutes a critical step forward providing both immediate insights for prosthesis implantation and enduring computational tools to support ongoing biomedical innovation.

Acknowledgments

Grazie al professor Pralits, Jan, per avermi aiutato nell'assurdo aggiustamento dei grafici all'ultimo minuto.

Grazie al professor Ferrari (ancora solo prof. per me!), per aver ascoltato ridendo i miei infiniti blateraggi alle ore più assurde, pronto a suggerire carriere alternative.

Grazie Eric. Senza di te, boh.

Grazie papino. Anche sbraitando e lamentandosi, c'è sempre stato e sempre ci sarà.

Grazie ai miei zii. Anche se distanti, inesorabilmente presenti, pieni di affetto e sostegno. E gatti.

Grazie alla mia ami, amica oramai da tempi quasi giurassici (è abbastanza incredibile che siamo ancora qui). Negli ultimi due anni sei stata la mia colonna in un caos in cui era impossibile stare in piedi, letteralmente. Hai ascoltato ogni mio pianto e gli stessi discorsi con una pazienza che farebbe invidia a Madre Teresa (o forse come nei film appoggiavi il telefono e tornavi a pianto finito). Mi hai sostenuta, incoraggiata e hai fatto un tifo per me che mi sono sentita una star nella mi stessa vita e sopratutto capace di fare tutto. Giuro che non so dove sarei ora se non ci fossi stata tu.. forse in un letto a fare la larva, sono però sicura che non sarei qui oggi. Sei stata il mio salvagente. Ma non hai solo fatto in modo che non affogassi, mi hai aiutata ad arrivare più in alto di quanto abbia mai fatto. Arrivando anche tu a vette altissime. E lo so che non è uno dei miei discorsi migliori, ma giuro che non esiste un modo per dirti quanto io sia fiera di te come persona, ti ammiri per quello che sei stata capace di raggiungere, apprezzi la tua amicizia

e quanto ti voglia bene. Perchè di voglio un bene veramente infinito. Grazie. (E giuro solennemente che la prossima crisi esistenziale sarà meno noiosa!)

Grazie ad Alessia, sempre e comunque coinquilina del cuore. Un orecchio attento. Una voce sempre dolce, ma anche decisa e tosta quando serve. Nonchè un'amica di bevute e di gatti di tutto rispetto.

Grazie Becca. Amico di viaggi bellissimi e da incubo allo stesso tempo, che spero non finiscano mai. Grazie delle giornate a tempo perso, degli sguardi carichi di affetto quando servivano e grazie per avermi ascoltata. Ah no aspetta, questo no!

Grazie ad Andrea Neri (siete stati decisamente troppi se devo mettere il cognome per specificare che sei tu), Claudia, Federica, Martina e Pietro .Con me da più o meno anni, ma tutti sempre costanti.

Grazie a Francesca, Michele e Roberta. Le new entry della mia vita, ma nonostante ciò una presenza già molto importante.. E ovvimanete divertente, dolce e sempre desiderata. Amici con cui fare e dire tutto, ma sopratutto fare sparlaggi esagerati...e venire criticati per gli stessi. Ogni riferimento a fatti o persone è puramente casuale.

Grazie Mirella, per la tua sfegatata tifoseria.

Grazie ai miei nipoti. Nipote (vabbè, Rita), Agnesina, Marione, Sofi e Annina. Detti anche sorcini o ciccini pasticcini. La cosa più dolce del mondo insieme ad Adino.

Amici del *A cena dalla violy*, anche se ringraziati in modi diversi, un grazie ulteriore vi spetta. Entrati nella mia vita nei modi e momenti più disparati, ma tutti con una cosa in comune.
L'incredibile affetto che mi dimostrate. Sempre in prima linea ad aiutarmi, anche quando neanche l'ho ancora chiesto. Sento la sincera felicità quando gioite con me dei miei (a volte minuscoli) traguardi, come se fossero vostri. E oddio, considerando la vostra presenza sicuramente siete un parametro da considerare. Un tifo degno di una squadra sportiva (lo so, ho usato questa parola troppe volte. Ma i sinonimi mi facevano anguscia). Sono davvero la persona più fortunata del

mondo ad avervi nella mia vita. Non esistono amici così. Belandi senza di voi sarebbe una vita veramente beige e scadente!! Vi voglio benissimo.

E comunque grazie anche alla mia testa dura come il marmo.

Bibliography

[1] G. Anastasi. *Trattato di anatomia umana*. Edi. Ermes, 2007.

[2] M.N. Levy, B.M. Koeppen, B.A. Stanton, and T. Manzoni. *Principi di fisiologia di Berne & Levy*. Elsevier, 2007.

[3] Ci and Elsevier Research. Biophysical aspects of blood flow in the microvasculature '. Technical report, 1996.

[4] T Kenner. The measurement of blood density and its meaning. Technical report, 1989.

[5] Claudia M. Vaz, S. van Tuijl, C. V.C. Bouten, and F. P.T. Baaijens. Design of scaffolds for blood vessel tissue engineering using a multi-layering electrospinning technique. *Acta Biomaterialia*, 1:575–582, 2005.

[6] Charanpreet Singh, Cynthia Wong, and Xungai Wang. Medical textiles as vascular implants and their success to mimic natural arteries. *Journal of Functional Biomaterials*, 6:500–525, 6 2015.

[7] Emelia J. Benjamin, Salim S. Virani, Clifton W. Callaway, Alanna M. Chamberlain, Alexander R. Chang, Susan Cheng, Stephanie E. Chiuve, Mary Cushman, Francesca N. Delling, Rajat Deo, Sarah D. De Ferranti, Jane F. Ferguson, Myriam Fornage, Cathleen Gillespie, Carmen R. Isasi, Monik C. Jiménez, Lori Chaffin Jordan, Suzanne E. Judd, Daniel Lackland, Judith H. Lichtman, Lynda Lisabeth, Simin Liu, Chris T. Longenecker, Pamela L. Lutsey, Jason S. MacKey, David B. Matchar, Kunihiro Matsushita, Michael E. Mussolino, Khurram Nasir, Martin O'Flaherty, Latha P. Palaniappan, Ambarish Pandey, Dilip K. Pandey, Mathew J. Reeves, Matthew D. Ritchey, Carlos J. Rodriguez, Gregory A. Roth, Wayne D. Rosamond, Uchechukwu K.A. Sampson, Gary M. Satou, Svati H. Shah, Nicole L. Spartano, David L.

Tirschwell, Connie W. Tsao, Jenifer H. Voeks, Joshua Z. Willey, John T. Wilkins, Jason H.Y. Wu, Heather M. Alger, Sally S. Wong, and Paul Muntner. Heart disease and stroke statistics - 2018 update: A report from the american heart association. *Circulation*, 137:E67–E492, 3 2018.

[8] H. Wang and C. Patterson. *Atherosclerosis: Risks, Mechanisms, and Therapies*. Wiley, 2015.

[9] J.S. Suri, C. Kathuria, and F. Molinari. *Atherosclerosis Disease Management*. Springer New York, 2010.

[10] Roberto Lorbeer, Andreas Grotz, Marcus Dörr, Henry Völzke, Wolfgang Lieb, Jens Peter Kühn, and Birger Mensel. Reference values of vessel diameters, stenosis prevalence, and arterial variations of the lower limb arteries in a male population sample using contrast-enhanced mr angiography. *PLoS ONE*, 13, 6 2018.

[11] Haifeng Liu, Xiaoming Li, Gang Zhou, Hongbin Fan, and Yubo Fan. Electrospun sulfated silk fibroin nanofibrous scaffolds for vascular tissue engineering. *Biomaterials*, 32:3784–3793, 5 2011.

[12] Jin Jia Hu, Wei Chih Chao, Pei Yuan Lee, and Chih Hao Huang. Construction and characterization of an electrospun tubular scaffold for small-diameter tissue-engineered vascular grafts: A scaffold membrane approach. *Journal of the Mechanical Behavior of Biomedical Materials*, 13:140–155, 9 2012.

[13] Benoit Lucereau, Foued Koffhi, Anne Lejay, Yannick Georg, Bernard Durand, Fabien Thaveau, Frédéric Heim, and Nabil Chakfe. Compliance of textile vascular prostheses is a fleeting reality. *European Journal of Vascular and Endovascular Surgery*, 60:773–779, 11 2020.

[14] Anwarul Hasan, Adnan Memic, Nasim Annabi, Monowar Hossain, Arghya Paul, Mehmet R. Dokmeci, Fariba Dehghani, and Ali Khademhosseini. Electrospun scaffolds for tissue engineering of vascular grafts, 2014.

[15] Valerie Barron, E. Lyons, C. Stenson-Cox, P. E. McHugh, and A. Pandit. Bioreactors for cardiovascular cell and tissue growth: A review, 2003.

[16] Avinash Baji, Yiu Wing Mai, Shing Chung Wong, Mojtaba Abtahi, and Pei Chen. Electrospinning of polymer nanofibers: Effects on oriented morphology, structures and tensile properties, 2010.

[17] Andrzej Polanczyk, Aleksandra Piechota-Polanczyk, Agnieszka W. Piastowska-Ciesielska, Ihor Huk, Christoph Neumayer, Julia Balcer, and Michal Strzelecki. Reconstruction of the physiological behavior of real and synthetic vessels in controlled conditions. *Applied Sciences (Switzerland)*, 14, 3 2024.

[18] Yuji Naito, Toshiharu Shinoka, Daniel Duncan, Narutoshi Hibino, Daniel Solomon, Muriel Cleary, Animesh Rathore, Corey Fein, Spencer Church, and Christopher Breuer. Vascular tissue engineering: Towards the next generation vascular grafts, 4 2011.

[19] Anita C. Thomas, Gordon R. Campbell, and Julie H. Campbell. Advances in vascular tissue engineering. *Cardiovascular Pathology*, 12:271–276, 2003.

[20] Ke Hu, Yuxuan Li, Zunxiang Ke, Hongjun Yang, Chanjun Lu, Yiqing Li, Yi Guo, and Weici Wang. History, progress and future challenges of artificial blood vessels: a narrative review, 3 2022.

[21] Dieter A. Schumann, Jens Wippermann, Dieter O. Klemm, Friederike Kramer, Daniel Koth, Hartwig Kosmehl, Thorsten Wahlers, and Schariar Salehi-Gelani. Artificial vascular implants from bacterial cellulose: Preliminary results of small arterial substitutes. *Cellulose*, 16:877–885, 2009.

[22] Mariah S. Hahn, Melissa K. McHale, Eva Wang, Rachael H. Schmedlen, and Jennifer L. West. Physiologic pulsatile flow bioreactor conditioning of poly(ethylene glycol)-based tissue engineered vascular grafts. *Annals of Biomedical Engineering*, 35:190–200, 2 2007.

[23] Michel R. Hoenig, Gordon R. Campbell, Barbara E. Rolfe, and Julie H. Campbell. Tissue-engineered blood vessels: Alternative to autologous grafts?, 6 2005.

[24] S E Greenwald and C L Berry. Improving vascular grafts: the importance of mechanical and haemodynamic properties. Technical report.

[25] John D. Kakisis, Christos D. Liapis, Christopher Breuer, and Bauer E. Sumpio. Artificial blood vessel: The holy grail of peripheral vascular surgery, 2005.

[26] Eugene D Boland, Jamil A Matthews, Kristin J Pawlowski, David G Simpson, Gary E Wnek, and Gary L Bowlin. Electrospinning collagen and elastin: Preliminary vascular tissue engineering. Technical report, 2004.

[27] Muneera R. Kapadia, Daniel A. Popowich, and Melina R. Kibbe. Modified prosthetic vascular conduits, 4 2008.

[28] Lei Song, Qiang Zhou, Ping Duan, Ping Guo, Dianwei Li, Yuan Xu, Songtao Li, Fei Luo, and Zehua Zhang. Successful development of small diameter tissue-engineering vascular vessels by our novel integrally designed pulsatile perfusion-based bioreactor. *PLoS ONE*, 7, 8 2012.

[29] Erman Pektok, Benjamin Nottelet, Jean Christophe Tille, Robert Gurny, Afksendiyos Kalangos, Michael Moeller, and Beat H. Walpoth. Degradation and healing characteristics of small-diameter poly(-caprolactone) vascular grafts in the rat systemic arterial circulation. *Circulation*, 118:2563–2570, 12 2008.

[30] Young Min Ju, Hyunhee Ahn, Juan Arenas-Herrera, Cheil Kim, Mehran Abolbashari, Anthony Atala, James J. Yoo, and Sang Jin Lee. Electrospun vascular scaffold for cellularized small diameter blood vessels: A preclinical large animal study. *Acta Biomaterialia*, 59:58–67, 9 2017.

[31] Bryan W. Tillman, Saami K. Yazdani, Sang Jin Lee, Randolph L. Geary, Anthony Atala, and James J. Yoo. The in vivo stability of electrospun polycaprolactone-collagen scaffolds in vascular reconstruction. *Biomaterials*, 30:583–588, 2 2009.

[32] S Ramakrishna, J Mayer, E Wintermantel, and Kam W Leong. Biomedical applications of polymer-composite materials: a review. Technical report.

[33] V. G. Borisov, Yu N. Zakharov, Yu I. Shokin, E. A. Ovcharenko, K. Yu Klyshnikov, I. N. Sizova, A. V. Batranin, Yu A. Kudryavtseva, and P. S. Onishchenko. Numerical method for predicting hemodynamic effects in vascular prostheses. *Numerical Analysis and Applications*, 12:326–337, 10 2019.

[34] Paola Serena Ginestra, Elisabetta Ceretti, and Antonio Fiorentino. Potential of modeling and simulations of bioengineered devices: Endoprostheses, prostheses and orthoses, 7 2016.

[35] C E Schmidt, Christine E Schmidt, and Jennie M Baier. Acellular vascular tissues: natural biomaterials for tissue repair and tissue engineering.

[36] Robeson and Lloyd M. Lloyd m. robeson polymer blends. Technical report.

[37] Joram Slager and Abraham J. Domb. Biopolymer stereocomplexes, 4 2003.

[38] Rachid Hsissou, Rajaa Seghiri, Zakaria Benzekri, Miloudi Hilali, Mohamed Rafik, and Ahmed Elharfi. Polymer composite materials: A comprehensive review, 4 2021.

[39] K. P. Matabola, A. R. De Vries, F. S. Moolman, and A. S. Luyt. Single polymer composites: A review, 12 2009.

[40] Wei Huang and Chenming Zhang. Tuning the size of plga nanoparticles fabricated by nanoprecipitation. *Biotechnology Journal*, 2018.

[41] Basheer Aaliya, Kappat Valiyapeediyekkal Sunooj, and Maximilian Lackner. Biopolymer composites: a review. *International Journal of Biobased Plastics*, 3:40–84, 1 2021.

[42] Jaya Baranwal, Brajesh Barse, Antonella Fais, Giovanna Lucia Delogu, and Amit Kumar. Biopolymer: A sustainable material for food and medical applications, 3 2022.

[43] Simzar Hosseinzadeh, Zeinab Zarei-Behjani, Mahboubeh Bohlouli, Arash Khojasteh, Nazanin Ghasemi, and Nasim Salehi-Nik. Fabrication and optimization of bioactive cylindrical scaffold prepared by electrospinning for vascular tissue engineering. *Iranian Polymer Journal (English Edition)*, 31:127–141, 2 2022.

[44] Grażyna Lewandowicz Katarzyna Leja. Polymer biodegradation and biodegradable polymers – a review. *Polish J. of Environ. Stud.*, 19:255–266, 2010.

[45] Swathi Ravi and Elliot L. Chaikof. Biomaterials for vascular tissue engineering, 1 2010.

[46] Faraz Fazal, Francisco Javier Diaz Sanchez, Muhammad Waqas, Vasileios Koutsos, Anthony Callanan, and Norbert Radacsi. A modified 3d printer as a hybrid bioprinting-electrospinning system for use in vascular tissue engineering applications. *Medical Engineering and Physics*, 94:52–60, 8 2021.

[47] Lien Van Der Schueren, Bert De Schoenmaker, Özlem I. Kalaoglu, and Karen De Clerck. An alternative solvent system for the steady state electrospinning of polycaprolactone. *European Polymer Journal*, 47:1256–1263, 6 2011.

[48] Manuel A. Alfaro De Prá, Rosa M. Ribeiro do Valle, M. Maraschin, and Beatriz Veleirinho. Effect of collector design on the morphological properties of polycaprolactone electrospun fibers. *Materials Letters*, 193:154–157, 4 2017.

[49] Ryan R. Duling, Rebecca B. Dupaix, Noriko Katsube, and John Lannutti. Mechanical characterization of electrospun polycaprolactone (pcl): A potential scaffold for tissue engineering. *Journal of Biomechanical Engineering*, 130, 1 2008.

[50] Jue Hu, Dan Kai, Hongye Ye, Lingling Tian, Xin Ding, Seeram Ramakrishna, and Xian Jun Loh. Electrospinning of poly(glycerol sebacate)-based nanofibers for nerve tissue engineering. *Materials Science and Engineering C*, 70:1089–1094, 1 2017.

[51] Ahmad Saudi, Mohammad Rafienia, Anousheh Zargar Kharazi, Hossein Salehi, Ali Zarrabi, and Mehdi Karevan. Design and fabrication of poly (glycerol sebacate)-based fibers for neural tissue engineering: Synthesis, electrospinning, and characterization. *Polymers for Advanced Technologies*, 30:1427–1440, 6 2019.

[52] Feng Yi and David A. La Van. Poly(glycerol sebacate) nanofiber scaffolds by core/shell electrospinning. *Macromolecular Bioscience*, 8:803–806, 9 2008.

[53] Yadong Liu, Kang Tian, Jun Hao, Tao Yang, Xiaoling Geng, and Weiguo Zhang. Biomimetic poly(glycerol sebacate)/polycaprolactone blend scaffolds for cartilage tissue engineering. *Journal of Materials Science: Materials in Medicine*, 30, 5 2019.

[54] Eric M. Jeffries, Robert A. Allen, Jin Gao, Matt Pesce, and Yadong Wang. Highly elastic and suturable electrospun poly(glycerol sebacate) fibrous scaffolds. *Acta Biomaterialia*, 18:30–39, 5 2015.

[55] Seema Agarwal, Joachim H. Wendorff, and Andreas Greiner. Use of electrospinning technique for biomedical applications, 12 2008.

[56] A. Martins, R. L. Reis, and N. M. Neves. Electrospinning: Processing technique for tissue engineering scaffolding, 9 2008.

[57] Sarah Drilling, Jeremy Gaumer, and John Lannutti. Fabrication of burst pressure competent vascular grafts via electrospinning: Effects of microstructure. *Journal of Biomedical Materials Research - Part A*, 88:923–934, 3 2009.

[58] Nandana Bhardwaj and Subhas C. Kundu. Electrospinning: A fascinating fiber fabrication technique, 5 2010.

[59] Wei He, Zuwei Ma, Eong Teo Wee, Xiang Dong Yi, Peter Ashley Robless, Chye Lim Thiam, and Seeram Ramakrishna. Tubular nanofiber scaffolds for tissue engineered small-diameter vascular grafts. *Journal of Biomedical Materials Research - Part A*, 90:205–216, 7 2009.

[60] Nannan Duan, Xue Geng, Lin Ye, Aiying Zhang, Zengguo Feng, Lianrui Guo, and Yongquan Gu. A vascular tissue engineering scaffold with core-shell structured nano-fibers formed by coaxial electrospinning and its biocompatibility evaluation. *Biomedical Materials (Bristol)*, 11, 5 2016.

[61] Sangwon Chung, Nilesh P. Ingle, Gerardo A. Montero, Soo Hyun Kim, and Martin W. King. Bioresorbable elastomeric vascular tissue engineering scaffolds via melt spinning and electrospinning. *Acta Biomaterialia*, 6:1958–1967, 2010.

[62] Wei Fu, Zhenling Liu, Bei Feng, Renjie Hu, Xiaomin He, Hao Wang, Meng Yin, Huimin Huang, Haibo Zhang, and Wei Wang. Electrospun gelatin/pcl and collagen/plcl scaffolds for vascular tissue engineering. *International Journal of Nanomedicine*, 9:2335–2344, 5 2014.

[63] Pier Francesco Ferrari, Bahar Aliakbarian, Domenico Palombo, and Patrizia Perego. Small diameter vascular grafts coated with gelatin. In *CHEMICAL ENGINEERING TRANSACTIONS*, volume 57, 2017.

[64] Pier Francesco Ferrari, Bahar Aliakbarian, Alberto Lagazzo, Ali Tamayol, Domenico Palombo, and Patrizia Perego. Tailored electrospun small-diameter graft for vascular prosthesis. *International Journal of Polymeric Materials and Polymeric Biomaterials*, 66:635–643, 8 2017.

[65] Shengchang Zhang, Christine Campagne, and Fabien Salaün. Influence of solvent selection in the electrospraying process of polycaprolactone, 1 2019.

[66] Björn Sonesson MD PhD Åsa Rydén Ahlgren MD Thomas Sandgren, MD and PhD Malmö Sweden Toste Länne, MD. The diameter of the common femoral artery in healthy human: Influence of sex, age, and body size. *JOURNAL OF VASCULAR SURGERY*, Volume 29, Number 3:846–853, 6 1999.

[67] P. Lewis, J.V. Psaila, W.T. Davies, K. McCarty, and J.P. Woodcock. Measurement of volume flow in the human common femoral artery using a duplex ultrasound system. *Ultrasound in Medicine Biology*, 12(10):777–784, 1986.

[68] jaroslaw Krejza et al. Carotid artery diameter in men and women. *American heart association journals*, 2006.

[69] Nigel Ackroyd, Robert Gill, Kaye Griffiths, George Kossoff, and Michael Appleberg. Quantitative common carotid artery blood flow: Prediction of internal carotid artery stenosis. *Journal of Vascular Surgery*, 3:846–853, 6 1986.

[70] J T Dodge, B G Brown, E L Bolson, and H T Dodge. Lumen diameter of normal human coronary arteries. influence of age, sex, anatomic variation, and left ventricular hypertrophy or dilation. *Circulation*, 86(1):232–246, 1992.

[71] Jean-Pierre Barral and Alain Croibier. 3 - homeostasis of the cardiovascular system. In Jean-Pierre Barral and Alain Croibier, editors, *Visceral Vascular Manipulations*, pages 46–60. Churchill Livingstone, Oxford, 2011.

[72] Trager et al.

[73] Shu Chien, Shunichi Usami, and Robert J Dellenback. Shear-dependent interaction of plasma proteins with erythrocytes in blood rheology. Technical report, 1970.

[74] Xiaojiang Xu, Timothy P. Rioux, and Michael P. Castellani. The specific heat of the human body is lower than previously believed: The journal temperature toolbox, 2023.

[75] HENNY H. BILLETT. Hemoglobin and hematocrit. 1990.

[76] Melissa C. Brindise, Margaret M. Busse, and Pavlos P. Vlachos. Density- and viscosity-matched newtonian and non-newtonian blood-analog solutions with pdms refractive index, 11 2018.

[77] Ping Yuan. Numerical analysis of an equivalent heat transfer coefficient in a porous model for simulating a biological tissue in a hyperthermia therapy. *International Journal of Heat and Mass Transfer*, 52(7):1734–1740, 2009.

[78] Li Li, Mingchao Liang, Boming Yu, and Shanshan Yang. Analysis of thermal conductivity in living biological tissue with vascular network and convection. *International Journal of Thermal Sciences*, 86:219–226, 2014.

[79] E. N. Ahmed, A. Bottaro, and G. Tanda. A homogenization approach for buoyancy-induced flows over micro-textured vertical surfaces. *Journal of Fluid Mechanics*, 941:A53, 2022.

[80] E. N. Ahmed, A. Bottaro, and G. Tanda. Conjugate natural convection along regularly ribbed vertical surfaces: A homogenization-based study. *Numerical Heat Transfer, Part A: Applications*, 85:1331–1355, 2023.

[81] E. N. Ahmed and G. Tanda. An experimental and numerical study of laminar natural convection along vertical rib-roughened surfaces. *International Journal of Heat and Mass Transfer*, 223:125227, 2024.

[82] Onshape Inc. Learning center, Onshape Inc.

[83] The OpenFoam Foundation. Guides and training.

[84] Wolf Dynamics. Wolf dynamics multiphysics simulation, optimization and data analytics.

[85] Kitware Inc. Paraview training course.